EFFECTS OF HIGH SATURATED FAT ON MYOCARDIAL CONTRACTILE AND MITOCHONDRIAL FUNCTION IN HEART FAILURE

by

JULIE HELENE RENNISON

Submitted in partial fulfillment of the requirements

For the degree of Doctor of Philosophy

Dissertation Adviser: Dr. Margaret P. Chandler

Department of Physiology and Biophysics

CASE WESTERN RESERVE UNIVERSITY

August, 2008

CASE WESTERN RESERVE UNIVERSITY

SCHOOL OF GRADUATE STUDIES

We hereby approve the thesis/dissertation of

Julie Rennison

candidate for the Doctoral degree *.

(signed) Thomas Nosek
(chair of the committee)

Margaret Chandler

John Kirwan

Steve Fisher

Charles Hoppel

Laura Nagy

Andrea Romani

(date) May 2, 2008

*We also certify that written approval has been obtained for any proprietary material contained therein.

DEDICATION

This work is dedicated to my husband and to my family who have always supported and encouraged me.

TABLE OF CONTENTS

List of Tables……..……ix

List of Figures……..…….……x

Acknowledgements…...…….……xii

List of Abbreviations……..xiii

Abstract…….……..……xvi

Chapter 1: Energy Metabolism in the Heart……..……1

1.1 Introduction**……..……1**

1.2 Heart Failure……..……1

1.3 Lipid Accumulation and Myocardial Function……..……...3

1.3.1 Obesity…….……..3

1.3.2 Animal Models of Lipid Accumulation…….……4

1.4 Myocardial Metabolism……5

1.4.1 Overview of Metabolism……...……5

1.4.2 Glucose Metabolism……..…6

1.4.3 Fatty Acid Metabolism……...…7

1.4.4 Oxidative Phosphorylation……...……10

1.4.5 Regulation of Myocardial Metabolism……12

1.5 Alterations in Myocardial Metabolism……...……15

1.5.1 Metabolic Alterations in Heart Failure……..…15

1.5.1.1 Abnormalities in Mitochondrial Structure…….……16

1.5.1.2 Abnormalities in Mitochondrial Function…….……16

1.5.2 Mitochondrial Alterations Associated with High Fat……...……19

1.5.2.1 Lipotoxicity……20

1.5.2.2 Lipotoxicity in Heart Failure……..……23

1.5.2.3 Obesity Paradox…….……24

1.6 Rationale and Hypothesis……26

Chapter 2: High Fat Diet Post Infarction Enhances Mitochondrial Function and Does Not Exacerbate Left Ventricular Dysfunction…….……29

2.1 Introduction……..……30

2.2 Methods…….……...…33

2.2.1 Study Design and Induction of Myocardial Infarction…….……33

2.2.2 Echocardiography…….……34

2.2.3 Hemodynamic Measurements……..…..……35

2.2.4 Preparation of Mitochondria…….……35

2.2.5 Mitochondrial Oxidative Phosphorylation……36

2.2.6 Mitochondrial Electron Transport Chain Complex Activity……37

2.2.7 Detection of Hydrogen Peroxide Production…….……...38

2.2.8 Plasma and Tissue Metabolic Products…….……38

2.2.9 Electron Microscopy…….……40

2.2.10 Statistical Analysis……..……40

2.3 Results……...……42

2.3.1 Coronary Artery Ligation Mortality Rates……..…….42

2.3.2 Body and Heart Mass……42

2.3.3 Cardiac Function and Left Ventricular Remodeling…….……42

2.3.4 Metabolic Substrates: Free fatty acids, triglyceride, ceramide, leptin, and

insulin……45

2.3.5 Electron Microscopy……45

2.3.6 Oxidative Phosphorylation……50

2.3.7 Mitochondrial Electron Transport Chain and Enzyme Activity……...52

2.3.8 Hydrogen Peroxide Production……54

2.4 Discussion……55

Chapter 3: Enhanced Acyl-CoA Dehydrogenase Activity is Associated with Improved Mitochondrial and Contractile Function in Heart Failure……62

3.1 Introduction……..63

3.2 Methods……65

3.2.1 Study Design and Induction of Myocardial Infarction……65

3.2.2 Echocardiography……65

3.2.3 Hemodynamic Measurements……..65

3.2.4 Preparation of Mitochondria……66

3.2.5 Mitochondrial Oxidative Phosphorylation……66

3.2.6 Mitochondrial Electron Transport Chain Complex Activity……67

3.2.7 Electron Microscopy……67

3.2.8 RNA Extraction and Quantitative RT-PCR……68

3.2.9 Western Immunoblot Analysis……69

3.2.10 Acyl-CoA Dehydrogenase Activity……70

3.2.11 Plasma and Tissue Metabolic Products……70

3.2.12 Statistical Analysis……71

3.3 Results……72

3.3.1 Body and Heart Mass……72

3.3.2 Cardiac Function and Echocardiographic Measures……..…72

3.3.3 Metabolic Substrates and Humoral Factors……..72

3.3.4 Mitochondrial Morphology……...……75

3.3.5 Oxidative Phosphorylation……79

3.3.6 Mitochondrial Electron Transport Chain Complex Activities……..……83

3.3.7 RNA Expression……...88

3.3.8 Acyl-CoA Dehydrogenase Protein Expression and Enzyme Activity……..88

3.3.9 Acylcarnitines……...93

3.4 Discussion……96

Chapter 4: Summary and Future Directions……..103

4.1 Summary of Primary Findings…….…..103

4.2 Future Directions……..…….105

4.2.1 Mechanism for Increased Acyl-CoA Dehydrogenase Activity……..105

4.2.2 High Fat Diet and Substrate Utilization in Heart Failure……...106

4.2.3 The Role of High Fat Feeding in Increased Surgical Mortality…….…..…107

4.2.4 Specificity of Findings to Model Used……...107

4.2.5 Time Course for Alterations Induced by High Fat……108

4.2.6 Diet Composition- The Role of Carbohydrates...……...109

4.3 Summary……110

Reference List……111

LIST OF TABLES

Table 2-1: Body and heart mass……..…44

Table 2-2: Plasma free fatty acids, triglycerides, leptin, and insulin……..…47

Table 2-3: Protein yield and mitochondrial oxidative phosphorylation rates in SSM and IFM……..…51

Table 2-4: Electron transport chain complex activities in SSM and IFM……...……53

Table 3-1: Body and heart mass…….....…73

Table 3-2: LV functional measurements…….....……74

Table 3-3: Plasma glucose, insulin, free fatty acids, triglycerides, and leptin, serum adiponectin, and tissue triglycerides……..…76

Table 3-4: Electron transport chain complex and enzyme activities in SSM……..…86

Table 3-5: Electron transport chain complex and enzyme activities in IFM…..……87

Table 3-6: Summary of changes induced by high fat in heart failure…….……...97

LIST OF FIGURES

Figure 1-1: Schematic of fatty acid metabolism……9

Figure 1-2: Subsarcolemmal and interfibrillar mitochondria……..…..11

Figure 1-3: Schematic of ceramide production and effects on the cell……22

Figure 2-1: Coronary artery ligation surgeries and the accompanying mortality due to sudden death……...……43

Figure 2-2: Left ventricular hemodynamics and echocardiographic measurements…46

Figure 2-3: Myocardial tissue triglyceride and tissue C16-ceramide content…..……48

Figure 2-4: Morphological comparison of SSM and IFM by electron microscopy….49

Figure 3-1: Electron micrographs of SSM and IFM……77

Figure 3-2: Electron micrographs of mitochondria in LV myocardial tissue…..……78

Figure 3-3: State 3 respiration in SSM ……..……..…...…80

Figure 3-4: State 3 respiration in IFM…….……81

Figure 3-5: State 4 respiration in SSM and IFM…….82

Figure 3-6: Respiratory control ratio in SSM and IFM……...……84

Figure 3-7: ADP/O in SSM and IFM……...…85

Figure 3-8: mRNA expression of PPARα regulated genes……...…89

Figure 3-9: MCAD mRNA and protein expression……..……90

Figure 3-10: Activity of short-, medium-, and long-chain acyl-coA dehydrogenase in SSM and IFM……91

Figure 3-11: Activity of MCAD correlated to state 3 respiration in the SSM ……...…92

Figure 3-12: CD36 and FATP-1 protein expression in myocardial tissue……....94

Figure 3-13: Myocardial tissue carnitine, acylcarnitine, and total carnitine content, acylcarnitine-to-carnitine ratio, and long-chain acylcarnitine content…..95

ACKNOWLEDGEMENTS

I would like to thank my advisor, Dr. Margaret Chandler, for her support both professionally and personally. I would also like to thank my committee members, Dr. Thomas Nosek, Dr. Charles Hoppel, Dr. Andrea Romani, Dr. Laura Nagy, Dr. John Kirwan, and Dr. Steven Fisher, as well as Dr. William Stanley, Dr. Janos Kerner, Dr. Martin Young, Dr. Hisashi Fujioka, and Dr. Kou-Yi Tserng for their guidance and support. Additionally, I would like to thank Tracy McMahon, Xiaoqin Chen, Ronda Griffen, Dr. Isidore Okere, Dr. Jessica Berthiaume, Dr. Naveen Sharma, and Yi-Hsien Cheng for technical assistance, personal support, and friendship. Finally, I would like to thank Dr. Hoppel and his extensive laboratory network. These individuals were instrumental in the development and implementation of my project, but also provided a source of personal support and friendship.

LIST OF ABBREVIATIONS

2D	Two-Dimensional
AHA	American Heart Association
ANF	Atrial Natriuretic Factor
ANOVA	Analysis of Variance
BMI	Body Mass Index
CACT	Carnitine-Acylcarnitine Translocase
CHARM	Candesartan in Heart Failure: Assessment of Reduction in Mortality and Morbidity
Complex I	NADH: Ubiquinone Oxidoreductase
Complex II	Succinate Ubiquinone-Reductase
Complex III	Ubiquinone-Cytochrome C Oxidoreductase
Complex IV	Cytochrome C Oxidase
Complex V	F_oF_1-ATP Synthetase
CI	Cardiac Index
CO	Cardiac Output
CPT-I	Carnitine Palmitoyltransferase-I
CPT-II	Carnitine Palmitoyltransferase-II
CTE1	Cytosolic Thioesterase 1
DHQ	Durohydroquinone
DMSO	Dimethyl Sulfoxide

+/- dP/dt	LV Maximum and Minimum Rate of Change of Pressure with Time
ETC	Electron Transport Chain
FABP	Fatty Acid Binding Protein
FAT/CD36	Fatty Acid Translocase
FATP	Fatty Acid Transport Protein
FS	Fractional Shortening
GAPDH	Glyceraldehyde-3-Phosphate Dehydrogenase
GLUT-4	Glucose Transporter-4
H_2O_2	Hydrogen Peroxide
IFM	Interfibrillar Mitochondria
LCAD	Long-Chain Acyl-CoA Dehydrogenase
LV	Left Ventricular
MCAD	Medium-Chain Acyl-CoA Dehydrogenase
MOPS	3-[N-Morpholino]propanesulfonic acid
MPI	Myocardial Performance Index
NYHA	New York Heart Association
PPARα	Peroxisome Proliferator Activated Receptor-α
PPARβ/δ	Peroxisome Proliferator Activated Receptor-β/δ
PPARγ	Peroxisome Proliferator Activated Receptor-γ
PDK4	Pyruvate Dehydrogenase Kinase-4
PGC-1α	PPAR Gamma Co-Activator-1α
RCR	Respiratory Control Ratio

RV	Right Ventricle
RXR	Retinoid X Receptor
SCAD	Short-Chain Acyl-CoA Dehydrogenase
SSM	Subsarcolemmal Mitochondria
TMPD	*N*,*N*,*N*',*N*'-tetramethyl-*p*-phenylenediamine
UCP2	Uncoupling Protein-2
UCP3	Uncoupling Protein-3
VLCAD	Very Long-Chain Acyl-CoA Dehydrogenase

Effects of High Saturated Fat on Myocardial Contractile and Mitochondrial Function in Heart Failure

Abstract

by

JULIE HELENE RENNISON

Lipid accumulation in non-adipose tissue may play a role in the pathophysiology of heart failure. Accumulation of myocardial lipids and ceramide is associated with decreased contractile function, mitochondrial oxidative phosphorylation, and electron transport chain (ETC) complex activities. We hypothesized that the progression of heart failure would be exacerbated by elevated myocardial lipids and a ceramide-induced inhibition of oxidative phosphorylation and ETC activities. Rats were fed a normal (14% kcal fat) or high fat diet (60% kcal fat) for two weeks. Heart failure was induced by coronary artery ligation. High fat feeding prior to ligation surgery increased surgical mortality, consequently the study was modified so that all rats remained on the normal diet prior to ligation surgery. Following ligation surgery, rats were fed a normal (HF) or high fat diet (HF+FAT) for eight weeks. Sham-operated animals were fed a normal diet. State 3 respiration and ETC complex activities were increased in subsarcolemmal mitochondria (SSM) of HF+FAT, despite elevated myocardial ceramide. No further progression of left ventricular dysfunction was evident in HF+FAT.

We then investigated possible mechanisms by which high fat improved mitochondrial function in heart failure. We hypothesized that a high fat diet during heart failure would increase mitochondrial fatty acid oxidation and state 3 respiration by activating genes involved in fatty acid uptake and utilization. Rats underwent ligation or sham surgery and were fed a normal (SHAM, HF) or high fat diet (SHAM+FAT, HF+FAT) for eight weeks. State 3 respiration using lipid substrates was elevated in SSM of HF+FAT and correlated to increased activities of short-, medium- and long-chain acyl-CoA dehydrogenase. This was associated with improved myocardial contractility as assessed by LV +dP/dt max. Despite decreased medium-chain acyl-CoA dehydrogenase mRNA in HF and HF+FAT, protein content was unchanged. Though high fat improved myocardial contractile and mitochondrial function in heart failure, these effects of high fat were not evident in sham animals. These studies clearly demonstrate a potential cardioprotective role for high fat during early stages of the progression of heart failure. Future studies should examine the mechanism(s) behind high fat induced alterations in mitochondrial and contractile function in heart failure.

Chapter 1

Energy Metabolism in the Heart

1.1 Introduction

Cardiovascular disease is a term that encompasses diseases of the heart, including coronary heart disease, hypertension, heart failure, stroke, and congenital cardiovascular defects (1). An estimated 1 in 3 Americans suffers from one or more of these diseases (1) resulting in 36.3 percent of total deaths in the United States in 2004 (106). The prevalence of cardiovascular disease is an enormous financial burden as well- the cost in the United States for 2008 is estimated at $448.5 billion (1). Given that many of the cardiovascular diseases are interrelated, the increased incidence of risk factors for cardiovascular disease (i.e. diabetes, obesity etc.), and the aging baby boomer population, the impact of cardiovascular disease is expected to rise.

1.2 Heart Failure

Clinically defined as "a complex clinical syndrome that can result from any structural or functional cardiac disorder that impairs the ability of the ventricle to fill with or eject blood" (49), heart failure accounts for seven percent of cardiovascular disease related deaths (1). Risk factors for heart failure include age, male sex, hypertension, left ventricular (LV) hypertrophy, myocardial infarction, diabetes mellitus, valve disease, and

overweight/obesity (59). Heart failure is generally characterized by dyspnea and fatigue (49), but a more specific classification system was developed by the New York Heart Association (NYHA). The NYHA classification system is comprised of four classes that quantify the degree of functional limitation based upon the degree of effort needed to elicit symptoms of heart failure, ranging from symptoms evident at rest (class IV) to symptoms evident at levels that would limit normal individuals (class I) (49). Current medical therapies for heart failure improve clinical symptoms and are able to slow, but not eliminate, the progression of contractile dysfunction. For the more than five million Americans who have been diagnosed with heart failure the prognosis is bleak- 80 percent of men and 70 percent of women under age 65 who are diagnosed with heart failure die within eight years (1), highlighting the need for alternative therapies.

Heart failure is a progressive process that can manifest itself as systolic dysfunction, diastolic dysfunction, or both (86; 127). LV dysfunction is typically initiated by an injury to the myocardium that leads to an abnormality in cardiac structure, function, rhythm, or conductance (49; 86). Injury can result from an acute event such as myocardial infarction, a chronic insult as would occur with pressure or volume overload, or a genetic abnormality (84). As the LV attempts to compensate for the loss of function in the injured area the myocardial wall thickens, a process known as remodeling (49). The patient may remain asymptomatic for many years because the remodeling process initially preserves the functional capacity of the heart (84). As the heart continues to remodel, the structural changes in the heart progress to ventricular hypertrophy and chamber dilation, and are accompanied by the activation of neurohormonal and cytokine systems, culminating in mechanical and electrical dysfunction (49; 84; 86). There is

evidence to suggest that the decreased contractile work that characterizes end-stage heart failure is closely linked to defects in myocardial metabolism and that therapies that inhibit fatty acid oxidation while promoting carbohydrate oxidation may improve LV function and prevent the progression of heart failure (122; 129). However, the exact role of myocardial metabolism in the progression of contractile dysfunction and ventricular remodeling in heart failure is poorly understood and warrants further investigation.

1.3 Lipid Accumulation and Myocardial Function

1.3.1 Obesity

There is overwhelming evidence for obesity-associated alterations in cardiac structure and function that include increased LV mass, LV hypertrophy, increased end-diastolic dimension, as well as impaired systolic and diastolic function (47; 59), and that these symptoms progress with the severity and duration of obesity (59). The prevalence of obesity, defined as a body mass index (BMI) greater than 30 kg/m^2, is also increasing in the United States. In 2005, an estimated 142 million American adults were overweight (66% of the adult population) and 67 million obese (31% of the adult population) (1). Obesity has been identified as a risk factor for heart failure and is associated with additional risk factors for cardiovascular disease such as hypertension, insulin resistance, and dyslipidemia (47; 59). Additionally, obesity is often coupled with metabolic derangements such as hyperinsulinemia, glucose intolerance, hypertriglyceridemia, and low plasma high-density lipoprotein content, all of which have been established to promote coronary heart disease (59). A reversal of heart failure symptoms upon weight loss has been described in morbidly obese patients (59). In fact, current American Heart

Association (AHA) guidelines recommend a low-fat diet in an effort to reduce cardiovascular disease risk factors (79) and the European Society of Cardiology recommends weight loss for all overweight and obese patients with heart failure (127). However, at present little is known about the role of dietary macronutrient composition on the progression of heart failure.

1.3.2 Animal Models of Lipid Accumulation

The excess lipid accumulation commonly associated with obesity is also linked to lipid deposition in non-adipose tissues such as liver, heart, pancreatic islets, and skeletal muscle (6; 115; 134; 142) and increases the risk of diseases such as hepatic steatosis, type 2 diabetes, coronary artery disease, and insulin resistance (1; 6; 134). Extensive animal studies have also demonstrated that lipid accumulation in non-adipose tissue may play an important role in these pathophysiological conditions (16; 27; 43; 111; 144; 148). Enhanced myocardial lipid accumulation is associated with a decrease in myocardial contractile function in several animal models, including the Zucker diabetic fatty rat. Sharma *et al.* (115) found that intramyocardial lipid deposition present in human non-ischemic failing hearts was accompanied by genetic alterations that mirrored those seen in the Zucker diabetic fatty rat. Chiu *et al.* (16) examined the effects of cardiac lipid accumulation in transgenic mice overexpressing cardiac acyl-CoA synthetase, an enzyme that catalyzes esterification of long-chain fatty acids. In this model, lipid accumulation was associated with cardiac hypertrophy, a decrease in systolic function, and premature death (16). Similarly, several studies have shown enhanced myocardial lipid deposition accompanied by marked contractile dysfunction (18; 27; 144; 148) and that this loss of

contractile function can be prevented and/or reversed by the reduction of cardiac lipid content (27; 144; 148). These studies suggest a link between adiposity and cardiovascular dysfunction.

It is important to note that some studies have shown no deleterious effects of high fat on ventricular function in normal animals. In a Wistar rat model neither a high saturated fat diet nor a diet enriched with carnitine palmitoyltransferase-I (CPT-1) inhibitor oxfenicine resulted in cardiac hypertrophy or dysfunction (92). Similarly, Chess *et al.* (14) showed that despite greater plasma free fatty acid and leptin concentrations, high fat feeding did not cause ventricular remodeling or dysfunction in mice. Ouwens *et al.* (97) reported increased papillary muscle basal developed force and maximal force in a Wistar rat model of high fat feeding compared to low fat fed rats. Additional studies from the same lab reported an ejection fraction of 85% in animals fed a high fat diet compared to 88% in control animals (98). Though statistically different, this would be considered very mild contractile dysfunction. Together, these studies indicate that the effects of high fat feeding on myocardial contractile function have not been fully elucidated.

1.4 Myocardial Metabolism

1.4.1 Overview of Metabolism

The heart has a low ATP content and high rate of ATP hydrolysis due to high demand for ATP for contractile work and pumping Ca^{2+} into the sarcoplasmic reticulum, and maintaining Na^{+} and K^{+} ion gradients (122; 123). Under normal conditions about two-thirds of the ATP hydrolyzed by the heart fuels contractile work while about one-third is used for ion pumps (122). In the healthy heart, increased contractile work is

linked to ATP production so that myocardial function does not become limited by ATP supply (123; 128). More than 95% of ATP production in the heart occurs in the mitochondrial electron transport chain (ETC) by a process known as oxidative phosphorylation (123; 128). Oxidative phosphorylation is fueled with energy from electrons that are passed to the ETC by reducing equivalents NADH and $FADH_2$. These reducing equivalents are generated as a result of dehydrogenation reactions that occur primarily in the citric acid cycle or the β-oxidation pathway. The β-oxidation pathway and decarboxylation of pyruvate by pyruvate dehydrogenase also generate acetyl-CoA, which fuels the citric acid cycle, providing additional reducing equivalents to the ETC. Under normal conditions, approximately 60-90% of the acetyl-CoA in the heart is a product of the β-oxidation of fatty acids, while 10-40% comes from the oxidation of pyruvate (10; 123; 129).

1.4.2 Glucose Metabolism

Glycolysis is the process by which the heart converts glucose to pyruvate (126). The heart's substrate supply for glycolysis comes predominantly from exogenous glucose uptake (129). Upon stimulation by insulin, increased work demand, or ischemia, the glucose transporter GLUT-4 is translocated to the plasma membrane to facilitate glucose uptake (123; 129). To prevent its transport out of the cell, glucose is phosphorylated by hexokinase to form glucose 6-phosphate (126). The isomerization of glucose 6-phosphate produces fructose 6-phosphate (126). The first irreversible and key regulatory step in glycolysis is catalyzed by phosphofructokinase, which produces fructose 1,6-bisphosphate (123; 126; 129). The next major regulatory step in the glycolytic pathway is

catalyzed by glyceraldehyde-3-phosphate dehydrogenase (GAPDH) and produces 1,3-bisphosphoglycerate and NADH (123), which is followed by a series of reactions whose end product is phosphoenolpyruvate (126). Pyruvate kinase catalyzes the final irreversible step of glycolysis, producing pyruvate from phosphoenolpyruvate (126). Pyruvate then has three main fates: decarboxylation to acetyl-CoA by pyruvate dehydrogenase, conversion to lactate, or carboxylation to oxaloacetate or malate (123; 129).

1.4.3 Fatty Acid Metabolism

Because the heart has a limited capacity for storage of fatty acids, β-oxidation relies heavily upon a continuous supply of fatty acids derived from the adipose tissue. The rate of fatty acid uptake by the cell is primarily dependent upon the plasma fatty acid concentration and the content of fatty acid transporters at the plasma membrane (138). Fatty acid transport across the plasma membrane is mediated by fatty acid translocase (FAT/CD36), fatty acid transport protein (FATP), and fatty acid binding protein (FABP), the rate of which increases when the concentration of nonesterified fatty acids in the plasma is elevated (65; 123; 129). FABP also enables transport of the fatty acid from the plasma membrane, through the cytoplasm, to the outer surface of the mitochondrial membrane (65). While FAT/CD36, FABP, and FATP are key components of fatty acid transport into the cell, there is little evidence to suggest a role for these transporters in channeling fatty acids towards a particular metabolic fate (i.e. esterification, oxidation) (40). Evidence to date suggests that the fate of fatty acids is determined by intracellular signals (40).

On the inner surface of the plasma membrane, acyl-CoA synthetase converts the fatty acid to fatty acyl-CoA which can then be stored as triacylglycerol, used as a membrane phospholipid, or be transported into the mitochondria to undergo β-oxidation (61; 65). The rate-limiting step for fatty acid transport into the mitochondria and a key regulatory step in β-oxidation is catalyzed by CPT-I (Figure 1-1), an enzyme located in the outer mitochondrial membrane (61). The inner mitochondrial membrane is impermeable to fatty acyl-CoA so CPT-I enables transport of fatty acyl-CoA across the inner mitochondrial membrane by converting fatty acyl-CoA to acylcarnitine in the mitochondrial inter-membrane space (61). The acylcarnitine is then transported into the mitochondrial matrix via the carnitine-acylcarnitine translocase (CACT), converted back to fatty acyl-CoA by carnitine palmitoyltransferase- II (CPT-II), and enters β-oxidation (61; 125).

The first and rate-limiting step of β-oxidation is catalyzed by a family of flavoproteins known as the acyl-CoA dehydrogenases (36). Members of this enzyme family can be found in the mitochondria (36) and have overlapping substrate specificity; short-chain acyl-CoA dehydrogenase (SCAD) for fatty acids of chain-length C_4-C_6, medium-chain acyl-CoA dehydrogenase (MCAD) for fatty acids of chain-length C_4-C_{16}, and long-chain acyl-CoA dehydrogenase (LCAD) for fatty acids of chain-length C_{10}-C_{18}, very long-chain acyl-CoA dehydrogenase (VLCAD), is specific for fatty acids of chain-length greater than C_{16} (36). Acyl-CoA dehydrogenases catalyze the α,β-dehydrogenation of fatty acyl-CoA (36). Two electrons are then transferred to the electron transferring flavoprotein and subsequently to complex III of the ETC. The remaining three steps of β-oxidation are catalyzed by enoyl-CoA hydratase, β-hydroxyacyl-CoA dehydrogenase,

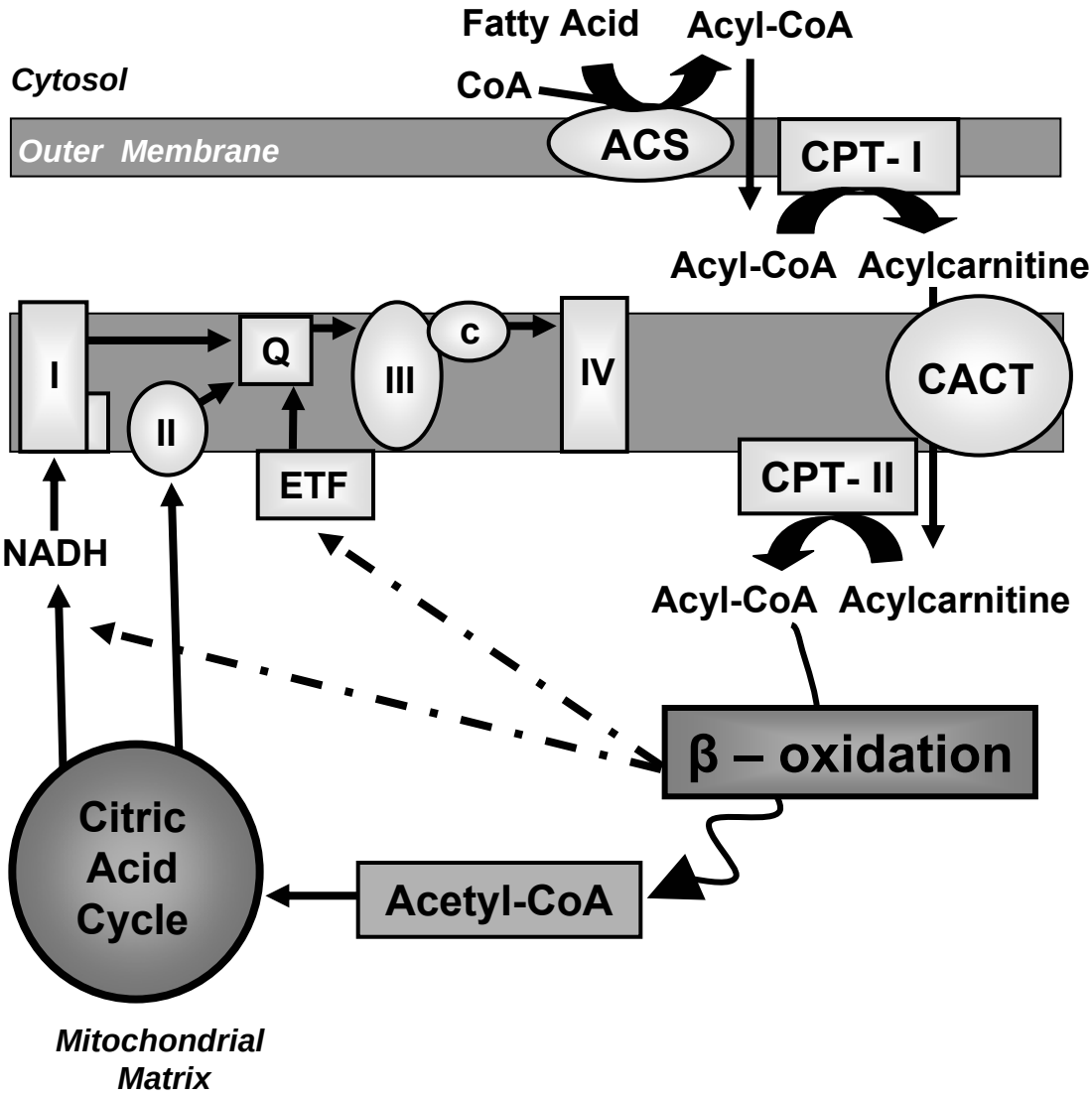

Figure 1-1. Schematic of fatty acid metabolism. Acyl-CoA synthetase (ACS) converts the fatty acid to fatty acyl-CoA. The rate-limiting step for fatty acyl-CoA transport into the mitochondria is catalyzed by carnitine palmitoyltransferase- I (CPT-I) which converts fatty acyl-CoA to acylcarnitine in the mitochondrial inter-membrane space. Acylcarnitine is then transported into the mitochondrial matrix via the carnitine-acylcarnitine translocase (CACT). Upon entering the mitochondria acylcarnitine is converted back to fatty acyl-CoA by CPT-II. Acyl-CoA dehydrogenases catalyze the first and rate-limiting step of β-oxidation. Two electrons are then transferred to the electron transferring flavoprotein (ETF) and subsequently through ubiquinone (coenzyme Q) to complex III of the electron transport chain (ETC). This process shortens a fatty acid by two carbons resulting in acetyl-CoA units that enter the citric acid cycle and generate reducing equivalents that enter the ETC at complex I or complex II.

and ketoacylthiolase, respectively (61; 122). Similar to acyl-CoA dehydrogenase, each of these enzymes also has chain-length specific isoforms (61; 122). The end product of β-oxidation is acetyl-CoA units that enter the citric acid cycle, generating reducing equivalents that enter the ETC at complex I or complex II.

1.4.4 Oxidative Phosphorylation

Due to the high demand for energy production, the heart has a high density of mitochondria compared to other tissues (128). There exists two distinct populations of mitochondria in the heart (Figure 1-2). Subsarcolemmal mitochondria (SSM) are located beneath the plasma membrane and interfibrillar mitochondria (IFM) are found between the myofibrils (99). Both populations of mitochondria exhibit similar respiratory coupling, but as they have been shown to respond differently to pathological conditions (74) it is important that they are assessed separately.

Embedded in the inner mitochondrial membrane, the ETC is composed of four multi-protein complexes (complexes I-IV) and two electron carriers (ubiquinone which is also known as coenzyme Q and cytochrome c) (Figure 1-1) (74; 76). NADH: ubiquinone oxidoreductase (complex I) is a multi-protein complex comprised of 45 or 46 proteins, and functions to transfer electrons from NADH to ubiquinone while pumping protons from the mitochondrial matrix to the inter-membrane space (110). NADH dehydrogenase is a three protein subunit of complex I which binds and oxidizes NADH thereby reducing flavin mononucleotide (32). Succinate ubiquinone-oxidoreductase (complex II) is a flavin-dependent dehydrogenase composed of five subunits and functions to transfer electrons from succinate to ubiquinone (76; 110). The proximal portion of complex II,

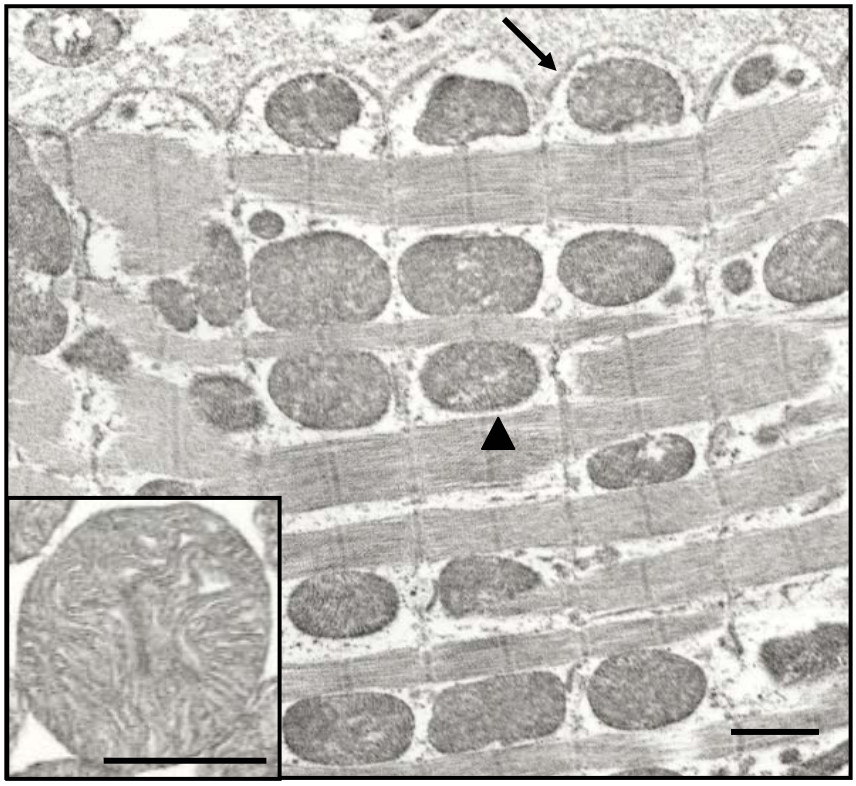

Figure 1-2. Electron micrographs of mitochondria in LV myocardial tissue. SSM are situated beneath the sarcolemma (↑). IFM (▲) are located between the myofibrils. Inset in bottom-left corner shows a single mitochondrion. Bars = 1 μm.

succinate dehydrogenase, is a component of the citric acid cycle and catalyzes the oxidation of succinate into fumarate (76; 110). Ubiquinol-cytochrome c oxidoreductase (complex III) oxidizes ubiquinol and reduces cytochrome c (76; 110). Cytochrome c oxidase (complex IV) is the final step in the transfer of electrons. Complex IV oxidizes cytochrome c and reduces molecular oxygen to water (76; 110). Similar to complex I, complexes III and IV also pump protons into the inter-membrane space as the electrons are transferred from one complex to the next. Because the inner mitochondrial membrane has a very low permeability for protons, this creates an electrochemical proton gradient. Protons then flow back down their electrochemical gradient through F_oF_1-ATP synthetase (complex V) which uses this electrochemical gradient to synthesize ATP from ADP and Pi (74; 110).

1.4.5 Regulation of Myocardial Metabolism

Myocardial metabolism is regulated by a number of factors, including arterial carbon substrate concentration, plasma hormone (e.g. insulin, glucagon, epinephrine, norepinephrine, thyroid hormone) and adipokine (e.g. leptin, adiponectin, resistin, ghrelin, visfatin) concentrations, coronary flow, inotropic state, allosteric control of fatty acid metabolic enzymes, and the nutritional status of the tissue (57; 123; 129). Regulation of myocardial metabolism also is mediated at the transcriptional level (129). The primary regulator of genes involved in key energy producing metabolic pathways is the family of ligand-activated transcriptional factors known as peroxisome proliferator activated receptors (PPARα, β/δ, and γ) (5; 10; 26; 51). Though PPARβ/δ is a necessary regulatory component of myocardial energy metabolism (26), PPARα is thought to be the primary

transcriptional regulator of fatty acid metabolism in the heart (26; 50). Long-chain fatty acids and eicosanoids are known natural ligands for PPARs, however their precise mechanism of action has not been elucidated (26; 30). Synthetic ligands for PPARα include fenofibrate and WY-14,643 (30). Conditions such as ischemia, fasting, diabetes, and high fat feeding which increase plasma fatty acids also have been shown to increase the expression of PPARα (50; 123), while hypertrophy, cardiomyopathy, and heart failure have been shown to decrease PPARα expression (10; 51; 122; 123).

Upon ligand binding, PPARs dimerize with retinoid X receptor (RXR). The PPAR/RXR complex recruits transcriptional coactivators that are necessary to initiate transcription of target genes, then binds direct repeat response elements in the target gene promoter region (26). PPARα activates the expression of genes encoding enzymes involved in nearly every aspect of fatty acid utilization including uptake and esterification (FAT/CD36, FATP, FABP, acyl-CoA synthetase), mitochondrial and peroxisomal β-oxidation (CPT-I, malonyl-CoA decarboxylase, acyl-CoA dehydrogenase, 3-ketoacyl-CoA thiolase, acyl-CoA oxidase), and mitochondrial uncoupling (UCP2, UCP3) (26; 28; 50; 83; 146). At the same time, PPARα activation inhibits glucose metabolism by altering the expression of genes involved in glucose uptake and utilization including glucose transporter (GLUT-4), glycolytic enzyme phosphofructokinase, and pyruvate dehydrogenase kinase-4 (PDK4), an enzyme that inhibits pyruvate dehydrogenase (28). There are several coactivators that interact with PPARs, however the best known is PPAR gamma co-activator-1α (PGC-1α). In addition to the PPAR family, PGC-1α also coactivates with estrogen-related receptors and the nuclear respiratory factor 1 thereby

augmenting myocardial metabolism by stimulating mitochondrial biogenesis and expression of various components of the ETC (26).

Myocardial metabolism also is modulated by a variety of hormones. Glycolysis is stimulated by insulin, glucagon, epinephrine, norepinephrine, and thyroid hormone (57). Insulin facilitates the transport of glucose into the cell, thereby stimulating glucose utilization and suppressing fatty acid oxidation (7). Diabetes, a condition characterized by low plasma insulin concentrations (Type 1) or insulin resistance (Type II), is associated with increased fatty acid oxidation and decreased glucose utilization (10). A similar phenotype is seen in fasting, a condition also characterized by low insulin and increased plasma free fatty acids (26). This phenotype is a combination of an absence of insulin-mediated regulation of myocardial metabolism associated with the diabetic condition and PPARα-mediated stimulation of the fatty acid oxidation pathway (as described above), highlighting the involvement of several different factors in the regulation of myocardial metabolism (26).

Of the adipokines, leptin and adiponectin are the most widely studied. Under normal conditions, leptin acts to trigger food satiety and decrease food intake, and is positively correlated with percentage body fat in patients (83; 113). Leptin also has been shown to play a role in LV hypertrophy (83; 113). Studies in isolated working rat hearts have shown that leptin increased exogenous and endogenous fatty acid oxidation and decreased triacylglycerol content, while glucose oxidation was unaltered (3). The increased fatty acid oxidation was blocked by co-administration of leptin and insulin. Although the precise mechanisms are unknown, adiponectin is a known regulator of myocardial metabolism and thought to play a protective role in the heart (83).

Adiponectin has been shown to enhance glucose and fatty acid uptake by cardiomyocytes and stimulate myocardial fatty acid oxidation (58) and glucose metabolism (96). This hormone is down-regulated in obesity (83; 96) and adiponectin deficiency is associated with insulin resistance, type 2 diabetes, increased risk of myocardial infarction, coronary artery disease, and increased cardiovascular risk factors (78; 96).

1.5 Alterations in Myocardial Metabolism

1.5.1 Metabolic Alterations in Heart Failure

It is well established that in the healthy heart fatty acids are the primary substrate for the production of ATP. However, the alterations in myocardial metabolism that occur in disease states such as hypertrophy and heart failure are less clear. Several studies have shown that as ventricular dysfunction progresses in heart failure, fatty acid oxidation is down-regulated and the heart begins to rely more on carbohydrate metabolism (10; 51; 122; 123). Sack *et al.* (108) established that mRNA expression of genes involved in fatty acid oxidation are down-regulated in the failing heart. Similarly, PPARα, its co-activator PGC-1α (a regulator of mitochondrial biogenesis) (50; 71; 123), and enzymes involved in fatty acid oxidation have been reported to be down-regulated in hypertrophied and failing hearts (34; 50; 71). Administration of a high fat diet, however, may provide the ligand for the activation of PPARα and PGC-1α, and subsequently increase the expression of the fatty acid metabolic enzymes, thereby enabling increased uptake, utilization, and storage of excess lipids that might, under other circumstances, be cytotoxic to the myocardium.

1.5.1.1 Abnormalities in Mitochondrial Structure

Alterations in myocardial metabolism are not limited to changes in gene expression. Heart failure also is associated with abnormalities in mitochondrial morphology as well. Studies in LV free wall, septum, and right ventricular free wall tissue report increased mitochondrial number, but decreased average size, in microembolism induced heart failure (107). The extent of mitochondrial injury varied from matrix depletion to membrane disruption (107). Isopycnic density gradient analysis of mitochondria isolated from hypertrophied and failing hearts revealed two distinct populations of mitochondria (118). Electron micrographs showed that while mitochondrial structure was primarily unaltered with hypertrophy, mitochondria isolated during early- and late-stage heart failure exhibited a greater variability in size (118). Conversely, studies in isolated mitochondria following ischemia (74; 75) and reperfusion (72) indicate that mitochondrial morphology remains largely intact.

1.5.1.2 Abnormalities in Mitochondrial Function

In addition to abnormalities in mitochondrial morphology, myocardial injury is associated with mitochondrial dysfunction in multiple models of cardiomyopathy. The SSM have been shown to be more susceptible than the IFM to ischemic damage (74; 75; 133). Brief periods of ischemia result in mitochondrial alterations that include decreased complex I activity and damage to the phosphorylation apparatus (48). However as ischemia continues, mitochondrial dysfunction progresses to include complexes III and IV (48). One mechanism by which oxidative phosphorylation and ETC activities are altered in ischemia was demonstrated in studies by Lesnefsky *et al.* (72; 74) using a

rabbit model of ischemia in which a decrease in oxidative phosphorylation using TMPD-ascorbate (complex IV respiratory substrate) was shown to occur concomitantly with a decrease in cardiolipin and cytochrome c content (72; 74). These alterations occur during the ischemic period rather than during reperfusion (72).

Altered mitochondrial function also was described in the rat model of coronary artery ligation-induced heart failure. Decreased mitochondrial respiration was reported in isolated mitochondria using glutamate and succinate as respiratory substrates (56) and in saponin-skinned LV myofibers using glutamate+malate as a respiratory substrate (109). Mitochondrial respiration in the IFM also was reported to be decreased in the cardiomyopathic Syrian hamster model (46). Similarly, ADP dependent respiration in saponin-skinned myofibers was decreased using glutamate+malate as a respiratory substrate in the canine microembolization-induced model of heart failure (116) and in the myocardium of failed explanted human hearts due to ischemic or idiopathic dilated cardiomyopathy (117).

In addition to decreased oxidative phosphorylation, evidence for abnormalities in the ETC complexes also has been reported in various models of heart failure. Ischemia has been shown to induce cytochrome c loss from the mitochondria (8; 54; 75). Additionally, Ide *et al.* (53) reported decreased complex I activity in submitochondrial particles in a pacing-induced canine model of heart failure, though other ETC complexes were not assessed. Using the same animal model of heart failure, Marin-Garcia *et al.* (85) found that complex III activity was decreased in whole tissue homogenates while activities of complexes I, II, and IV were unaltered. In a mouse myocardial infarction model of heart failure, decreased activity of complexes I, III, and IV was accompanied by

a downregulation of the mRNA for mitochondrial encoded subunits of the same complexes (52). There also is evidence of ETC abnormalities in human patients with heart failure. Buchwald *et al.* (9) reported decreased activity of ETC complexes III, IV, and V in mitochondria isolated from hearts of transplant patients with advanced heart failure (NYHA IV). Decreased activity of complex III of the ETC also was found in both patients with idiopathic dilated cardiomyopathy and heart failure patients with a history of ischemic coronary artery disease, though complexes I, II, and IV were unaffected (55).

It is important to note that defects in mitochondrial structure and function may be dependent upon the method by which heart failure is induced. This may account for the different mitochondrial alterations observed in various models of heart failure. For example, the microembolization model of heart failure results in global ischemia in the heart, whereas the coronary artery ligation model of heart failure results in scar tissue formation that develops in the infarcted area of the LV. In the coronary artery ligation model, the damage to the myocardium is more localized. The scar that develops is fibrous tissue and contains no viable mitochondria, while the mitochondria in the viable myocardium may remain unaffected. Defects in mitochondrial function also may depend upon the severity of LV dysfunction. For example, Sordahl *et al.* (118) reported increased mitochondrial respiration during the early stages of hypertrophy, however as ventricular dysfunction progressed to failure mitochondrial function declined as well. Similarly, Javadov *et al.* (56) demonstrated significant reductions in mitochondrial respiration 12 and 18 weeks following ligation surgery, but reported no alterations in mitochondrial function six weeks following the induction of heart failure. Mitochondrial dysfunction

may be evident only when the progression of LV dysfunction and remodeling results in a more severe or decompensated stage of heart failure.

1.5.2 Mitochondrial Alterations Associated with High Fat

While fatty acids are the dominant energy source for the adult mammalian heart, the role of fatty acids extends far beyond that of providing energy for the cell. Fatty acids are utilized for membrane biosynthesis, generation of lipid signaling molecules, post-translational protein modification, and transcriptional regulation (111) and can have multiple effects on mitochondrial function. Ouwens *et al.* (97) examined the effects of seven weeks of high fat feeding on cardiomyocyte mitochondrial structure. Electron microscopy revealed mitochondrial ultrastructural abnormalities that included matrix dilution, cristolysis, and mitochondria-associated lamellar bodies (97).

Depending upon their composition (saturation, chain-length, etc.), fatty acids can differentially affect mitochondrial function. Previous studies performed *in vitro* have clearly shown that long-chain saturated fatty acids are involved in toxic pathways leading to cardiomyopathy, whereas mono- and polyunsaturated fatty acids are not (80; 101; 120). In these studies, the long-chain saturated fatty acid was shown to induce apoptosis, cytochrome c release, caspase activation, and DNA laddering, all markers of cell death (80; 120). Conversely, saturated fatty acids also stimulate mitochondrial oxidation in rats, whereas monounsaturated fatty acids have no effect (39). Similarly, unsaturated fatty acids are associated with greater lipoperoxidation (24), mitochondrial uncoupling, and reactive oxygen species production (20) than saturated fatty acids. The fatty acid composition of the diet has been shown to alter the myocardial composition of

cardiolipin, a phospholipid that plays an essential role in the assembly of mitochondrial supercomplexes, mitochondrial biogenesis, and the structure and activity of several ETC complexes (119). Further studies are required to elucidate the mechanisms responsible for these differential effects of saturated and unsaturated fatty acids, particularly in respect to their effect on mitochondrial respiration and ETC complex activities.

1.5.2.1 Lipotoxicity

Fatty acids taken up by the cardiomyocyte, but not immediately oxidized through β-oxidation pathways, are esterified and stored as triglycerides. As a non-adipose tissue the heart has a limited capacity to store triglycerides. Studies have suggested that under normal conditions only 10-30% of the fatty acids that enter the cardiomyocyte are converted to triglycerides, while as much as 70-90% are converted to acylcarnitines and immediately oxidized (123). When there is a loss of synchronization between fatty acid availability and fatty acid utilization in cardiomyocytes, the excess fatty acids will accumulate, resulting in toxic lipid intermediates that can lead to contractile dysfunction and cell death (43; 111; 136; 144; 148) a condition referred to as "lipotoxicity" (111; 136). The lipotoxic condition is characterized by generation of reactive oxygen species and nitric oxide, decreased phosphatidyl-3-kinase content, and alterations in mitochondrial structure and function, and is associated with a dysregulation of insulin secretion, insulin resistance, and heart failure (80). Apoptotic cell death and lipotoxicity can be prevented by activation of PPARα expression by fenofibrate, an action which would be expected to improve the synchronization between fatty acid availability and utilization (64).

Lipotoxicity also is associated with an increase in ceramide content (Figure 1-3). Ceramides (N-acylsphingosines) comprise the hydrophobic backbone of complex sphingolipids and consist of a long-chain sphingoid base linked by an amide bond to a fatty acid (130). They are produced by either the hydrolysis of membrane sphingomyelin or by the *de novo* synthesis from palmitoyl-CoA and serine (130). Ceramides have been implicated in mitochondrial alterations that include the inhibition of ETC complex III activity (38), increased generation of hydrogen peroxide (33; 103), peroxidation of membrane lipids (33), release of cytochrome c from the mitochondria (23; 35), and apoptosis (23; 43). At the same time, ischemic preconditioning has been shown to limit myocardial apoptosis, an effect that was accompanied by decreased myocardial ceramide content (2).

Similar to fatty acid induced alterations in mitochondrial function, the lipotoxic effect of a fatty acid also is specific to the fatty acid composition. Long-chain saturated fatty acids palmitate and stearate increased ceramide and induced cell death in murine hematopoietic cell lines (101). As palmitoyl-CoA and stearoyl-CoA are precursors for *de novo* ceramide synthesis, it was not surprising that this effect was not evident using other saturated, unsaturated, or branched-chain fatty acids (101). Similar *in vitro* studies have shown that palmitate, but not oleate, increased ceramide content and induced apoptosis (42; 81). These findings have been corroborated in an *in vivo* model in which a high unsaturated fat (oleate) diet decreased ceramide content and resulted in fewer apoptotic events relative to a high saturated fat (palmitate) diet (93). It has been proposed that unsaturated fatty acids have an enhanced ability to be incorporated into triglycerides, an effect that may play a critical role in protection from lipotoxicity by diverting excess fatty

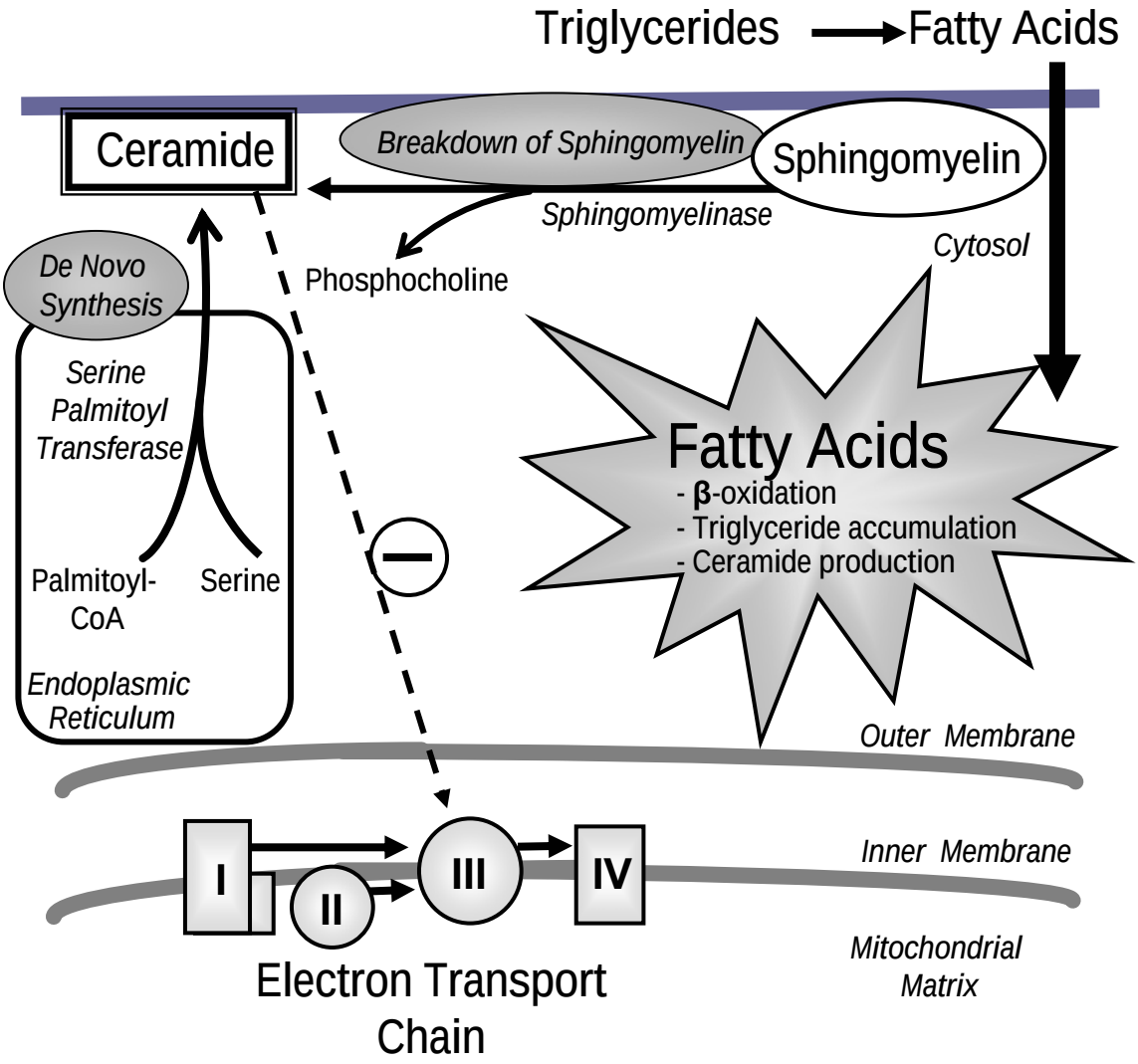

Figure 1-3. Fatty acids are utilized for membrane biosynthesis, generation of lipid signaling molecules, post-translational protein modification, and transcriptional regulation. Chronic exposure to fatty acids can result in an imbalance between fatty acid uptake and utilization that can trigger cytotoxic mechanisms leading to cell dysfunction or death, a phenomenon known as lipotoxicity. The accumulation of ceramide from either the hydrolysis of membrane sphingomyelin or from *de novo* synthesis from palmitoyl-CoA and serine has been implicated in the development of a "lipotoxic" cardiomyopathy. Direct inhibition by ceramide of mitochondrial ETC complex III activity, and the associated reductions in oxidative phosphorylation, could provide a novel mechanism of modulating mitochondrial function and thereby alter myocardial contractile function.

acids from more cytotoxic pathways (80). This concept is supported in studies by Morgan *et al.* (91) in which myocardial triglycerides were elevated, however no further elevation in ceramide content or progression of myocardial contractile dysfunction was evident in heart failure animals fed a high fat diet when compared to heart failure animals fed a normal diet.

1.5.2.2 Lipotoxicity in Heart Failure

Ceramide content has been shown to be elevated in coronary artery ligation induced heart failure (91). Additionally, numerous studies have shown that elevations in ceramide content are associated with cardiac contractile dysfunction and remodeling, and that this loss of contractile function can be prevented and/or reversed by the reduction of these toxic lipid intermediates (15; 16; 144; 148). In the diabetic PPARα overexpressing mouse fed a high fat diet Finck *et al.* (27) reported an imbalance between fatty acid uptake and utilization, resulting in enhanced triglyceride accumulation and ceramide production. Lipid accumulation was associated with ventricular hypertrophy and decreased fractional shortening, thereby exacerbating the cardiomyopathy (27). Likewise, increased myocardial triglyceride stores in Zucker Diabetic Fatty rats have been shown to be accompanied by marked elevations in tissue ceramide, apoptotic cardiomyocyte death, and a decrease in myocardial function (43). However, troglitazone therapy, a PPARγ agonist that reduced cardiac triglyceride accumulation, prevented both the increased ceramide production and the loss of myocardial function (43).

It is important to note that *in vitro* studies commonly use exogenous ceramide (C2-ceramide) which is ampiphilic and can translocate from the plasma membrane to

other cellular membranes, while endogenous ceramide (C16-ceramide) remains tightly bound to the membrane where it is produced (22). Therefore, the biochemical and biophysical action of exogenous ceramide may not mimic the behavior of endogenous ceramide. Exogenous ceramide also has a fluidizing effect on membrane phospholipids while endogenous long-chain ceramide exerts an ordering/packing effect (137). It also is unknown whether the magnitude of increase in endogenous ceramide needed to elicit an effect on mitochondrial function is comparable to the effects of exogenous ceramide as demonstrated *in vitro*. Additionally, as ceramide has been shown to exist on the plasma membrane, as well as the mitochondrial membrane, the relationship between the localization of ceramide and its effects on mitochondrial and cellular function should be investigated. Finally, despite numerous studies that have shown deleterious effects of ceramide, the absence of a lipotoxic effect of ceramide was demonstrated by Relling *et al.* (104) in that acute exposure of ventricular myocytes to ceramide directly enhanced peak cardiomyocyte shortening. Therefore, further studies are needed to assess the relationship between myocardial tissue ceramide and integrated function in isolated mitochondria in an *in vivo* model of heart failure.

1.5.2.3 Obesity Paradox

Despite the considerable body of literature supporting the notion that high dietary fats, tissue lipid accumulation, and elevations in lipotoxic intermediates such as ceramide are detrimental to myocardial contractile function, dietary fat has shown a different effect on cardiac function in multiple animal models of LV dysfunction and heart failure. Okere *et al.* (93) demonstrated that administration of a 60% high fat diet in a Dahl Salt-Sensitive

rat model of hypertension induced cardiomyopathy, reduced LV hypertrophy, improved contractile function, and prevented LV dilation. These findings were confirmed in a mouse model of hypertrophy in which 60% high fat feeding did not exacerbate the hypertrophic response to transverse aortic constriction (14). It is important to note that the fat content of a diet is increased at the expense of the carbohydrate content. Recent studies have shown a high fructose diet exacerbated LV dysfunction and increased mortality in a Dahl Salt-Sensitive rat model of hypertension (113) and a mouse model of transverse aortic constriction induced LV hypertrophy (13), suggesting that the protective effects of high fat may actually be a result of a reduced carbohydrate content. However, the effects of dietary manipulation, specifically high fat feeding, on mitochondrial function in an injury model have not been examined and represent the focus of the present investigation.

There also is evidence for a cardioprotective role of fat in human patients with established LV dysfunction. Recent clinical studies have examined the relationship between BMI and mortality in patients with established heart failure. Several clinical trials have shown that obese and overweight patients with mild to moderate (21; 68) and advanced (29; 47) heart failure have better long-term survival relative to patients with a low BMI. More recently, as part of the Candesartan in Heart Failure: Assessment of Reduction in Mortality and Morbidity (CHARM) program, lower BMI was associated with increased mortality in patients with symptomatic heart failure (NYHA II-IV) while patients in the mild to moderate overweight class were found to have the lowest risk of mortality (60). Additionally, the Women's Health Initiative reported a low-fat diet did not significantly affect the incidence of cardiovascular disease and only modestly altered the

risk factors for cardiovascular disease (48). These findings highlight the need for additional research to determine the effects of dietary macronutrient composition and body composition on the progression of heart failure.

1.6 Rationale and Hypothesis

In summary, extensive clinical and animal studies suggest that excess lipid accumulation in non-adipose tissue plays an important role in the pathophysiology of heart failure, obesity, insulin resistance, and diabetes. However, recent clinical observations indicate that high fat, in existing pathophysiological conditions, may be cardioprotective. The paradoxical nature of these findings highlights the need for further investigation into the role of high saturated fat diet on myocardial contractile and mitochondrial function.

Lipid accumulation due to a mismatch between fatty acid uptake and utilization can trigger cytotoxic mechanisms that lead to cell dysfunction or death, a phenomenon known as lipotoxicity. Specifically, the long-chain saturated fatty acid palmitate can be readily converted to the lipotoxic intermediate ceramide which can impair mitochondrial function and trigger apoptotic cell death. Furthermore, lipid accumulation has also been shown to trigger pathologic hypertrophic growth. However, the cellular mechanisms that determine whether excess lipids are well tolerated or toxic to the heart are unknown.

A possible mechanism of action by which ceramides could lead to myocardial dysfunction has been proposed in studies in isolated rat heart mitochondria in which a rapid decline in mitochondrial oxidative phosphorylation and inhibition of ETC complex III occurred in the presence of ceramide (38). Several human and animal models of heart

failure have demonstrated that myocardial dysfunction is accompanied by alterations in oxidative phosphorylation and ETC abnormalities (46; 48; 52; 53; 55; 56; 72; 74; 85; 109). Thus, direct inhibition of mitochondrial ETC complex III activity by ceramide, and the associated inhibition of oxidative phosphorylation, may provide a novel mechanism of modulating mitochondrial function and thereby alter myocardial contractile function.

The effects of saturated fatty acids on myocardial function in physiological and pathophysiological conditions are poorly understood. It remains to be determined whether myocardial injury (with and without dietary manipulations) is accompanied by increased myocardial ceramide content. Likewise, it is unclear if the LV dysfunction reported in coronary artery ligation induced heart failure would be exacerbated by high fat feeding and increased myocardial ceramide content. Furthermore, the effect of enhanced lipid accumulation and increased ceramide content on mitochondrial function has not been systemically evaluated in a model of coronary artery ligation induced heart failure.

This study investigated the impact of elevated dietary lipids on the progression of myocardial contractile and mitochondrial dysfunction in heart failure. Specifically we investigated whether accumulation of excess myocardial lipids and coronary artery ligation are accompanied by elevated myocardial ceramide content. Additionally, we sought to determine whether myocardial ceramide accumulation, in the context of heart failure and elevated saturated fat, is accompanied by alterations in mitochondrial respiration and ETC complex activity thereby exacerbating the progression of LV dysfunction. I hypothesized that heart failure, induced by coronary artery ligation, would be exacerbated by elevated lipids and a ceramide induced inhibition of mitochondrial

respiration (specifically through inhibition of complex III). We found that administration of a high saturated fat diet in a model of coronary artery ligation-induced heart failure resulted in no impairments in mitochondrial oxidative phosphorylation or ETC complex activities. Instead state 3 respiration and activities of ETC complexes II and IV were elevated. Additionally, administration of a high saturated fat diet did not adversely affect LV contractile function or the progression of LV remodeling despite elevated myocardial ceramide.

We therefore investigated possible mechanisms by which high fat feeding improved mitochondrial and contractile function in heart failure. We also sought to determine whether these effects of the high fat diet are specific to heart failure. I hypothesized that a high fat diet during heart failure would result in improved mitochondrial fatty acid oxidation and increased state 3 respiration by activating genes involved in fatty acid uptake and utilization (including *cpt-I*, *scad*, *mcad*, *lcad*, *ucp3*, *pdk4*, and cytosolic thioesterase 1 (*cte1*). Additionally, I hypothesized that these effects of a high fat diet are specific to heart failure, and therefore would not be evident in normal animals fed a high fat diet. These hypotheses were tested in a rat model of coronary artery ligation induced heart failure. We found that administration of a high fat diet increased state 3 respiration and acyl-CoA dehydrogenase activities, but did not normalize mRNA or protein levels of acyl-CoA dehydrogenases in coronary artery ligation-induced heart failure rats. Though high fat improved myocardial contractile and mitochondrial function in heart failure, these effects of high fat were not evident in sham animals.

Chapter 2

High Fat Diet Post Infarction Enhances Mitochondrial Function and Does Not Exacerbate Left Ventricular Dysfunction

Julie H. Rennison[1], Tracy A. McElfresh[1], Isidore C. Okere[1], Edwin J. Vazquez[3], Hiral V. Patel[3], Amy B. Foster[3], Kalpana K. Patel[3], Qun Chen[3], Brian D. Hoit[3,5], Kou-Yi Tserng[4], Medhat O. Hassan[4], Charles L. Hoppel[2,3,4], and Margaret P. Chandler[1]

From: [1]Departments of Physiology and Biophysics, [2]Pharmacology, and [3]Medicine, Case Western Reserve University, Cleveland, OH, [4]Louis Stokes VA Medical Center, Cleveland, OH & [5]University Hospitals of Cleveland, Cleveland, OH.

Am J Physiol Heart Circ Physiol. 2007 Mar;292(3):H1498-506

Running title: High Fat Improves Mitochondrial Function in Heart Failure

2.1 Introduction

Fatty acids are the dominant energy source for the adult mammalian heart and also are utilized for membrane biosynthesis, generation of lipid signaling molecules, post-translational protein modification, and transcriptional regulation (111). Chronic exposure to fatty acids can result in an imbalance between fatty acid uptake and utilization that potentially can trigger cytotoxic mechanisms leading to cell dysfunction or death, a phenomenon known as lipotoxicity. Extensive clinical and animal studies have shown that excess lipid accumulation in non-adipose tissue due to enhanced circulating fatty acids, may play an important role in pathophysiological conditions such as heart failure, obesity, insulin resistance, and diabetes (43; 111; 148).

A loss of synchronization between fatty acid availability and utilization in cardiomyocytes, despite otherwise normal or up-regulated β-oxidation capacity, can lead to an increase in the accumulation of tissue ceramide (63). Ceramide, a lipid signaling molecule, has been implicated in the formation of reactive oxygen species and peroxidation of membrane lipids (33), as well as apoptosis (43). The accumulation of ceramide from either the hydrolysis of membrane sphingomyelin or from *de novo* synthesis from palmitoyl-CoA and serine (141) has been implicated in the development of a "lipotoxic" cardiomyopathy. Severe myocardial contractile dysfunction has been observed in mice with increased cardiac fatty acid import due to cardiac specific over-expression of acyl-CoA synthetase, an enzyme that catalyzes esterification of long-chain fatty acids resulting in lipid accumulation (16). In this model, lipid accumulation was associated with cardiac hypertrophy, followed by the development of LV dysfunction, increased ceramide content, and premature death. Studies in Zucker diabetic fatty rats

found that increased myocardial triglyceride stores were accompanied by marked elevations in tissue ceramide and a decrease in contractile function. These effects were prevented by a reduction in cardiac triglyceride over-accumulation (148). Similarly, mice over-expressing PPARα develop a severe cardiomyopathy characterized by marked lipid accumulation, enhanced ceramide production and a decrease in fractional shortening, which is exacerbated when mice are fed a high fat diet. Interestingly, the lipotoxic cardiomyopathy was reversed by discontinuing the high fat diet (27). A potential mechanism by which ceramide could lead to myocardial dysfunction was proposed following studies in isolated rat heart mitochondria in which a rapid decline in mitochondrial oxidative phosphorylation and inhibition of complex III occurred in the presence of ceramide (38). Direct inhibition by ceramide of mitochondrial ETC complex III activity, and the associated reductions in oxidative phosphorylation, could provide a novel mechanism of modulating mitochondrial function and thereby alter myocardial contractile function.

Enhanced myocardial lipid accumulation appears to be associated with impaired myocardial contractile function. However, the effect of enhanced lipid accumulation and increased ceramide production on mitochondrial function and their concomitant effects on ventricular function under pathophysiological conditions such as heart failure have not been systemically evaluated. This study was designed to test the hypothesis that the progression of heart failure would be exacerbated by elevated myocardial lipids and an associated ceramide-induced inhibition of mitochondrial oxidative phosphorylation (specifically through inhibition of complex III activity). We tested our hypothesis in rats

fed a high saturated fat diet following coronary artery ligation surgery to induce heart failure.

2.2 Methods

2.2.1 Study Design and Induction of Myocardial Infarction

This study was conducted in accordance with the *Guide for the Care and Use of Laboratory Animals* (NIH publication NO. 85-23) and the Institutional Animal Care and Use Committee at Case Western Reserve University. Animals were maintained on a reverse 12h:12h light:dark cycle (i.e. lights off at 6:00 AM), and all procedures and tissue harvests were performed in the fasted state between three and six hours into the dark phase of the cycle.

In the initial design of this study, 8-week-old male Wistar rats were fed normal diet (14% calories from fat, 26% calories from protein, 60% calories from carbohydrate) or a high saturated fat diet (60% calories from fat (25% palmitic, 33% stearic and 33% oleic acid), 20% calories from protein, 20% calories from carbohydrate) (Research Diets, Inc.) for 2 weeks. For the induction of heart failure, rats were anaesthetized with isoflurane (1.5–2.0%), intubated, and ventilated. Heart failure was induced by ligation of the left main coronary artery (4). The lungs were inflated, the ribs were then approximated, and the chest was closed. Sham animals were subjected to the same surgical procedure without coronary artery ligation

As reported under results, there was such a marked and significant surgical mortality in rats fed a high saturated fat diet prior to ligation surgery, the study design subsequently was modified such that all rats remained on the normal diet prior to ligation surgery. Following the induction of heart failure by coronary artery ligation, rats were randomly assigned to either a heart failure group fed a normal diet (HF, n=8) or a heart

failure group fed a high saturated fat diet (HF+FAT, n=7) for eight weeks. Sham operated animals (n=8) were fed a normal diet.

2.2.2 Echocardiography

LV function was evaluated by echocardiography before coronary artery ligation and eight weeks post coronary artery ligation using a Sequoia C256 System (Siemens Medical) with a 15 MHz linear array transducer (90). Briefly, rats were anesthetized with 1.5-2.0% isoflurane by mask, the chest was shaved, the animal was situated in the supine position on a warming pad, and ECG limb electrodes were placed. Two-dimensional (2D), 2D-guided M-mode, and Doppler echocardiographic studies of aortic and transmitral flows were performed via parasternal and foreshortened apical windows. All data were analyzed offline with software resident on the ultrasound system at the end of the study. LV wall motion was analyzed with a 13-segment model. The wall segments were visualized from two-dimensional images taken from the parasternal long axis and from the basal and midpapillary short axes. Regional wall motion was graded in each segment according to the scheme adopted by the American Society of Echocardiography. End-diastolic and end-systolic dimensions were measured using software resident on the ultrasonograph. Myocardial performance index (MPI) was defined as the sum of the isovolumic contraction and relaxation times divided by the ejection time. Cardiac output (CO) was estimated as follows

$$CO = VTI \times \pi \times (\text{aortic diameter}/2)^2 \times HR$$

where VTI is the velocity-time integral of aortic flow, HR is heart rate, and the aortic diameter was measured from the parasternal long-axis two-dimensional view. Cardiac

index (CI) was calculated by dividing CO by body weight. Percent fractional shortening (FS) was calculated according to the following equation

$$FS = [(LVDd - LVSd)/LVDd] \times 100\%$$

2.2.3 Hemodynamic Measurements

Eight weeks post coronary artery ligation, a terminal surgical procedure was performed to evaluate LV pressure and contractile properties. Rats were anesthetized (1.5-2.0% isoflurane), intubated, and ventilated. A microtip pressure transducer catheter (3.5 Fr, Millar Instruments) was introduced via the right carotid artery into the LV. Measurements of heart rate, maximum LV pressure, and peak LV maximum and minimum rate of change of pressure with time (+/- dP/dt) were recorded over a 30 s period using a Digi-Med® Heart Performance Analyzer-τ ™.

2.2.4 Preparation of Mitochondria

Following LV cannulation, blood samples were drawn from the inferior vena cava. LV, right ventricle (RV), and scar mass were obtained by gravimetric measurements. A myocardial tissue sample (approximately 100 mg) was harvested and immediately quick-frozen. The scar and the balance of the LV were placed in KME (100 mM KCl, 50 mM 3-[N-Morpholino]propanesulfonic acid (MOPS), internal salt, and 0.5 mM EGTA). Cardiac SSM and IFM were isolated using the procedure of Palmer *et al.* (99) except that a modified Chappell-Perry buffer (containing 100 mM KCl, 50 mM MOPS, 1 mM EGTA, 5 mM $MgSO_4 \cdot 7H_2O$, and 1 mM ATP, pH 7.4 at 4 °C) was used for isolation of both mitochondrial populations. The IFM were harvested following treatment

of skinned fibers with 5 mg/g ww trypsin for 10 minutes at 4 °C (89). Mitochondrial protein concentration was determined by the Lowry method using bovine serum albumin as a standard.

2.2.5 Mitochondrial Oxidative Phosphorylation

Oxygen consumption in SSM and IFM was measured using a Clark-type oxygen electrode at 30 °C (131). Mitochondria were incubated in a solution consisting of 80 mM KCl, 50 mM MOPS, 1 mM EGTA, 5 mM KH_2PO_4, and 1 mg/ml bovine serum albumin at pH 7.4. The rate of oxidative phosphorylation and uncoupled respiration was measured using several substrates. Glutamate assesses complexes I, III, and IV. Durohydroquinone (DHQ), an analog of coenzyme Q, assesses complexes III and IV. *N*,*N*,*N*',*N*'-tetramethyl-*p*-phenylenediamine (TMPD), an electron carrier that reduces complex IV, was used in conjunction with ascorbate to assess complex IV. Mitochondrial respiration also was measured using lipid substrates carnitine-dependent palmitoyl-CoA plus malate and palmitoylcarnitine plus malate (62). Palmitoyl-CoA is converted to palmitoylcarnitine in the mitochondrial inter-membrane space by CPT-I and can then be transported into the mitochondrial matrix via the carnitine-acylcarnitine transporter. Palmitoylcarnitine bypasses CPT-I and enters the matrix directly. These two substrates assess whether an effect on lipid metabolism is due to CPT-I activity or the oxidation of the fatty acid. State 3 (ADP-stimulated) respiration, state 4 (ADP-limited) respiration, respiratory control ratio (RCR) (state 3/state 4), and ADP/O ratio (ADP added per oxygen consumed) were determined (11; 25).

2.2.6 Mitochondrial Electron Transport Chain Complex Activity

Samples of SSM and IFM (10 mg cholate/ 1mg mitochondrial protein) were mixed in 1 ml buffer (75 mM mannitol, 220 mM sucrose, 2 mM EDTA, and 5 mM MOPS, (pH 7.4)) with mammalian protease inhibitor cocktail (1 µl/ 1 ml buffer) and were kept on ice. Assays were completed on the day of preparation.

All ETC complex activities were measured as specific donor-acceptor oxidoreductase activities using a diode array spectrophotometer (45; 66; 67). Donors and acceptors were chosen to span specific regions of the complete ETC. NADH Q reductase (complex I) was measured as the rotenone-sensitive reductase and assesses complex I. NADH ferricyanide reductase is a measure of the proximal portion of complex I. Ubiquinol-cytochrome c oxidoreductase was measured as the antimycin-sensitive decyubiquinol-cytochrome c oxidoreductase to assess complex III. NADH-cytochrome c oxidoreductase was measured as the rotenone-sensitive reductase, assessing complexes I and III. Succinate-cytochrome c oxidoreductase was measured as the antimycin-sensitive reductase to assess complexes II and III. Succinate dehydrogenase measures the proximal portion of complex II. Complex II activity was measured in the presence (complex II+coenzyme Q) and absence (complex II) of exogenous coenzyme Q. Cytochrome c oxidase assay measures complex IV activity and is expressed as the first order rate constant (143). Citrate synthase, a mitochondrial marker enzyme was measured spectrophotometrically in cholate-solubilized SSM or IFM by measuring the rate of 5,5'-dithiobis(nitrobenzoic acid)-reactive reduced coenzyme A (412 nm) at 37°C (121). Aconitase, a mitochondrial matrix enzyme used as a marker of oxidative stress, was measured as the rate of isomerization of citrate from the substrate isocitrate.

2.2.7 Detection of Hydrogen Peroxide Production

The rate of hydrogen peroxide (H_2O_2) production in mitochondria was determined using the oxidation of the fluorogenic indicator, amplex red, in the presence of horseradish peroxidase (88). The concentrations of horseradish peroxidase and amplex red in the incubation mixture were 0.1 unit/ml and 50 μM, respectively. Fluorescence was recorded in a microplate reader (1420 Victor2, PerkinElmer Life Sciences) with 530 nm excitation and 590 nm emission wavelengths. Standard curves obtained by adding known amounts of H_2O_2 to assay medium in the presence of the reactants (amplex red and horseradish peroxidase) were linear up to 2 μM. Background fluorescence was measured in the absence of mitochondria and data was presented as fluorescence minus background (pmol/mg of protein/30 min). Mitochondria were incubated at 0.1 mg of protein/ml at 30 °C. H_2O_2 production was initiated using succinate (5 mM). Rotenone (2.4 μM) was used to inhibit the reverse flow of electrons to complex I. Maximal radical production at complex III was induced by inhibition of the Qi (the inner binding site for coenzyme Q binding on the outer surface of Complex III) by antimycin A (10 μM). Stigmatellin (6.6 μM) was used to test whether blockade of complex III at the Qo (the outer binding site for coenzyme Q binding on the outer surface of Complex III) reduced H_2O_2 generation. Catalase (643 units/ml) was used to dissipate H_2O_2 in the incubation system.

2.2.8 Plasma and Tissue Metabolic Products

C16-ceramide content in the LV was measured by a capillary gas chromatographic procedure with a flame ionization detector using C17-ceramide as an

internal standard (132). LV homogenates or an aliqot of isolated SSM or IFM were mixed with 2.25 nmol C17-ceramide as the internal standard in 0.1 M phosphate buffer (pH 6.2). This mixture was then extracted with chloroform:methanol (3:1). After evaporating the separated organic layer to dryness, the residue was taken up by isooctane:ethyl acetate (10:1) and applied to a silica gel column (pasteur pipet, 4 cm height, preequilibrated with isooctane:ethyl acetate 10:1). Following extraction of cholesterol esters and triglycerides, diacylglyceride, and nonesterified fatty acids, the residue from the original tube was extracted further with methanol. This extract was applied to the same silica gel column followed by 3.4 ml of methanol. The fraction eluted from the column contained ceramides and phosphatidylethanolamines. Ceramides were extracted from this fraction with isooctane:ethyl acetate (3:1) and dried. The samples were analyzed by gas chromatography (Hewlett–Packard (HP) 5980). The separation was achieved with a short (5 m; 0.25mm ID; 0.25 lm coating) column of methylsilicone (ZB-1 Phenomenex, Torrance, CA). The temperature zones for the instrument were set at 290^{o}C for both injector and flame ionization detector. The initial oven temperature was at 200 ^{o}C and then increased at 20^{o}C /min to 280 ^{o}C. A splitless injection was used. The data analysis was performed with HP ChemStation software.

Tissue triglyceride content was measured in homogenate extracts using an enzymatic spectrophotometer method (Wako Chemicals, USA, Richmond, VA). Plasma free fatty acids and triglycerides were measured using a commercially available enzymatic spectrophotometric kit (100). Plasma concentration of insulin and leptin were assayed by ELISA immunoassay (ALPCO Diagnostics, Salem, NH).

2.2.9 Electron Microscopy

Electron microscopic analysis was performed as described in Lesnefsky *et al.* (75). An aliquot of each SSM or IFM was added to an equal volume of phosphate-buffered, full-strength Karnovsky's fixative, mixed, and immediately spun down for 30 seconds in a microcentrifuge. The fixation continued in half-strength Karnovsky's fixative for a total of 2 hours at room temperature. The SSM or IFM pellets were thoroughly rinsed in distilled water, then post-fixed for 2 hours in an unbuffered 1:1 mixture of 2% osmium tetroxide and 3% potassium ferricyanide. After rinsing with distilled water, the specimens were soaked overnight in an acidified solution of 0.25% uranyl acetate. After another rinse in distilled water, they were dehydrated in ascending concentrations of ethanol, passed through propylene oxide, and embedded in a Poly/Bed 812 embedding media (Polysciences, Warrington, PA). Thin sections (70nm) were cut on a RMC MT6000-XL ultramicrotome. These were mounted on Gilder square 300 mesh nickel grids (Electron Microscopy Sciences, PA) then sequentially stained with acidified methanolic uranyl acetate and stable lead staining solution (41). These were coated on a Denton DV-401 carbon coater (Denton Vacuum LLC, NJ), and examined in a Zeiss CEM 902 electron microscope (Oberkochen, Germany). Electron micrographs were assessed in an investigator-blinded fashion.

2.2.10 Statistical Analysis

Differences among SHAM, HF, and HF+FAT were determined using a one-way analysis of variance (ANOVA) followed by Bonferroni t-tests for multiple comparisons.

Data are expressed as group means ± SEM. For all statistical analysis, significance was accepted at $p<0.05$.

2.3 Results

2.3.1 Coronary Artery Ligation Mortality Rates

Surgical mortality for the SHAM animals was 0% (0/8). Administration of high saturated fat diet for 2 weeks prior to coronary artery ligation resulted in an increased surgical mortality rate in saturated fat fed (30/45, 67%) (Figure 2-1) compared to normal chow fed rats (9/24, 38%) (P=0.0007 by Chi-square Analysis). Given the significantly higher mortality rate in the animals fed saturated fat diet prior to coronary artery ligation compared to those fed normal diet, the group fed a high saturated fat diet prior to coronary artery ligation was subsequently removed from the study due to a potential "survivor bias" in this group of animals.

2.3.2 Body and Heart Mass

High saturated fat feeding initiated immediately following coronary artery ligation increased body mass compared to SHAM and HF (Table 2-1). Total LV mass (LV mass + scar tissue mass) was increased in HF+FAT compared to SHAM; however, when normalized to body weight (Total LV Mass/Body Mass), there were no differences between groups. Mean scar tissue mass did not differ between the two ligated groups (HF and HF+FAT).

2.3.3 Cardiac Function and Left Ventricular Remodeling

LV function prior to coronary artery ligation did not differ between groups. Coronary artery ligation-induced heart failure resulted in impaired LV contractile function eight weeks post ligation as assessed by decreased peak LV +/- dP/dt

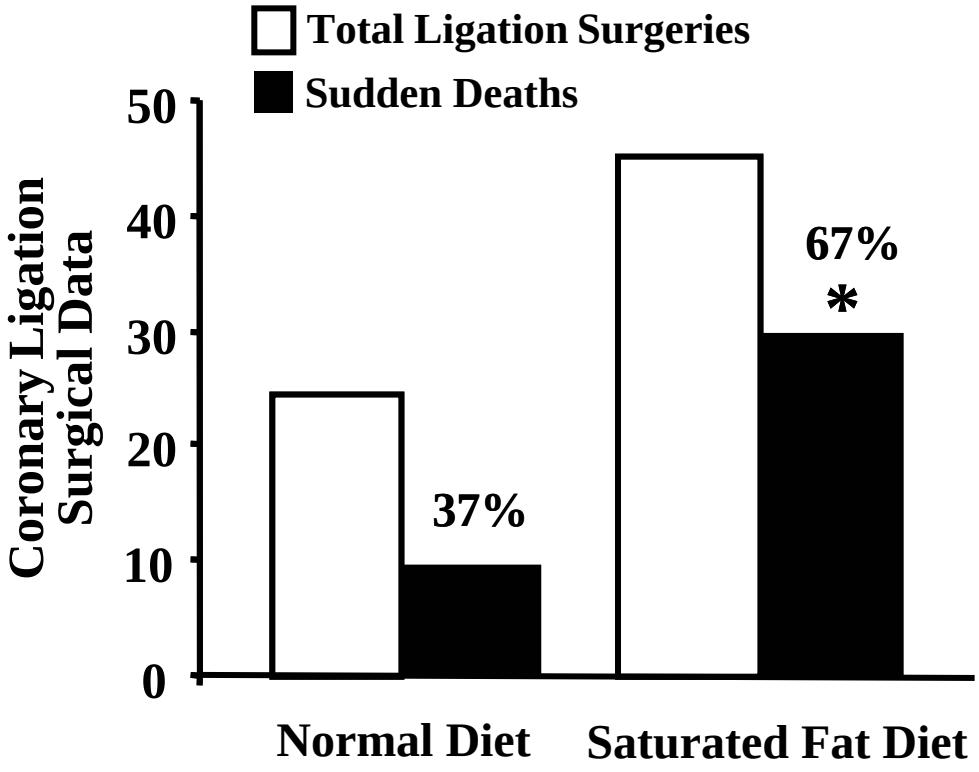

Figure 2-1. Coronary artery ligation surgeries and the accompanying mortality due to sudden death in rats fed high saturated fat or normal diet prior to the ligation surgery. SHAM, n=8; HF, n=8; HF+FAT, n=7. * P=0.0007 by Chi-square Analysis

Table 2-1. Body and heart mass in SHAM, HF, and HF+FAT eight weeks following coronary artery ligation surgery.

	SHAM	HF	HF+FAT
Body Mass (g)	458 ± 9	466 ± 11	540 ± 15 *†
Total LV Mass (mg)	929 ± 32	956 ± 41	1067 ± 41 *
Total LV Mass/Body Mass (mg/g)	2.03 ± 0.06	2.05 ± 0.06	1.98 ± 0.07
Scar (mg)		104 ± 16	133 ± 44

SHAM, n=8; HF, n=8; HF+FAT, n=7. Values are expressed as mean ± SEM. * $p<0.05$ vs SHAM; † $p<0.05$ vs HF

and increased MPI in HF compared to SHAM, but not in the HF+FAT group (Figure 2-2). Percent fractional shortening was decreased in HF and HF+FAT compared to SHAM. LV remodeling also was evident from increased end-diastolic and end-systolic dimensions in HF compared to SHAM (Figure 2-2). Peak LV systolic pressure (SHAM 115±6; HF 101±7; HF+FAT 108±6 mmHg) and heart rate (SHAM 339±17; HF 300±16; HF+FAT 319±10 beats·min^{-1}) were unchanged following coronary artery ligation. High saturated fat feeding immediately post coronary artery ligation (HF+FAT) caused no further decrease in LV contractile function or progression of LV remodeling compared to HF.

2.3.4 Metabolic Substrates

Plasma free fatty acids were not altered by heart failure or high fat feeding (Table 2-2). Plasma triglycerides (Table 2-2) and myocardial tissue triglycerides (Figure 2-3) were increased in HF+FAT compared to SHAM and HF. Similarly, myocardial tissue C16-ceramide content was elevated in HF+FAT compared to SHAM and HF (Figure 2-3). C16-ceramide content also was measured in the SSM and IFM; however, in 33% of SSM samples and 84% of IFM samples, the ceramide content was below the level of detection by gas chromatography. Plasma leptin was elevated in HF+FAT compared to SHAM and HF (Table 2-2). Insulin levels in the plasma were not different (Table 2-2).

2.3.5 Electron Microscopy

Neither heart failure, nor high saturated fat feeding had an effect on the morphology of the SSM or IFM, as noted by electron microscopy (Figure 2-4).

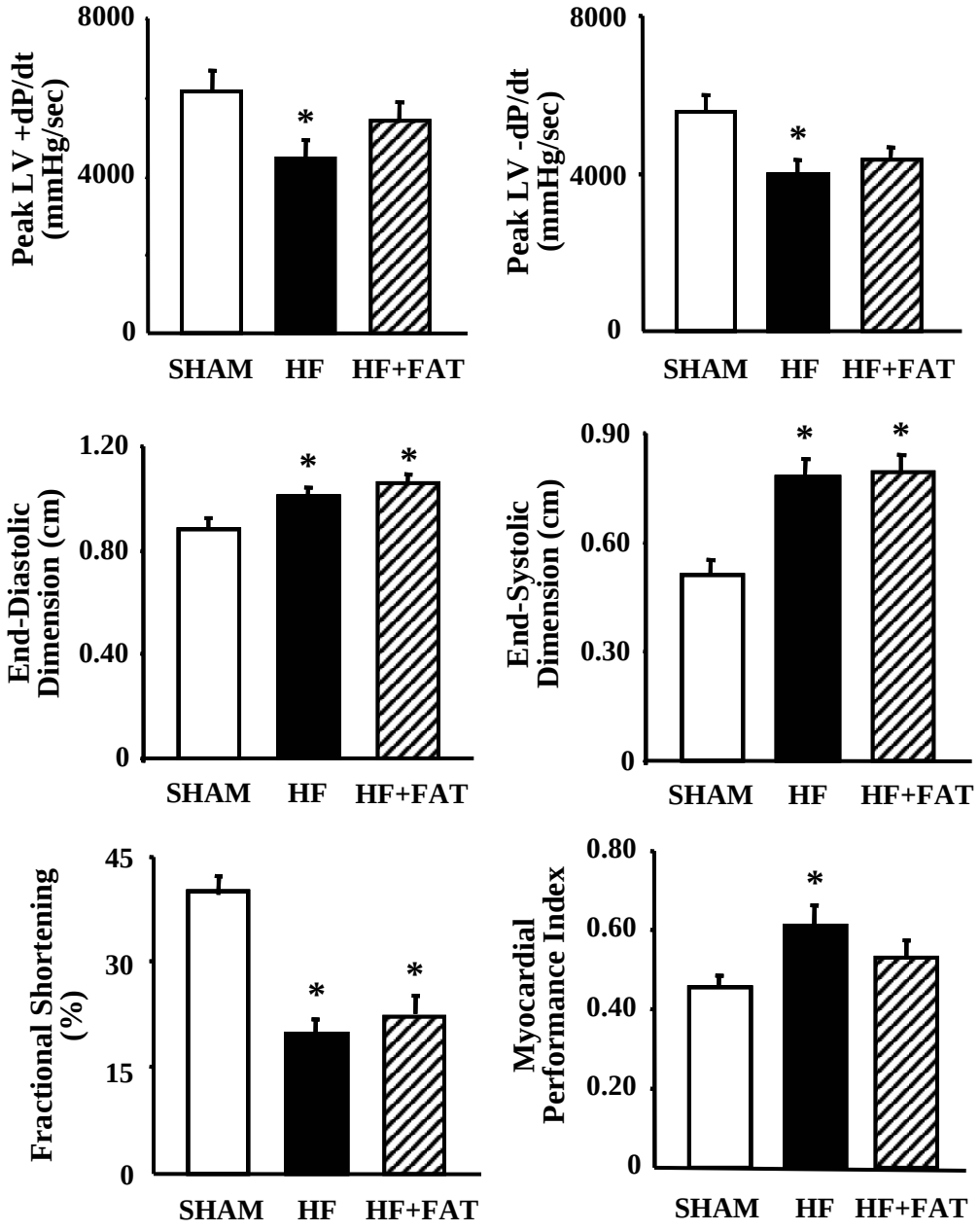

Figure 2-2. Left ventricular hemodynamics and echocardiographic measurements in SHAM (n=8), HF (n=8), and HF+FAT (n=7). Peak LV +/- dP/dt measurements were obtained from a Millar pressure transducer. Echocardiographic measurements including end-diastolic and end-systolic dimensions, percent fractional shortening, and myocardial performance index were obtained from parasternal long- and short-axis views. Values are mean ± SEM. ***** $p<0.05$ compared to SHAM.

Table 2-2. Plasma free fatty acids, triglycerides, leptin, and insulin in SHAM, HF, and HF+FAT eight weeks following coronary artery ligation surgery.

	SHAM	HF	HF+FAT
Free Fatty Acids (µmol/mL)	0.39 ± 0.09	0.32 ± 0.04	0.55 ± 0.12
Triglycerides (mg/mL)	0.15 ± 0.03	0.18 ± 0.05	0.37 ± 0.08 *†
Leptin (pg/mL)	518 ± 140	656 ± 183	1527 ± 243 *†
Insulin (pmol/mL)	94.1 ± 24.7	139 ± 56	200 ± 55

SHAM, n=8; HF, n=8; HF+FAT, n=7. Values are expressed as mean ± SEM. * $p<0.05$ vs SHAM; † $p<0.05$ vs HF

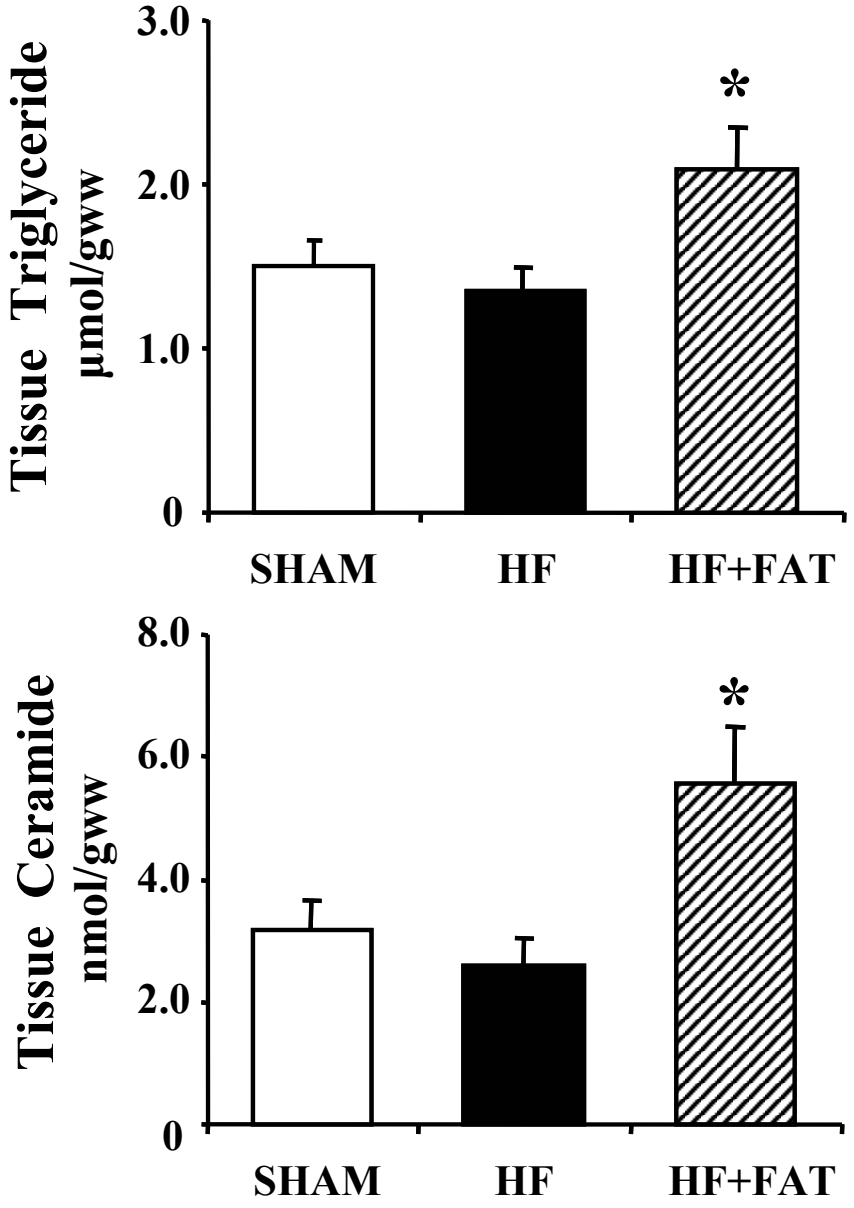

Figure 2-3. Myocardial tissue triglyceride and tissue C16-ceramide content in SHAM (n=8), HF (n=8), and HF+FAT (n=7). Values are mean ± SEM. *$p<0.05$ compared to SHAM and HF.

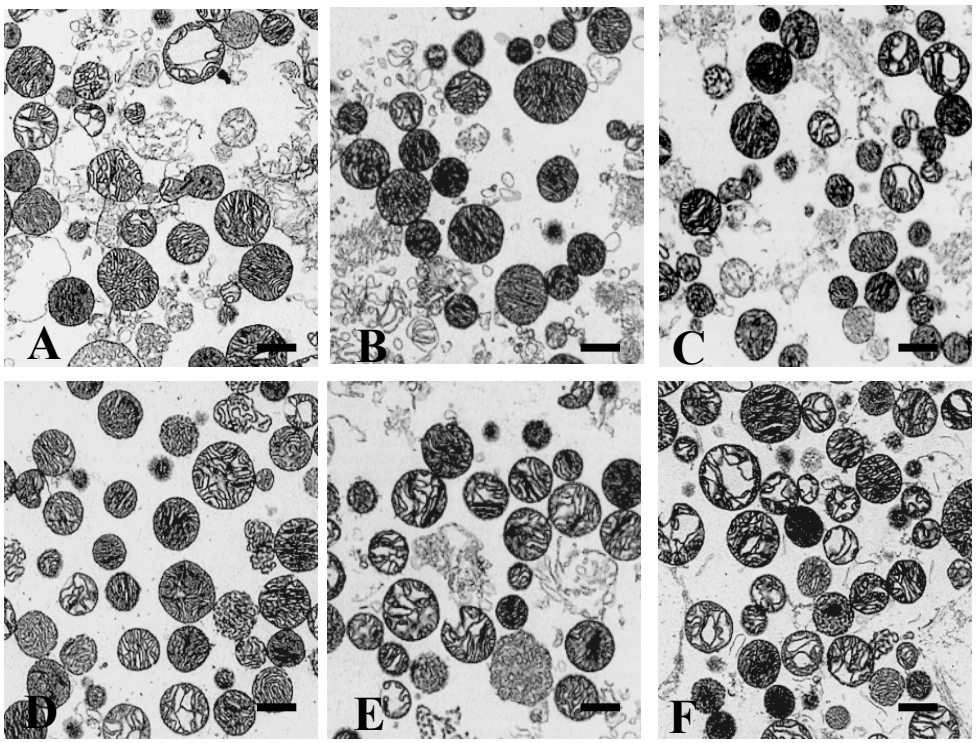

Figure 2-4. Electron micrographs of SSM and IFM. SSM in (A) SHAM, (B) HF, (C) HF+FAT. IFM in (D) SHAM, (E) HF, (F) HF+FAT. SHAM, n=3; HF, n=3; HF+FAT, n=3. Bars = 1 μm.

2.3.6 Oxidative Phosphorylation

Protein yield in the SSM and IFM was not altered by heart failure or high saturated fat feeding (Table 2-3). Mitochondrial recovery during the isolation protocol also did not differ between groups. State 3 respiration was not altered by heart failure using glutamate, DHQ, or TMPD-ascorbate as respiratory substrates. However, using glutamate and DHQ it was elevated in both mitochondrial populations of HF+FAT (Table 2-3).

State 4 respiration was not altered by heart failure (Table 2-3). It was not different using glutamate, but using DHQ it was elevated in both populations of HF+FAT. RCR was not altered by heart failure or high fat feeding in the SSM (SHAM, glutamate 5.26±0.42, DHQ 3.81±0.64) or IFM (SHAM, glutamate 7.8±1.5, DHQ 3.99±0.37). ADP/O also did not differ with heart failure or high fat feeding in the SSM (SHAM, glutamate 2.35±0.09, DHQ 1.47±0.11) or IFM (SHAM, glutamate 2.44±0.07, DHQ 1.54±0.13).

Mitochondrial respiration was measured using lipid substrates carnitine-dependent palmitoyl-CoA+malate and palmitoylcarnitine+malate in order to assess their ability to oxidize fatty acids. State 3 respiration was not altered by heart failure using either lipid substrate (Table 2-3). However, it was elevated in the SSM and IFM of HF+FAT using both lipid substrates.

Heart failure did not alter state 4 respiration using either lipid substrate (Table 2-3). It was elevated in the SSM of HF+FAT using carnitine dependent palmitoyl-CoA+malate and in both populations of HF+FAT using palmitoylcarnitine+malate. RCR was not altered by heart failure or high fat feeding in the SSM (SHAM, palmitoyl-

Table 2-3. Protein yield and mitochondrial oxidative phosphorylation rates in subsarcolemmal (SSM) and interfibrillar (IFM) mitochondria of SHAM, HF and HF+FAT eight weeks post coronary artery ligation surgery.

	SSM			IFM		
	SHAM	**HF**	**HF+FAT**	**SHAM**	**HF**	**HF+FAT**
Protein Yield (mg·g ww^{-1})	8.7 ± 1.1	10.1 ± 1.3	7.3 ± 0.6	8.56 ± 0.60	7.50 ± 0.89	6.36 ± 0.58
State 3 Respiration						
Glutamate	187 ± 13	155 ± 11	206 ± 11 †	253 ± 27	231 ± 14	307 ± 11 †
DHQ	407 ± 39	368 ± 47	609 ± 47 *†	575 ± 92	543 ± 37	793 ± 48 †
TMPD-Ascorbate	844 ± 85	747 ± 64	984 ± 73	1058 ± 127	1007 ± 68	1241 ± 62
Palmitoyl-CoA+Carnitine	141 ± 10	126 ± 10	191 ± 16 *†	193 ± 29	193 ± 7	301 ± 21 *†
Palmitoylcarnitine	173 ± 11	142 ± 11	229 ± 25 †	257 ± 45	219 ± 11	354 ± 17 *†
State 4 Respiration						
Glutamate	36.8 ± 3.0	33.7 ± 4.0	44.6 ± 3.5	37.5 ± 5.2	36.6 ± 3.5	50.2 ± 5.1
DHQ	125 ± 18	104 ± 25	194 ± 21 †	148 ± 25	133 ± 22	212 ± 14 †
Palmitoyl-CoA+Carnitine	44.6 ± 5.6	35.4 ± 3.3	53.1 ± 4.5 †	46.4 ± 3.4	47.6 ± 2.7	58.7 ± 6.4
Palmitoylcarnitine	54.3 ± 5.9 †	40.0 ± 1.9	64.0 ± 4.9 †	67.6 ± 8.1	55.9 ± 3.7	87.9 ± 2.7 *†

SHAM, n=8; HF, n=8; HF+FAT, n=7. Respiratory rates are expressed as nAO·min^{-1}·mg^{-1}. Values are expressed as mean ± SEM . *p<0.05 vs SHAM; † p<0.05 vs HF

CoA+malate 3.26±0.27, palmitoylcarnitine+malate 3.26±0.29) or IFM (SHAM, palmitoyl-CoA+malate 4.13±0.45, palmitoylcarnitine+malate 3.83±0.44). ADP/O also did not differ with heart failure or high fat feeding in the SSM (SHAM, palmitoyl-CoA+malate 2.37±0.16, palmitoylcarnitine+malate 2.24±0.20) or IFM (SHAM, palmitoyl-CoA+malate 2.54±0.13, palmitoylcarnitine+malate 2.31±0.12).

2.3.7 Mitochondrial Electron Transport Chain and Enzyme Activity

Complex III activity was not inhibited in either HF or HF+FAT compared to SHAM (Table 2-4). Activities of complex II in the SSM and complex IV in the SSM and IFM were elevated in HF+FAT compared to SHAM and HF. Complex I+III, complex I, NADH-dehydrogenase, complex II+III, complex II+Q, and succinate dehydrogenase activities in the SSM and IFM were unchanged in both HF and HF+FAT compared to SHAM.

Citrate synthase activity was elevated in the SSM of HF+FAT compared to HF (Table 2-4). The increased activity was not accompanied by greater increases in state 3 respiration (relative to the IFM), but may simply reflect differential responses of the SSM and IFM in diseased states, as previously reported (74). Aconitase was elevated in HF+FAT compared to SHAM and HF in the SSM, and in HF+FAT compared to HF in the IFM (Table 2-4). A loss or decrease in mitochondrial aconitase activity is an intracellular indicator of oxidative damage. Thus, the increased aconitase activity in our SSM and IFM indicates an increased anti-oxidant capacity which is consistent with the lack of increase in H_2O_2 production (see below).

Table 2-4. Electron transport chain complex activities in subsarcolemmal (SSM) and interfibrillar (IFM) mitochondria of SHAM, HF, and HF+FAT eight weeks post coronary artery ligation surgery.

	SSM			IFM		
	SHAM	**HF**	**HF+FAT**	**SHAM**	**HF**	**HF+FAT**
Complexes I and III	2897 ± 308	2474 ± 403	2439 ± 125	2910 ± 415	2936 ± 456	2176 ± 281
Complex I	330 ± 44	327 ± 31	319 ± 15	321 ± 37	337 ± 49	325 ± 16
NADH-Dehydrogenase	2725 ± 202	2428 ± 165	2622 ± 221	2975 ± 2673	2673 ± 188	2553 ± 132
Complex III	4083 ± 664	3471 ± 612	5171 ± 964	5035 ± 693	4324 ± 737	4678 ± 394
Complexes II and III	295 ± 24	225 ±39	322 ± 59	360 ± 20	315 ± 49	408 ± 67
Complex II	31.5 ± 9.2	31.5 ± 5.8	57.2 ± 8.5*†	51.8 ± 6.8	44.8 ± 7.5	64.7 ± 11.4
Complex II + Q	56.7 ± 7.2	61.6 ± 6.9	81.5 ± 9.9	83.0 ± 7.0	84.9 ± 8.2	95.9 ± 14.7
Succinate Dehydrogenase	212 ± 23	191 ± 21	258 ± 28	261 ± 31	248 ± 25	315 ± 50
Complex IV ($x10^4$)	63.1 ± 5.7	54.0 ±5.6	81.5 ± 4.5*†	70.9 ± 6.2	69.8 ± 7.6	90.3 ± 10.3‡
Citrate Synthase	2102 ± 155	2048 ± 132	2644 ± 194†	2725 ± 189	2865 ± 225	3019 ± 162
Aconitase	740 ± 79	628 ± 45	1018 ± 75*†	896 ± 105	844 ± 55	1181 ± 52†

Electron transport chain complex and enzyme activities are expressed as nmoles·min^{-1}·mg^{-1} mitochondrial protein with the exception of complex IV which is expressed as the first order rate constant (k:1 x min^{-1} x mg $protein^{-1}$). SHAM, n=8; HF, n=8; HF+FAT, n=7. Values are expressed as mean ± SEM. *p<0.05 vs SHAM; † p<0.05 vs HF; ‡ p=0.058 vs SHAM and HF.

2.3.8 Hydrogen Peroxide Production

H_2O_2 production using succinate as a substrate in the presence of rotenone did not change in the SSM (673±98, 677±118, 817±76 pmol·mg^{-1}·30 min^{-1}) or IFM (658±102, 719±190, 735±55 pmol·mg^{-1}·30 min^{-1}) of SHAM, HF, and HF+FAT respectively. Maximal H_2O_2 production in the presence of antimycin A was unaltered by heart failure or high fat feeding. Inhibition of maximal H_2O_2 production by stigmatellin was similar in all groups.

2.4 Discussion

The principal finding of this study is that administration of a high saturated fat diet in a model of coronary artery ligation-induced heart failure increased mitochondrial oxidative phosphorylation and ETC complex activities. Additionally, administration of a high saturated fat diet did not adversely affect LV contractile function or the progression of LV remodeling. Despite elevations in myocardial ceramide, there was no evidence of a lipotoxic effect on either contractile or mitochondrial function.

Numerous studies have shown that elevations in myocardial triglycerides and/or ceramide content are associated with cardiac contractile dysfunction and remodeling, and that this loss of contractile function can be prevented and/or reversed by the reduction of these toxic lipid intermediates (15; 16; 144; 148). In this study, we hypothesized that the progression of heart failure would be exacerbated by elevated myocardial lipids and an associated ceramide-induced inhibition of mitochondrial respiration and ETC complex activities. Coronary artery ligation resulted in a predictable increase in LV contractile dysfunction and remodeling that is considered to be characteristic of mild to moderate heart failure. However, high saturated fat feeding elevated myocardial ceramide and triglycerides without any further progression of heart failure or evidence of a lipotoxic effect. In point of fact, contractile function (peak +/- dP/dt and MPI see Figure 2-2) in the HF+FAT group was not significantly decreased relative to the SHAM group. These results are consistent with recently published data from our laboratory in a model of hypertension induced cardiomyopathy, where administration of a high saturated fat diet reduced LV hypertrophy, improved contractile function, and prevented LV dilation despite elevated plasma fatty acids and myocardial triglycerides (94). Furthermore,

Listenberger *et al.* (2003) has suggested that in response to an acute lipid overload, the ability to synthesize cardiac triglycerides could play a critical role in protection from "lipotoxicity" by diverting excess fatty acids from more cytotoxic pathways (80). The absence of a lipotoxic effect of ceramide has been demonstrated by Relling *et al.* (104), where acute ceramide exposure to ventricular myocytes directly enhanced peak cardiomyocyte shortening. However, longer durations of exposure caused a reversal of the positive peak shortening response to ceramide. Therefore, despite previous suggestions of a direct link between "lipotoxic" intermediates and LV contractile dysfunction, our results clearly demonstrate that high saturated fat feeding following coronary artery ligation is associated with accumulation of myocardial triglycerides and ceramide, but does not exacerbate LV dysfunction and dilatation.

Coronary artery ligation-induced heart failure in this study was not associated with decreased oxidative phosphorylation or ETC complex activities in the SSM or IFM. Abnormalities in mitochondrial oxidative phosphorylation have been reported to occur in the rat model of coronary artery ligation-induced heart failure (56; 109), the cardiomyopathic Syrian hamster model (46), the canine microembolization-induced heart failure model (116) and in the myocardium of failed explanted human hearts due to ischemic or idiopathic dilated cardiomyopathy (117). There also is evidence of ETC abnormalities. For example, abnormalities in mitochondrial morphology (77; 107) and in complexes I, III, IV and V of the ETC have been reported to occur in animal models of heart failure (52; 85) and human patients with heart failure (9; 55). However, defects in mitochondrial function may be dependent upon the method by which heart failure is induced. For example, the microembolization model of heart failure results in global

ischemia in the heart, whereas the coronary artery ligation model of heart failure used in this study results in scar tissue formation that develops in the infarcted area of the LV. Although the scar was included with the LV in the mitochondrial preparation, it can be assumed that the scar is fibrous tissue and contains no viable mitochondria. Therefore, the isolated mitochondria are from viable LV tissue and should be functioning. Defects in mitochondrial function also may depend on the severity of LV dysfunction. Javadov *et al.* (56) demonstrated significant reductions in mitochondrial respiration 12 and 18 weeks following ligation surgery, but reported no alterations in mitochondrial function six weeks following the induction of heart failure. Our study examines mitochondrial function eight weeks post ligation surgery and therefore reflects early stages of heart failure. Mitochondrial dysfunction may be evident only when the progression of LV dysfunction and remodeling results in a more severe or decompensated stage of heart failure rather than the more mild to moderate dysfunction evident in our study.

We hypothesized that high saturated fat feeding in a model of coronary artery ligation-induced heart failure would decrease mitochondrial respiration and inhibit ETC complex III. Our results have shown that high saturated fat feeding in this model of heart failure resulted in no impairments in mitochondrial oxidative phosphorylation or ETC complex activities. Instead state 3 respiration (using glutatmate, DHQ, palmitoylcarnitine+malate, and carnitine dependent palmitoyl-CoA+malate as respiratory substrates) and activities of ETC complexes II and IV were elevated with high saturated fat feeding. One possible explanation for these observations may be a fatty acid-induced activation of PPARα (a nuclear transcription factor that activates the expression of genes encoding enzymes involved in fatty acid uptake and metabolism) and its co-activator

PGC-1α (51; 71; 123). PPARα and PGC-1α have been reported to be down-regulated in hypertrophied and failing hearts and have been shown to stimulate cardiac gene expression of the fatty acid metabolic pathways and regulate oxidative phosphorylation and mitochondrial biogenesis (34; 51; 71). Administration of a high fat diet provides ligand for the activation of PPARα and PGC-1α and subsequently increases the expression of the fatty acid metabolic enzymes (including CPT-I, MCAD, UCP3, and mitochondrial thioesterase 1) (51; 124). An increase in the expression of these fatty acid metabolic enzymes could account for an increased ability of the mitochondria to utilize fatty acids and consequently, for the increased state 3 respiration rates seen with lipid substrates. This proposed mechanism contrasts with other studies that reported impaired contractile function in PPARα overexpressing mice (27) and in rats fed a PPARα agonist (145). However, we believe that in the presence of elevated lipids (as occurs with high fat feeding), an induction of the PPARα regulated genes would prevent an imbalance between substrate supply and substrate utilization and as a result, prevent further deterioration in contractile function. Additionally, PGC-1α increases mitochondrial number, up-regulates the expression of mitochondrial enzymes, and increases rates of fatty acid oxidation and coupled respiration (51) which also might account for the increased respiration and ETC complex activities reported in this study. Therefore, it will be important in future studies to elucidate the potential role of PPARα and PGC-1α in the enhanced mitochondrial function observed in heart failure animals fed a high fat diet.

Another potential explanation for the absence of lipotoxicity in this investigation is the anti-lipolytic action of leptin. It has been suggested that the primary physiological role of leptin is to prevent fatty acid accumulation in non-adipose tissues such as skeletal

muscle, liver, pancreas, and heart (135). In mice with severe lipotoxic cardiomyopathy, induced transgenically by cardiomyocyte-specific over-expression of the acyl-CoA synthase, elevations in plasma leptin levels completely prevented the dilated cardiomyopathy, elevations in myocardial triglyceride stores and cardiomyocyte hypertrophy (69). Similarly, during dietary induced obesity, hyperleptinemia protected nonadipocytes from steatosis and lipotoxicity (70). It is important to note however, that the plasma leptin levels reported in these studies far exceed the levels reported in our HF+FAT group. Thus, the absence of lipotoxicity in HF+FAT may be partially accounted for by elevations in plasma leptin that may be acting in a cardioprotective manner.

To our knowledge, this is the first study to assess the relationship between myocardial tissue ceramide and integrated function in isolated mitochondria in an *in vivo* model of heart failure. Elevations in myocardial ceramide were not associated with inhibition of mitochondrial respiration and ETC complex activities or the production of H_2O_2 in isolated mitochondria of HF+FAT. Although ceramide also is known to act as an intracellular signal to trigger apoptosis (43) and in the peroxidation of membrane lipids (33), these effects were not assessed in the current study. One potential explanation that could account for the lack of a "lipotoxic" effect of ceramide on mitochondrial function is that the magnitude of increase in whole tissue ceramide reported in this study was insufficient to inhibit mitochondrial function. C2-ceramide (a membrane permeable form) has been shown to reduce the activity of respiratory chain complex III in isolated mitochondria with a half maximum effect at 5–7 μM (38). How whole tissue ceramide content reported here compares to that of a cell-permeable ceramide in isolated mitochondria is unknown. However, the biochemical and

biophysical action of an exogenous ceramide may not mimic the behavior of endogenous ceramide. Exogenous C2-ceramide is ampiphilic and can translocate from the plasma membrane to other cellular membranes, while endogenous ceramide remains tightly bound to the membrane where it is produced.

The absence of a lipotoxic effect of ceramide could also be explained by its origin. Inhibition of complex III by ceramide could be initiated at either the plasma membrane or the mitochondrial membrane. We have shown that elevated myocardial tissue ceramide (which would reflect ceramide located on the plasma membrane as well as the mitochondrial membranes) did not correspond to alterations in mitochondrial oxidative phosphorylation or ETC activities. However, the ceramide on the plasma membrane is lost during the isolation of mitochondria. Although the mitochondrial pool of ceramide was measured in both the SSM and IFM, the ceramide content was below the level of detection by gas chromatography. Therefore, it is unlikely that the mitochondrial pool of ceramide was sufficient to result in inhibition of complex III (12; 140). It is important to acknowledge though that the absence of a significant lipotoxic effect of ceramide on mitochondrial function eight weeks following the induction of heart failure may simply reflect the impact of elevations in myocardial ceramide during the early stages of disease progression. It remains to be established what effect continued high fat feeding and increases in ceramide might have at later stages in the progression of heart failure.

The composition of the fatty acid may also play a role in mitochondrial function due to the differential effects of saturated vs unsaturated fats. Previous studies performed *in vitro* have clearly shown that long-chain saturated fatty acids are involved in lipotoxic

pathways leading to cardiomyopathy, whereas mono- and polyunsaturated fatty acids are not (80; 120). In these studies, the long-chain saturated fatty acid has been shown to induce apoptosis, cyctochrome c release, caspase activation, and DNA laddering, all markers of cell death. However, saturated fatty acids also stimulate mitochondrial oxidation in rats, whereas monounsaturated fatty acids had no effect (39). Unsaturated fatty acids are also associated with greater lipoperoxidation (24), mitochondrial uncoupling, and reactive oxygen species production (20) compared to saturated fatty acids. Thus, further studies are required to elucidate the mechanisms responsible for these differential effects of saturated and unsaturated fatty acids, particularly in respect to their effect on mitochondrial respiration and ETC complex activities.

In summary, despite previous suggestions of a direct link between "lipotoxic" intermediates and LV contractile dysfunction, our results clearly show that high saturated fat feeding following coronary artery ligation did not exacerbate LV dysfunction and remodeling, at the time point examined. Furthermore, administration of a high saturated fat diet in a model of ligation-induced heart failure increased mitochondrial oxidative phosphorylation and ETC complex activities. The absence of a lipotoxic effect coincident with elevations in myocardial ceramide was an unexpected outcome of this study that warrants further investigation. Future studies should also examine whether the effects of high saturated fat feeding on myocardial contractile and mitochondrial function are observed under control conditions and not unique to injury models such as ligation-induced heart failure.

Chapter 3

Enhanced Acyl-CoA Dehydrogenase Activity is Associated with Improved Mitochondrial and Contractile Function in Heart Failure

Julie H. Rennison[1], Tracy A. McElfresh[1], Isidore C. Okere[1], Hiral V. Patel[2], Amy B. Foster[2], Kalpana K. Patel[2], Maria S. Stoll[2], Paul E. Minkler[2], Hisashi Fujioka[2], Brian D. Hoit[3,4], Martin E. Young[5], Charles L. Hoppel[2,3], and Margaret P. Chandler[1]

From: [1]Departments of Physiology and Biophysics, [2]Pharmacology, and [3]Medicine, Case Western Reserve University, Cleveland, OH, [4]University Hospitals Case Medical Center, Cleveland, OH and [5]Baylor College of Medicine, Houston, TX.

Cardiovasc Res. 2008

Running title: High Fat Enhances Acyl-CoA Dehydrogenase Activity in Heart Failure

3.1 Introduction

A variety of pathophysiological conditions including obesity, insulin resistance, diabetes and heart failure have been shown to be associated with excess lipid accumulation in non-adipose tissue because of enhanced circulating fatty acids (111; 148). In particular, enhanced myocardial lipid accumulation appears to be associated with impaired myocardial contractile function and could exacerbate the progression of heart failure. However, the effect of enhanced lipid accumulation on mitochondrial and contractile function under pathophysiological conditions such as heart failure had not been systemically evaluated until recently. We reported that high saturated fat feeding in a Wistar rat model of coronary artery ligation-induced heart failure resulted in no impairments in mitochondrial oxidative phosphorylation, ETC complex activities, or myocardial contractile function (105). Instead, state 3 respiration and ETC activities were elevated. These results are in agreement with another recently published study from our laboratory in a Dahl Salt-Sensitive rat model of hypertension induced cardiomyopathy, where administration of a high saturated fat diet reduced LV hypertrophy, improved contractile function, and prevented LV dilation despite elevated plasma fatty acids and myocardial triglycerides (92).

One possible explanation for these observations may be a fatty acid-induced activation of PPARs, which are known to regulate the expression of genes involved in key energy producing metabolic pathways. Although the three primary PPAR isoforms, PPARα, β/δ, and γ are all known to be activated by fatty acids, PPARα is thought to be a major transcriptional regulator of fatty acid metabolism in the heart (50). PPARα activates the expression of genes encoding enzymes involved in fatty acid uptake and

metabolism (including *cpt-I*, *scad*, *mcad*, *lcad*, *ucp3*, *pdk4*, and *cte1*) (50; 124). PPARα, its co-activator PGC-1α (a regulator of mitochondrial biogenesis (50; 71; 123)), and enzymes involved in fatty acid oxidation have been reported to be down-regulated in hypertrophied and failing hearts (34; 50; 71). Administration of a high fat diet, however, may provide the ligand for the activation of PPARα and PGC-1α, and subsequently increase the expression of the fatty acid metabolic enzymes, thereby enabling increased uptake, utilization, and storage of excess lipids that might, under other circumstances, be cytotoxic to the myocardium.

The aim of the present study was to investigate possible mechanisms by which high fat feeding improved mitochondrial function and prevented the decline in contractile function in heart failure. We hypothesized that a high fat diet during heart failure would result in improved mitochondrial fatty acid oxidation and increased state 3 respiration by activating genes involved in fatty acid uptake and utilization. We tested our hypothesis in rats fed a high saturated fat diet following coronary artery ligation surgery to induce heart failure.

3.2 Methods

3.2.1 Study Design and Induction of Myocardial Infarction

The investigation conforms with *Guide for the Care and Use of Laboratory Animals* published by the US National Institutes of Health (NIH Publication No. 85-23, revised 1996) and the Institutional Animal Care and Use Committee at Case Western Reserve University. Animals were maintained on a reverse 12h:12h light:dark cycle, and all procedures/tissue harvests were performed 2-4 hours into the dark cycle.

Heart failure was induced by ligation of the left main coronary artery as described in Chapter 2 (90; 105). Following ligation or sham surgery, rats were randomly assigned to either normal chow (SHAM n=10, HF n=9) (Caloric content; 14% fat, 26% protein, 60% carbohydrate) or a high saturated fat chow (SHAM+FAT n=10, HF+FAT n=10), [Caloric content; 60% fat (25% palmitic, 33% stearic and 33% oleic acid), 20% protein, 20% complex carbohydrates] (Research Diets, Inc.) for eight weeks.

3.2.2 Echocardiography

Myocardial function was evaluated by echocardiography eight weeks post ligation using a Sequoia C256 System (Siemens Medical) with a 15 MHz linear array transducer as described in Chapter 2 (90). All data were analyzed in an investigator-blinded fashion.

3.2.3 Hemodynamic Measurements

LV pressure and contractile properties were assessed 8wks following ligation surgery. Rats were anesthetized (1.5-2.0% isoflurane), intubated, and ventilated. A microtip pressure transducer catheter (3.5 Fr, Millar Instruments) was introduced via the

right carotid artery. Measurements of HR, peak LV pressure, end diastolic pressure, and +/- dP/dt were recorded over a 30s period using a Digi-Med® Heart Performance Analyzer-τ ™.

3.2.4 Preparation of Mitochondria

Following LV cannulation, blood samples were drawn from the inferior vena cava. RV, LV, and scar mass were obtained by gravimetric measurements. A myocardial tissue sample was harvested and quick-frozen. The scar and balance of the LV were placed in KME (100mM KCl, 50mM MOPS, internal salt, and 0.5mM EGTA, pH 7.4). Cardiac SSM and IFM were isolated according to Palmer *et al.* (99) except that a modified Chappell-Perry buffer (containing 100mM KCl, 50mM MOPS, 1mM EGTA, 5mM $MgSO_4 \cdot 7H_2O$, and 1mM ATP, pH 7.4, 4°C) was used for isolation of mitochondria. IFM were harvested following treatment of skinned fibers with 5mg/gww trypsin for 10 minutes at 4°C (89). Mitochondrial protein concentration was determined by the Lowry method using bovine serum albumin as a standard.

3.2.5 Mitochondrial Oxidative Phosphorylation

Oxygen consumption in SSM and IFM was measured using a Clark-type oxygen electrode (Strathkelvin) at 30°C (131). Mitochondria were incubated in a solution consisting of 80mM KCl, 50mM MOPS, 1mM EGTA, 5mM KH_2PO_4, and 1mg/ml defatted bovine serum albumin at pH 7.4. The rate of oxidative phosphorylation and uncoupled respiration was measured using several substrates. Glutamate assesses complexes I, III, and IV. Succinate assesses complexes II, III, and IV. DHQ, an analog of

coenzyme Q, assesses complexes III and IV. TMPD, an electron carrier that reduces cytochrome c, used in conjunction with ascorbate, assesses complex IV. Mitochondrial respiration was measured using lipid substrates octanoylcarnitine plus malate and palmitoylcarnitine plus malate (62). State 3 (ADP-stimulated) respiration, state 4 (ADP-limited) respiration, RCR (state 3/state 4), and ADP/O ratio (ADP added per oxygen consumed) were determined (11; 25).

3.2.6 Mitochondrial Electron Transport Chain Complex Activity

Samples of SSM and IFM (10mg cholate/1mg mitochondrial protein) were mixed in 1ml buffer (75mM mannitol, 220mM sucrose, 2mM EDTA, and 5mM MOPS, pH 7.4) with mammalian protease inhibitor cocktail (1µl/1ml buffer) and kept on ice. Assays were completed on the day of preparation.

All ETC complex activities were measured as specific donor-acceptor oxidoreductase activities using a diode array spectrophotometer as described in Chapter 2 (45; 66; 67; 105; 143). Donors and acceptors were chosen to span specific regions of the complete ETC.

3.2.7 Electron Microscopy

Freshly isolated SSM and IFM were prepared for transmission electron microscopy as described in Chapter 2 (75; 105), with the exception that samples were fixed using one-quarter-strength Karnovsky's fixative. A myocardial tissue sample from the LV, obtained during the terminal surgery, also was prepared for analysis by electron microscopy as described in Lesnefsky *et al.* (75). LV tissue was minced in triple-

aldehyde-dimethyl sulfoxide (DMSO) and the fixation continued in fresh triple-aldehyde-DMSO for a total of 2 hours at room temperature. From this point all specimens were processed in the same fashion as the SSM and IFM. Electron micrographs were assessed in an investigator-blinded fashion.

3.2.8 RNA Extraction and Quantitative RT-PCR

RNA extraction (and subsequent quantitative RT-PCR) was performed on frozen powdered LV tissue as previously described (17; 37). Specific quantitative assays were designed from rat sequences available in GenBank for expression of *pparα*, atrial natriuretic factor (*anf*), and genes known to be regulated by PPARα: *scad, mcad*, *lcad*, *cpt-I*, *pdk4*, *ucp3*, and *cte-1*. Primer and probe sequences for these Taqman assays have previously been published (124; 145; 146), with the exception of *scad*. Sequences for *scad* are 5'-CAAAATCGGCTGTTTTGCC-3' (forward primer), 5'-AAGCTTTGGTGCCGTTGAG-3' (reverse primer), and 5'-FAM-CAGTGAGCCAGGCAATGGCAGTGA-TAMRA-3' (probe). Standard RNA was made for all assays by the T7 polymerase method (Ambion), using total RNA isolated from rat hearts. The correlation between the C_t (the number of PCR cycles required for the fluorescent signal to reach a detection threshold) and the amount of standard was linear over at least a 5-log range of RNA for all assays. The PCR data are reported as the number of transcripts per nanogram RNA.

3.2.9 Western Immunoblot Analysis

For the analysis of MCAD protein expression, SSM and IFM protein samples (100μg) were resuspended in a standard Laemmli buffer (XT sample buffer, BioRad) and boiled for 5 minutes. To assess the potential contribution of proteins involved in substrate flux across the plasma membrane, CD36 and FATP-1 protein expression was measured in myocardial tissue. Protein was extracted from frozen powdered LV tissue. Briefly, 25 mg of frozen LV tissue was homogenized in 75 ul ice-cold RIPA buffer (5000 ul RIPA, 50 ul PMSF, 50 ul sodium orthovanadate, 50 ul protease inhibitor, 50 ul each protein phosphatase inhibitor cocktails 1 and 2 (Sigma)). Homogenates were incubated on ice for 30 minutes then centrifuged at 10,000 x g for 5 minutes at 4^{o}C. The supernatant (total cell lysate) was transferred to a new eppendorf, protein concentration was determined by Lowry method, then samples were diluted with an equal volume of 2X electrophoresis sample buffer and boiled for 2-3 minutes. In order to allow for gel to gel comparisons, a standard sample was loaded onto each gel and protein bands detected in samples were then normalized to their respective gel control band. Sample proteins were separated using SDS-PAGE on a 10% tris-glycine polyacrylamide gel and transferred onto a nitrocellulose membrane. Protein transfer was verified with Ponceau staining. Membranes were washed in TBS plus tween and blocked with 5% nonfat dry milk in TBS plus tween. Membranes were incubated with a mouse polyclonal antibody for MCAD (1:500; Abnova), a goat polyclonal antibody for FATP-1 (1:100; Santa Cruz), a mouse polyclonal antibody for CD36 (1:5000; a gift from Maria Febbraio, Cleveland, Ohio), or a mouse monoclonal antibody for calsequestrin (1:1000; Affinity Bioreagents) overnight at room temperature. Membranes were then incubated for one hour with a

HRP-linked secondary antibodies for MCAD and calsequestrin (goat anti-mouse, Pierce), for FATP-1 (donkey anti-goat, Jackson Laboratories), or for CD36 (goat anti-rabbit, Pierce) for one hour. Protein bands were visualized via chemiluminescent detection (Supersignal, Pierce) on film and bands were quantified using Image J (http://rsb.info.nih.gov/ij/). For MCAD, each protein band was normalized to citrate synthase activity in the individual mitochondrial fractions. For CD36 and FATP-1, each protein band was normalized to calsequestrin.

3.2.10 Acyl-CoA Dehydrogenase Activity

Short-, medium-, and long-chain acyl-CoA dehydrogenase activities were measured in isolated SSM and IFM as the phenazine ethosulfate stimulated reduction of cytochrome c using 2μM butyryl-CoA (a 4-carbon substrate), 0.2mM octanoyl-CoA (an 8-carbon substrate), or 50μM palmitoyl-CoA (a 16-carbon substrate) respectively (44).

3.2.11 Plasma and Tissue Metabolic Products

Glucose, free fatty acids, and triglyceride concentrations in plasma were measured using an enzymatic spectrophotometric kit (100). Tissue triglyceride content was measured in homogenate extracts using an enzymatic spectrophotometer method (Wako Chemicals). Insulin and leptin concentrations in plasma were assayed by ELISA (ALPCO Diagnostics). Adiponectin concentrations in serum were measured by ELISA (B-Bridge, San Diego CA). Citrate synthase was measured as described in Chapter 2 (121).

Carnitine and acylcarnitine content in LV myocardial tissue were assessed by HPLC/ESI/MS/MS (87). For acylcarnitines, LV tissue homogenates were mixed with

internal standard solution (50 nmol/ml d6-acetylcarnitine, 10 nmol/ml d_3-propionylcarnitine, 2.5 nmol/ml nonanoylcarnitine and 1 nmol/ml heptadecanoylcarnitine). Following addition of 1 ml acetonitrile/methanol (3:1), samples were vortexed and centrifuged for 5 minutes. Samples were then loaded onto a solid-phase extraction column, eluted with 1.0 ml water/methanol/acetic acid (10:9:1), and evaporated to dryness with N_2. Using 200 µl acetonitrile/methanol (3+1) samples were reconstituted, transferred to an HPLC autosampler vial, and evaporated to dryness. Sample residues were reconstituted using 50 µl N,N-diisopropylethylamine in acetonitrile and 50 µl pentafluorophenacyl trifluoromethanesulfonate in acetonitrile.

For free and total carnitine, LV tissue homogenates were mixed with 50 µl d_3-carnitine and 1 ml acetonitrile/methanol (3+1), vortexed, and centrifuged for 5 minutes. For free carnitine an aliquot was then applied to a solid-phase extraction column. For total carnitine, a 400 µl aliquot was mixed with 100 µl 1 M KOH in methanol, vortexed, and placed in a waterbath at 50^{o}C for 60 minutes. Samples were then transferred to a microcentrifuge tube, mixed with 50 µl 10% phosphoric acid and 750 µl acetonitrile/methanol (3+1), vortexed, and centrifuged for 5 minutes. The supernatant was then loaded onto a solid-phase extraction column. Total carnitine was the sum of carnitine and acylcarnitine.

3.2.12 Statistical Analysis

Differences among SHAM, SHAM+FAT, HF, and HF+FAT were determined using a 2-Way ANOVA followed by Bonferroni t-tests for multiple comparisons. Data are expressed as group means±SEM. Significance was established at $P<0.05$.

3.3 Results

3.3.1 Body and Heart Mass

Heart failure increased LV and RV mass when normalized to body mass (Table 3-1). High fat in SHAM animals did not alter LV or RV mass, but in HF+FAT high fat attenuated the increases in RV/body mass and biventricular mass/body mass seen in HF. Mean scar tissue mass did not differ between the two ligated groups (Table 3-1). Body mass, as indicated in Table 3-1, was slightly elevated when compared to body mass in Table 2-1, however it is important to note that animals included in Table 3-1 were older than those in Table 2-1.

3.3.2 Cardiac Function and Echocardiographic Measures

High fat did not alter LV contractile function or remodeling in SHAM animals. Coronary ligation resulted in impaired LV contractile function and remodeling in HF and HF+FAT compared to SHAM and SHAM+FAT as assessed by increased MPI, end diastolic area, and end systolic area, as well as decreased peak LV +/-dP/dt, cardiac index, and area fractional shortening (Table 3-2). Interestingly, peak LV +dP/dt, an index of myocardial contractility, was increased in HF+FAT compared to HF. Thus, LV contractile function and the progression of LV remodeling were not exacerbated by high fat feeding in HF; instead, peak LV + dP/dt was improved.

3.3.3 Metabolic Substrates and Humoral Factors

Plasma glucose, plasma insulin, and tissue triglycerides were not altered by heart failure or high fat feeding. As expected, plasma free fatty acids, leptin, and

Table 3-1. Body and heart mass in SHAM, SHAM+FAT, HF, and HF+FAT eight weeks following coronary artery ligation surgery.

	SHAM	SHAM+FAT	HF	HF+FAT
Body Mass (g)	477 ± 6	484 ± 8	490 ± 10	515 ± 15
LV Mass/Body Mass (mg/g)	1.92 ± 0.05	1.82 ± 0.04	2.26 ± 0.05*	2.16 ± 0.06†
Biventricular Mass/ Body Mass (mg/g)	2.36 ± 0.06	2.30 ± 0.06	2.88 ± 0.09*	2.67 ± 0.08†‡
Scar (mg)			141 ± 11	140 ± 14

SHAM (n=10), SHAM+FAT (n=10), HF (n=9); and HF+FAT (n=10). Values are expressed as mean ± SEM. * $p<0.05$ vs SHAM; † $p<0.05$ vs SHAM+FAT; ‡ $p<0.05$ vs HF

Table 3-2. LV functional measurements obtained by LV cannulation and echocardiography in SHAM, SHAM+FAT, HF, and HF+FAT eight weeks following coronary artery ligation surgery.

	SHAM	SHAM+FAT	HF	HF+FAT
LV Cannulation				
Heart Rate (bpm)	331 ± 16	334 ± 13	285 ± 6 *	319 ± 13
Peak Systolic LV Pressure (mmHg)	119 ± 7	124 ± 4	95 ± 3 *	108 ± 6 †
Peak LV End Diastolic Pressure (mmHg)	7.6 ± 1.0	5.7 ± 0.5	10.1 ± 2.3	7.1 ± 1.7
Peak LV +dP/dt (mmHg/sec)	7014 ± 592	7637 ± 374	4679 ± 251 *	6135 ± 620 †‡
Peak LV -dP/dt (mmHg/sec)	5950 ± 484	6497 ± 393	3714 ± 230 *	4608 ± 436 †
Echocardiography				
End Diastolic Area (cm^2)	0.91 ± 0.06	0.88 ± 0.04	1.16 ± 0.12 *	1.12 ± 0.06 †
End Systolic Area (cm^2)	0.382 ± 0.058	0.359 ± 0.034	0.679 ± 0.090 *	0.748 ± 0.098 †
Cardiac Index ($ml \cdot^{-1} min \cdot^{-1} mg$)	171 ± 26	155 ± 20	116 ± 14 *	137 ± 12
Area Fractional Shortening (cm^2)	0.593 ± 0.046	0.595 ± 0.031	0.415 ± 0.047 *	0.341 ± 0.075 †
Myocardial Performance Index	0.408 ± 0.025	0.417 ± 0.028	0.557 ± 0.039 *	0.525 ± 0.027 †

Cardiac index was calculated by dividing cardiac output by body weight. Area fractional shortening was calculated as the sum of LV end-systolic and end-diastolic areas divided by end-diastolic area. Myocardial performance index was defined as the sum of the isovolumic contraction and relaxation times divided by the ejection time. SHAM (n=10), SHAM+FAT (n=10), HF (n=9); and HF+FAT (n=10). Values are expressed as mean ± SEM. * $p<0.05$ vs SHAM; † $p<0.05$ vs SHAM+FAT; ‡ $p<0.05$ vs HF

adiponectin were elevated in both SHAM+FAT and HF+FAT. Plasma triglycerides were elevated in HF compared to SHAM (Table 3-3). The discrepancy between values in Table 3-3 and those listed in Table 2-2 and Figure 2-3 can be accounted for by the fact that the data shown in Table 2-2 and Figure 2-3 was obtained from fasted animals while the date presented in Table 3-3 was obtained from non-fasted animals.

3.3.4 Mitochondrial Morphology

Neither heart failure nor high fat feeding altered the morphology of isolated SSM and IFM (Figure 3-1). In keeping with previous studies of cardiac mitochondria, these organelles have assumed a spherical shape. A small number of mitochondria exhibit a degree of extraction of matrix material. A few mitochondria show blebbing of their outer membrane. This description applies equally to SSM and IFM, however, IFM (Figure 3-1E-H) appear to be, on average slightly larger than the SSM (Figure 3-1A-D). Myocardial tissue samples of the LV were fixed in order to assess the integrity of both SSM and IFM within the myocardial tissue as well as the overall structure of the cardiomyocytes per se. Mitochondrial shape, size, and density *in situ* also were not altered by heart failure or high fat feeding (Figure 3-2). Although the myofibrils show a degree of contraction, they are identical in appearance under all conditions of this study. In a similar fashion, all cardiomyocyte nuclei have the same appearance, i.e., they are euchromatic, often exhibiting a single nucleolus.

Table 3-3. Plasma glucose, insulin, free fatty acids, triglycerides, and leptin, serum adiponectin, and tissue triglycerides in SHAM, SHAM+FAT, HF, and HF+FAT eight weeks following coronary artery ligation surgery.

	SHAM	SHAM+FAT	HF	HF+FAT
Glucose (µmol/mL)	4.61 ± 0.18	4.50 ± 0.14	4.58 ± 0.12	4.59 ± 0.20
Insulin (pmol/mL)	82 ± 23	98 ± 14	75 ± 16	122 ± 17
Free Fatty Acids (µmol/mL)	0.236 ± 0.026	0.422 ± 0.019 *	0.220 ± 0.031	0.380 ± 0.032 †
Plasma Triglycerides (mg/mL)	1.09 ± 0.11	1.12 ± 0.09	1.42 ± 0.11 *	1.29 ± 0.13
Leptin (pg/mL)	1287 ± 136	1970 ± 183 *	1363 ± 113	1832 ± 179 †
Adiponectin (µg/mL)	2.79 ± 0.18	4.63 ± 0.28 *	2.88 ± 0.26	4.03 ± 0.37 †
Tissue Triglycerides (µmol/g ww)	6.01 ± 0.97	7.29 ± 1.37	5.97 ± 1.05	5.39 ± 1.06

SHAM (n=10), SHAM+FAT (n=10), HF (n=9); and HF+FAT (n=10). Values are expressed as mean ± SEM. * $p<0.05$ vs SHAM; † $p<0.05$ vs HF

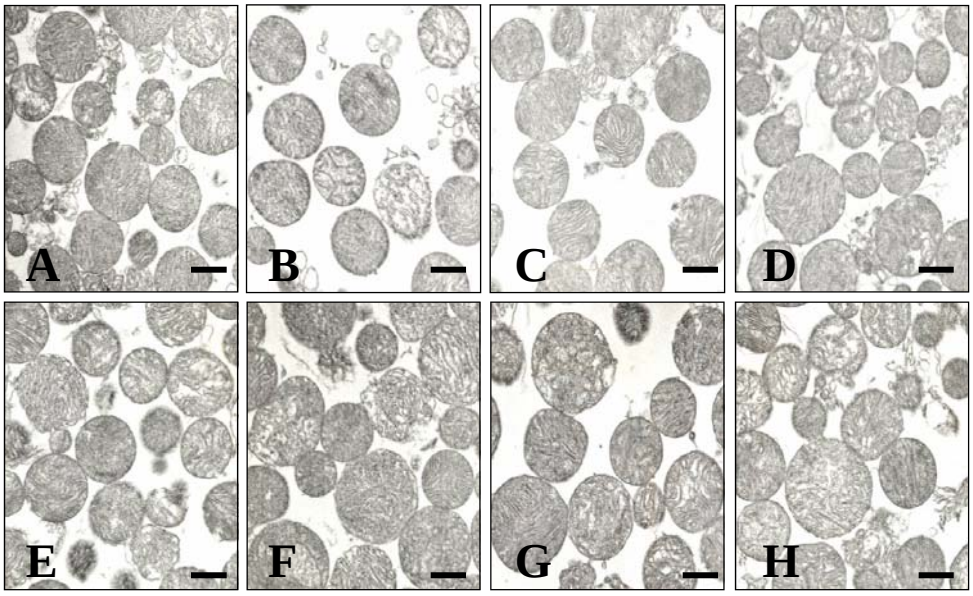

Figure 3-1. Electron micrographs of SSM and IFM. SSM in (A) SHAM, (B) SHAM+FAT, (C) HF, (D) HF+FAT. IFM in (E) SHAM, (F) SHAM+FAT, (G) HF, (H) HF+FAT. n=2 per group. Bars = 1 μm.

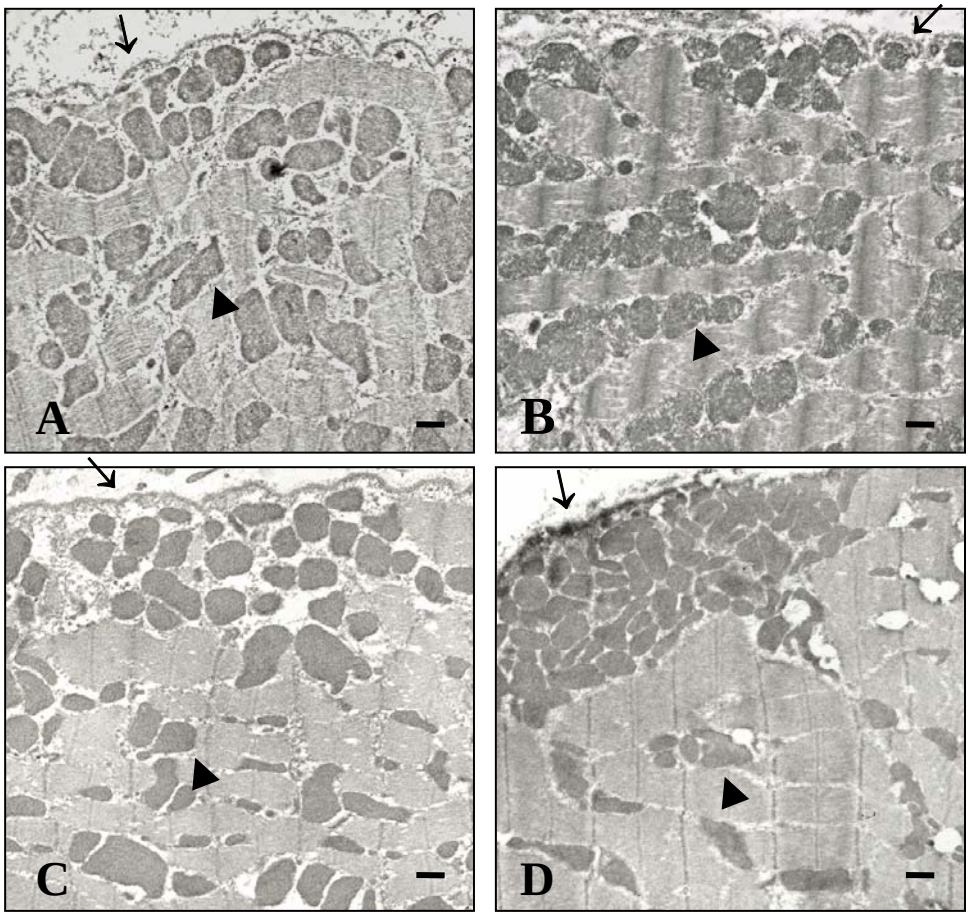

Figure 3-2. Electron micrographs of mitochondria in LV myocardial tissue in (A) SHAM, (B) SHAM+FAT, (C) HF, (D) HF+FAT. SSM are situated beneath the sarcolemma (↑). IFM (▲) are located between the myofibrils. The cluster of SSM (D) is not the result of treatment; such aggregates occasionally are present in untreated cardiomyocytes. n=2 per group. Bars = 1 μm.

3.3.5 Oxidative Phosphorylation

Protein yield in SSM was not altered by heart failure or high fat (SHAM 11.8±0.8, SHAM+FAT 10.2±0.4, HF 10.8±1.1, HF+FAT 11.9±1.1 $mg \cdot gww^{-1}$), but was significantly decreased in IFM in both heart failure groups compared to SHAM (SHAM 8.35±0.39, SHAM+FAT 8.37±0.49, HF 6.46±0.55, HF+FAT 6.20±0.69 $mg \cdot gww^{-1}$). Citrate synthase activity in myocardial tissue was also significantly decreased in both heart failure groups (SHAM 115±3, SHAM+FAT 120±3, HF 99±4, HF+FAT 102±5 $\mu mol \cdot min^{-1} \cdot gww^{-1}$), consistent with the decreased IFM protein yield.

Mitochondrial respiration was measured using lipid substrates octanoylcarnitine and palmitoylcarnitine to assess the ability of the mitochondria to oxidize fatty acids of different chain lengths. State 3 respiration in SSM was not altered in SHAM+FAT or HF using either lipid substrate (Figure 3-3A), but was elevated in HF+FAT compared to SHAM+FAT and HF using both octanoylcarnitine and palmitoylcarnitine. Similarly, state 3 respiration was not altered in SSM of SHAM+FAT or HF using glutamate, but was elevated in HF+FAT. In SSM, state 3 respiration was not altered using succinate, DHQ, or TMPD-ascorbate (Figure 3-4A). State 3 respiration did not differ in IFM with any of the respiratory substrates used (Figure 3-3B, 3-4B). The differential effects observed in SSM and IFM are not surprising as they have previously been shown to be distinct populations that respond differently under pathological conditions (73).

In SSM, state 4 respiration was not altered in SHAM+FAT or HF, but was elevated using octanoylcarnitine in HF+FAT compared to SHAM+FAT (Figure 3-5A). In IFM, state 4 respiration was not altered in SHAM+FAT or HF+FAT, but was increased in HF compared to SHAM using octanoylcarnitine and glutamate (Figure 3-5B).

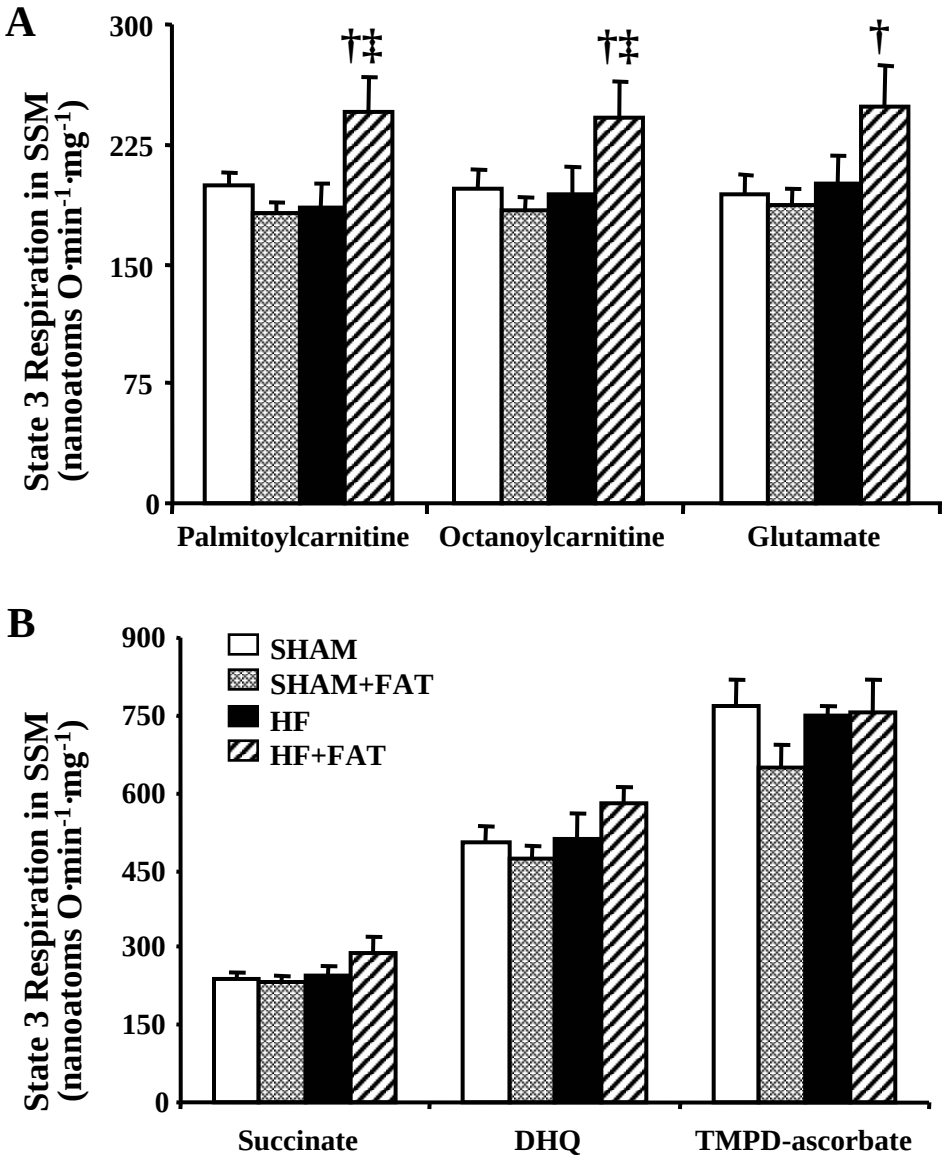

Figure 3-3. State 3 respiration (A) using palmitoylcarnitine, octanoylcarnitine, and glutamate and (B) using succinate, DHQ, and TMPD-ascorbate as respiratory substrates in SSM of SHAM (n=10), SHAM+FAT (n=10), HF (n=9); and HF+FAT (n=10). Values are mean±SEM. *****P<0.05 compared to SHAM; †P<0.05 compared to SHAM+FAT; ‡P<0.05 compared to HF.

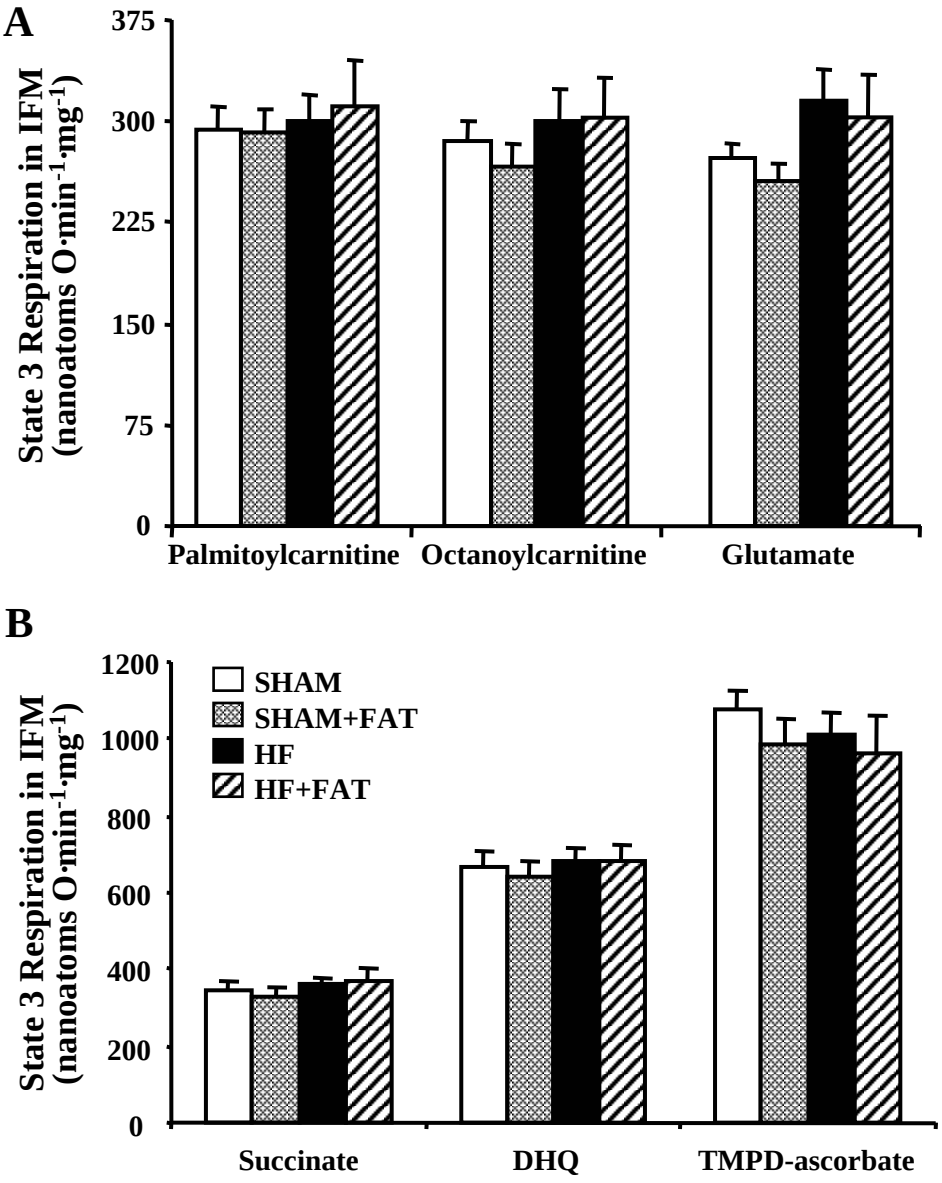

Figure 3-4. State 3 respiration (A) using palmitoylcarnitine, octanoylcarnitine, and glutamate and (B) using succinate, DHQ, and TMPD-ascorbate as respiratory substrates in IFM of SHAM (n=10), SHAM+FAT (n=10), HF (n=9); and HF+FAT (n=10). Values are mean±SEM. *****P<0.05 compared to SHAM; †P<0.05 compared to SHAM+FAT; ‡P<0.05 compared to HF.

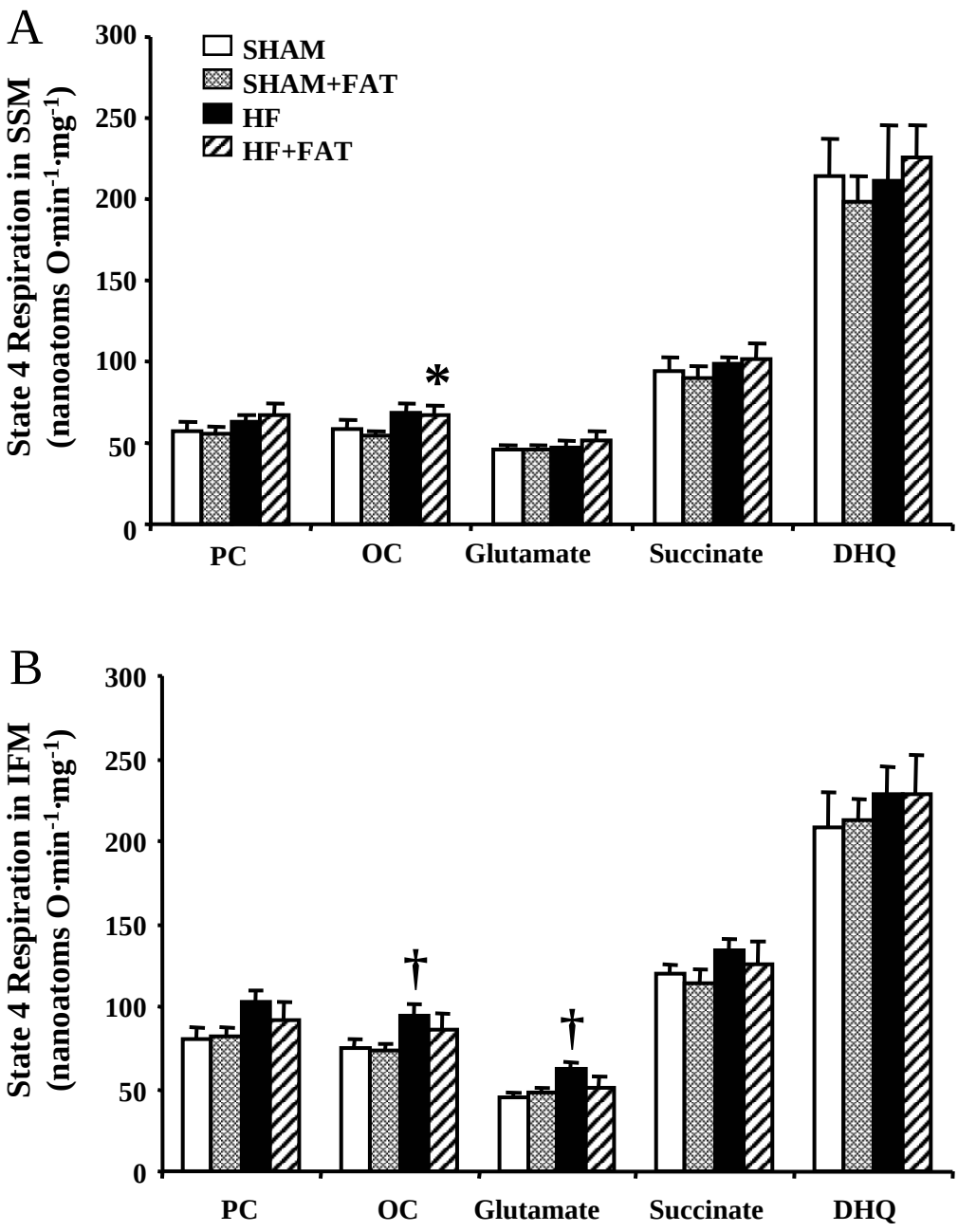

Figure 3-5. State 4 respiration in (A) SSM and (B) IFM using palmitoylcarnitine (PC), octanoylcarnitine (OC), glutamate, succinate, and DHQ as respiratory substrates in SHAM (n=10), SHAM+FAT (n=10), HF (n=9); and HF+FAT (n=10). Values are mean±SEM. *****P<0.05 compared to SHAM+FAT, †P<0.05 compared to SHAM.

RCR was not altered in either high fat group, but was decreased in SSM of HF compared to SHAM and HF+FAT using both octanoylcarnitine and palmitoylcarnitine (Figure 3-6A). In IFM, RCR was decreased in HF with palmitoylcarnitine, octanoylcarnitine, and glutamate compared to SHAM, but was increased in HF+FAT compared to HF with glutamate only (Figure 3-6B). ADP/O did not differ in the SSM or IFM with any lipid substrate (Figure 3-7A-B).

3.3.6 Mitochondrial Electron Transport Chain Complex Activities

Activity of complex II+coenzyme Q was elevated in SSM (SHAM 78.0±8.8, SHAM+FAT 61.7±5.8, HF 60.6±5.7, HF+FAT 85.4±10.0 nmoles·min^{-1}·mg^{-1}) and IFM (SHAM 88.9±7.7, SHAM+FAT 71.5±7.0, HF 72.4±8.3, HF+FAT 93.9±8.8 nmoles·min^{-1}·mg^{-1}) of HF+FAT compared to SHAM+FAT. In the SSM, the activity of complex II+coenzyme Q also was elevated in HF+FAT compared to HF. Complex III activity in IFM was elevated in HF+FAT compared to SHAM+FAT (SHAM 5623±620, SHAM+FAT 5066±594, HF 6766±498, HF+FAT 7437±1373 nmoles·min^{-1}·mg^{-1}). Complex I, complex I+III, NADH-dehydrogenase, complex II, complex II+III, complex IV, and succinate dehydrogenase activities were not altered in SSM (Table 3-4) or IFM (Table 3-5). The increase in complex II+coenzyme Q and complex III activities was not reflected in increased state 3 respiration using complex I (glutamate), complex II (succinate), or complex III (DHQ) substrates. Additionally, without a concomitant increase in the activity of the other complexes of the ETC, the increase in complex II+coenzyme Q is unlikely to account for the increased state 3 respiration evident in the SSM of HF+FAT.

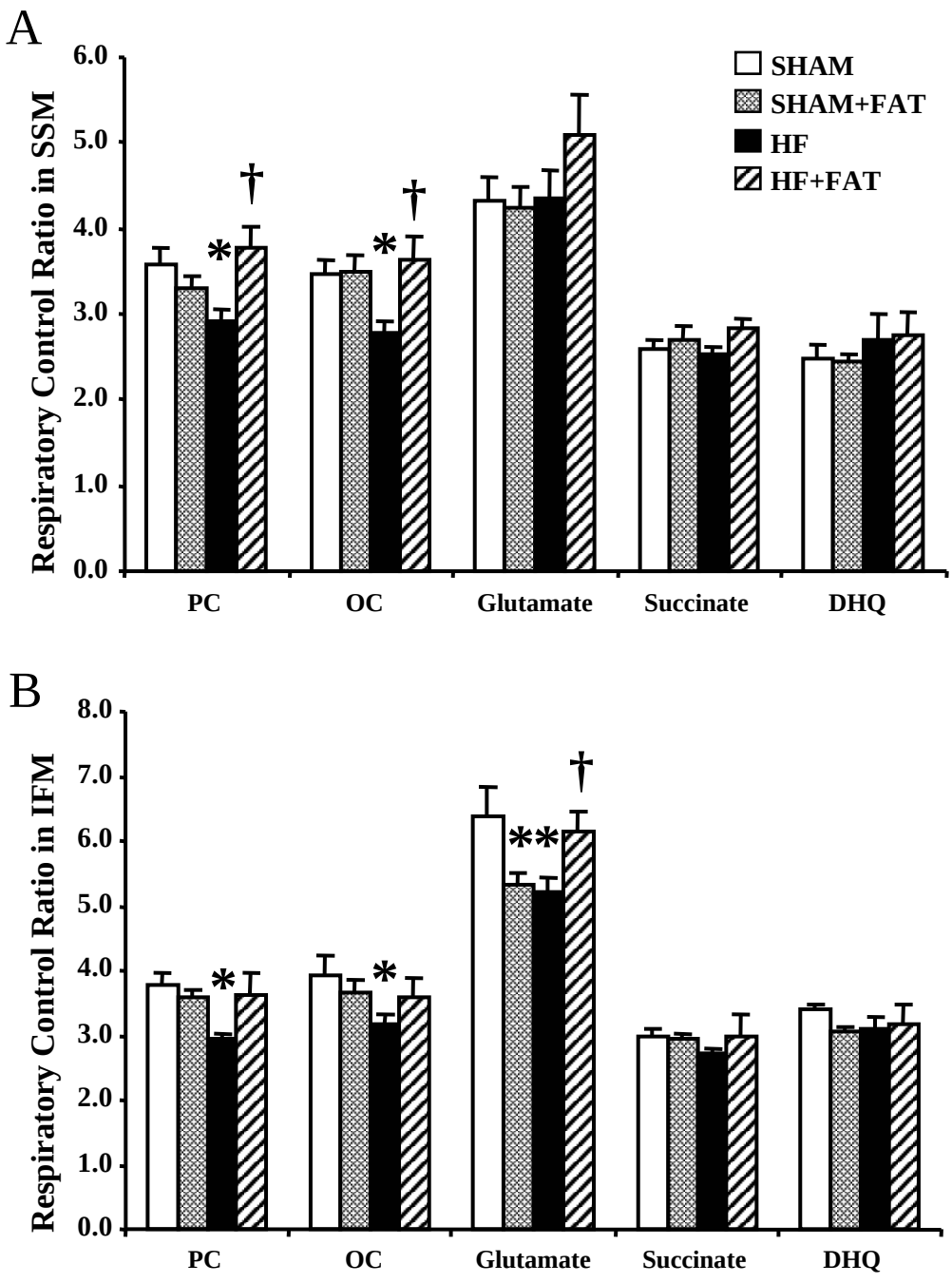

Figure 3-6. Respiratory control ratio (state 3/state 4) in (A) SSM and (B) IFM using palmitoylcarnitine (PC), octanoylcarnitine (OC), glutamate, succinate, and DHQ as respiratory substrates in SHAM (n=10), SHAM+FAT (n=10), HF (n=9); and HF+FAT (n=10). Values are mean±SEM. *P<0.05 compared to SHAM; †P<0.05 compared to HF.

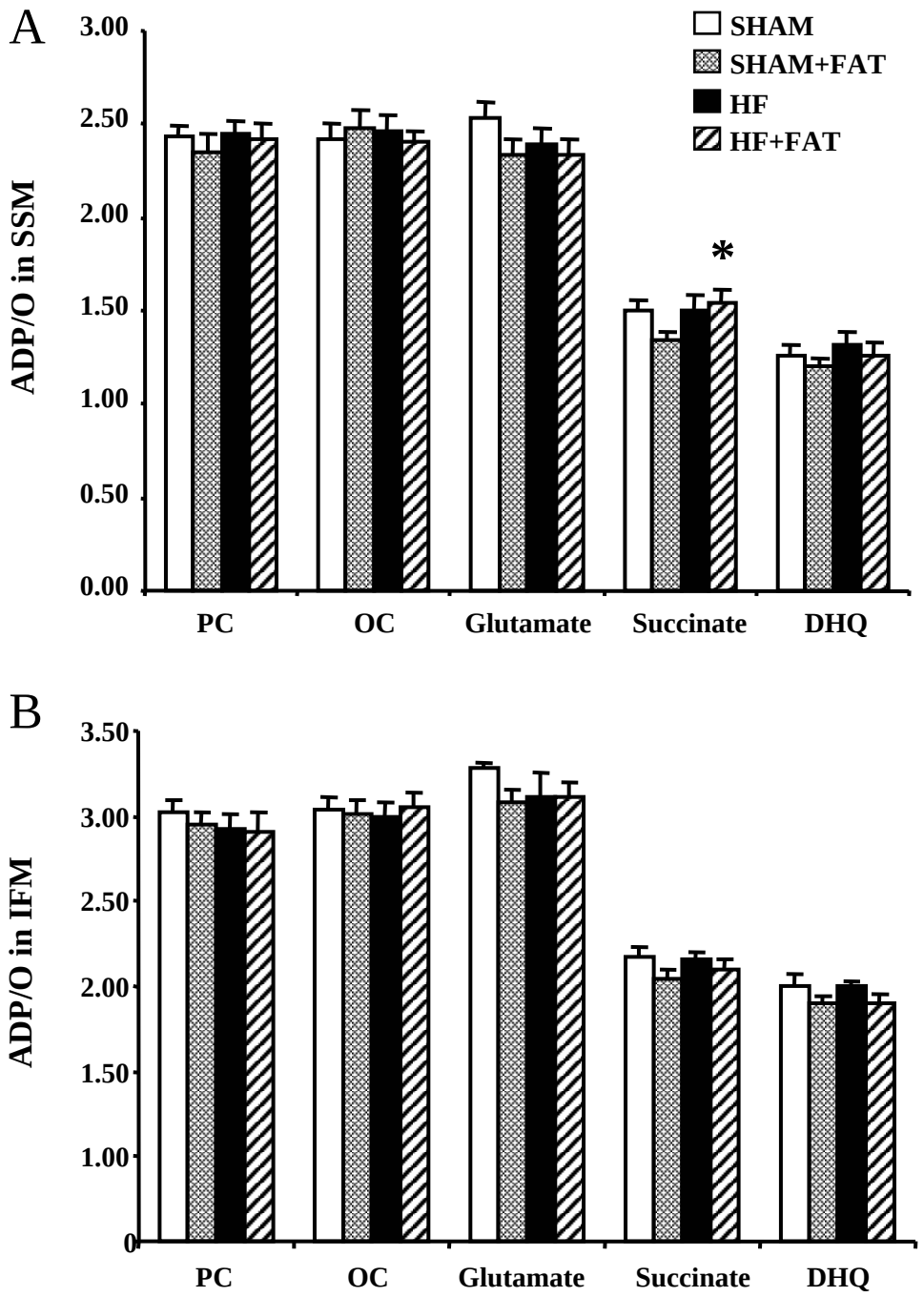

Figure 3-7. ADP/O in (A) SSM and (B) IFM using palmitoylcarnitine (PC), octanoylcarnitine (OC), glutamate, succinate, and DHQ as respiratory substrates in SHAM (n=10), SHAM+FAT (n=10), HF (n=9); and HF+FAT (n=10). Values are mean±SEM. *****P<0.05 compared to SHAM+FAT

Table 3-4. Electron transport chain complex and enzyme activities in SSM of SHAM, SHAM+FAT, HF, and HF+FAT eight weeks post coronary artery ligation surgery.

	SHAM	SHAM+FAT	HF	HF+FAT
Complexes I and III	3837 ± 435	4024 ± 245	3482 ± 263	3984 ± 532
Complex I	817 ± 81	722 ± 32	744 ± 56	736 ± 48
NADH-Dehydrogenase	2528 ± 213	2357 ± 100	2588 ± 149	2673 ± 253
Complex III	4719 ± 729	3986 ± 548	4872 ± 444	6128 ± 1056
Complexes II and III	338 ± 46	292 ± 29	260 ± 22	358 ± 72
Complex II	65.7 ± 6.7	55.6 ± 4.9	58.1 ± 2.8	71.0 ± 8.2
Complex II + Coenzyme Q	78.0 ± 8.8	61.7 ± 5.8	60.6 ± 5.7	85.4 ± 10.0 *†
Succinate Dehydrogenase	221 ± 19	219 ± 15	201 ± 8	238 ± 19
Complex IV ($x10^4$)	47.4 ± 3.9	43.0 ± 3.0	47.4 ± 2.7	50.8 ± 4.1
Citrate Synthase	1771 ± 136	1625 ± 88	1782 ± 51	2067 ± 108*
Aconitase	616 ± 65	577 ± 45	636 ± 62	809 ± 99

Electron transport chain complex and enzyme activities are expressed as nmoles·min^{-1}·mg^{-1} mitochondrial protein with the exception of complex IV which is expressed as the first order rate constant (k:1 x min^{-1} x mg $protein^{-1}$). SHAM (n=10), SHAM+FAT (n=10), HF (n=9); and HF+FAT (n=10). Values are expressed as mean ± SEM. *P<0.05 vs SHAM+FAT; † p<0.05 vs HF.

Table 3-5. Electron transport chain complex and enzyme activities in IFM of SHAM, SHAM+FAT, HF, and HF+FAT eight weeks post coronary artery ligation surgery.

	SHAM	SHAM+FAT	HF	HF+FAT
Complexes I and III	4471 ± 437	4382 ± 306	4822 ± 459	4745 ± 842
Complex I	820 ± 63	708 ± 36	767 ± 42	720 ± 49
NADH-Dehydrogenase	2896 ± 218	2585 ± 92	2959 ± 126	3120 ± 537
Complex III	5623 ± 620	5066 ± 594	6766 ± 498	7437 ± 1373 *
Complexes II and III	431 ± 43	353 ± 37	365 ± 29	453 ± 95
Complex II	74.9 ± 6.4	58.7 ± 6.0	71.8 ± 4.9	77.0 ± 8.1
Complex II + Coenzyme Q	88.9 ± 7.7	71.5 ± 7.0	72.4 ± 8.3	93.9 ± 8.8 *
Succinate Dehydrogenase	275 ± 18	250 ± 17	258 ± 14	292 ± 23
Complex IV ($x10^4$)	60.9 ± 5.6	52.1 ± 2.7	57.2 ± 3.1	64.5 ± 9.5
Citrate Synthase	2481 ± 134	2368 ± 109	2478 ± 93	2750 ± 256
Aconitase	871 ± 68	850 ± 61	841 ± 125	1008 ± 117

Electron transport chain complex and enzyme activities are expressed as nmoles·min^{-1}·mg^{-1} mitochondrial protein with the exception of complex IV which is expressed as the first order rate constant (k:1 x min^{-1} x mg $protein^{-1}$). SHAM (n=10), SHAM+FAT (n=10), HF (n=9); and HF+FAT (n=10). Values are expressed as mean ± SEM. *$p<0.05$ vs SHAM+FAT.

3.3.7 RNA Expression

Expression of *anf* was not altered with high fat feeding in sham animals (SHAM 105±23, SHAM+FAT 100±16). Heart failure resulted in an 8-fold increase in *anf* expression; however, *anf* did not differ between HF and HF+FAT (HF 920±268, HF+FAT 814±168). mRNA expression of fatty acid-responsive genes *cte-1* (Figure 3-8) and *mcad* (Figure 3-9) was significantly decreased in HF compared to SHAM; a similar trend was observed for *pdk4* (P=0.065). Whereas high fat diet increased the expression of *pdk4* and *cte-1* in both SHAM+FAT and HF+FAT, there was no effect of high fat on the expression of other genes investigated (Figure 3-8).

3.3.8 Acyl-CoA Dehydrogenase Protein Expression and Enzyme Activity

Despite decreased mRNA expression of *mcad* in HF compared to SHAM (Figure 3-9A), MCAD protein expression (Figure 3-9B) and activities of SCAD, MCAD, and LCAD (Figure 3-10A-B) were not altered. MCAD protein expression also was not altered by high fat feeding in SSM or IFM (Figure 3-9B). Interestingly, the activities of acyl-CoA dehydrogenases (SCAD, MCAD, and LCAD) were elevated in SSM of HF+FAT despite no alterations in mRNA and protein expression (Figure 3-10A). Furthermore, there was a strong positive relationship between MCAD activity and state 3 respiration in SSM using palmitoylcarnitine (Figure 3-11A) and octanoylcarnitine (Figure 3-11B) as respiratory substrates. This positive relationship with state 3 respiration also existed for SCAD (octanoylcarnitine $R=0.631$, $p<0.0001$; palmitoylcarnitine $R=0.651$, $p<0.0001$) and LCAD activity (octanoylcarnitine $R=0.606$, $p<0.0001$; palmitoylcarnitine $R=0.609$, $p<0.0001$).

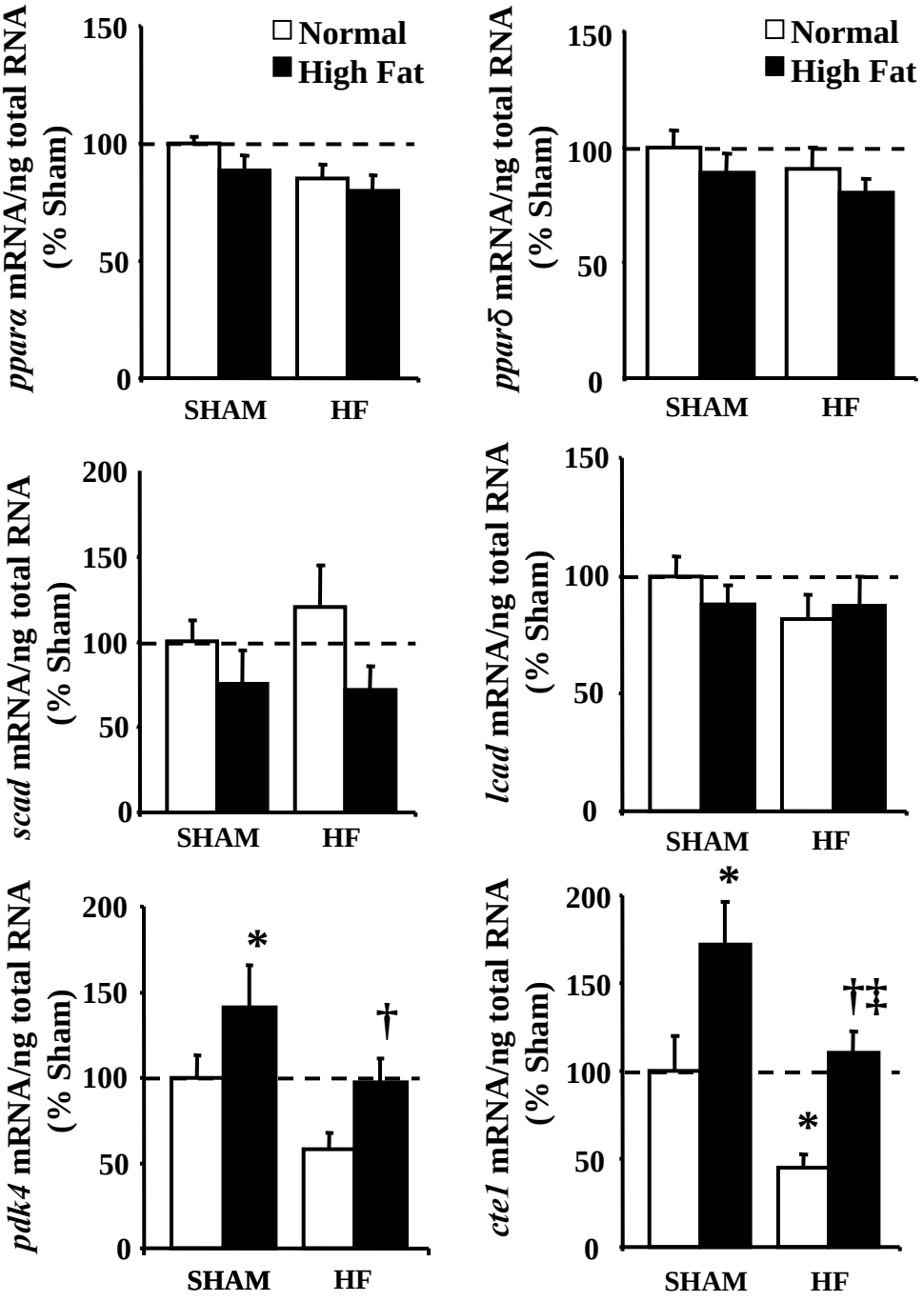

Figure 3-8. mRNA expression of PPARα regulated genes in SHAM (n=10), SHAM+FAT (n=10), HF (n=9); and HF+FAT (n=10). Values are mean±SEM and expressed as a percentage of SHAM. *P<0.05 compared to SHAM; †P<0.05 compared to SHAM+FAT; ‡P<0.05 compared to HF.

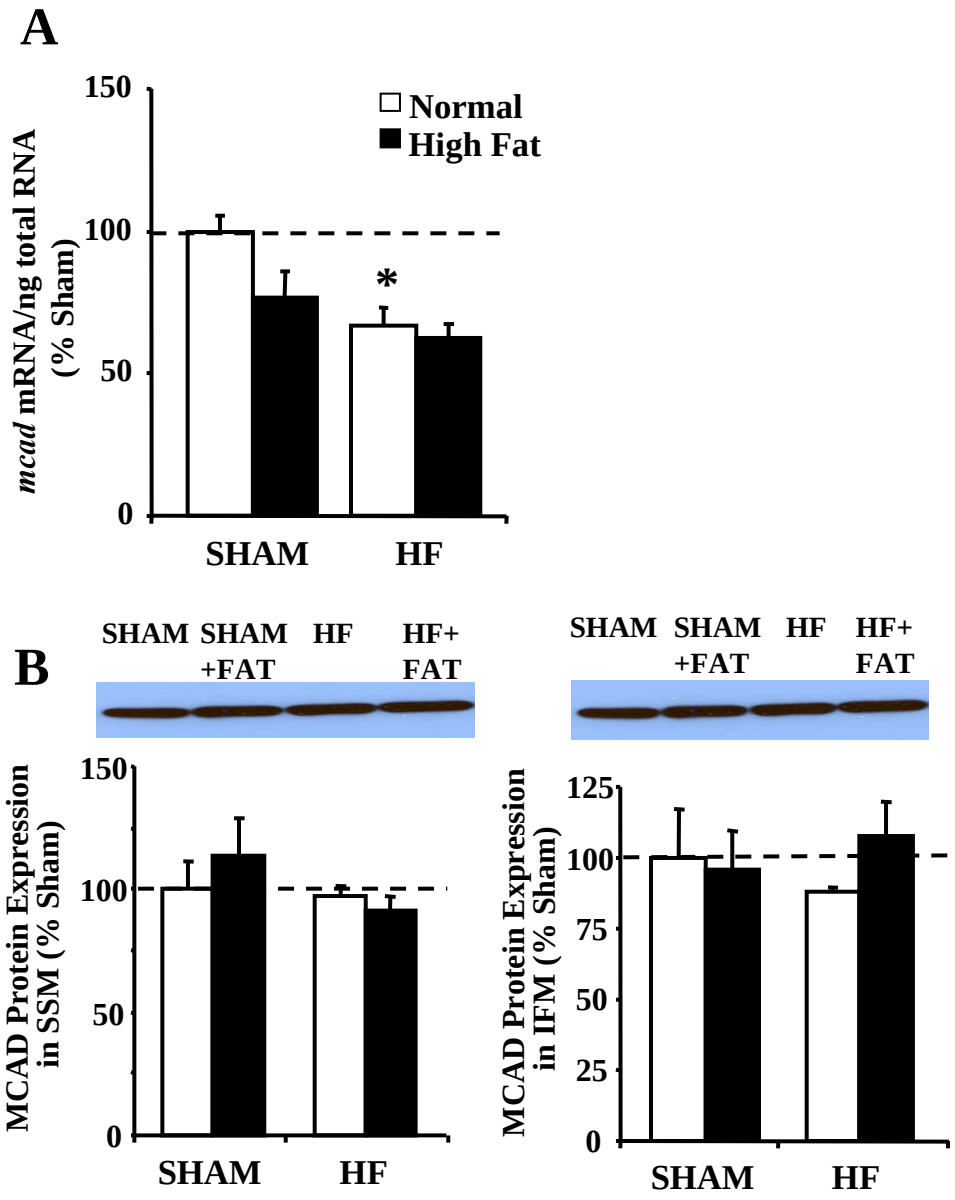

Figure 3-9. (A) mRNA expression of MCAD in myocardial tissue and (B) representative immunoblot and densitometry of MCAD protein expression in SSM and IFM of SHAM (n=10), SHAM+FAT (n=10), HF (n=9); and HF+FAT (n=10). Each protein band was normalized to its respective mitochondrial citrate synthase activity. Values are mean±SEM and expressed as a percentage of SHAM. *P<0.05 compared to SHAM.

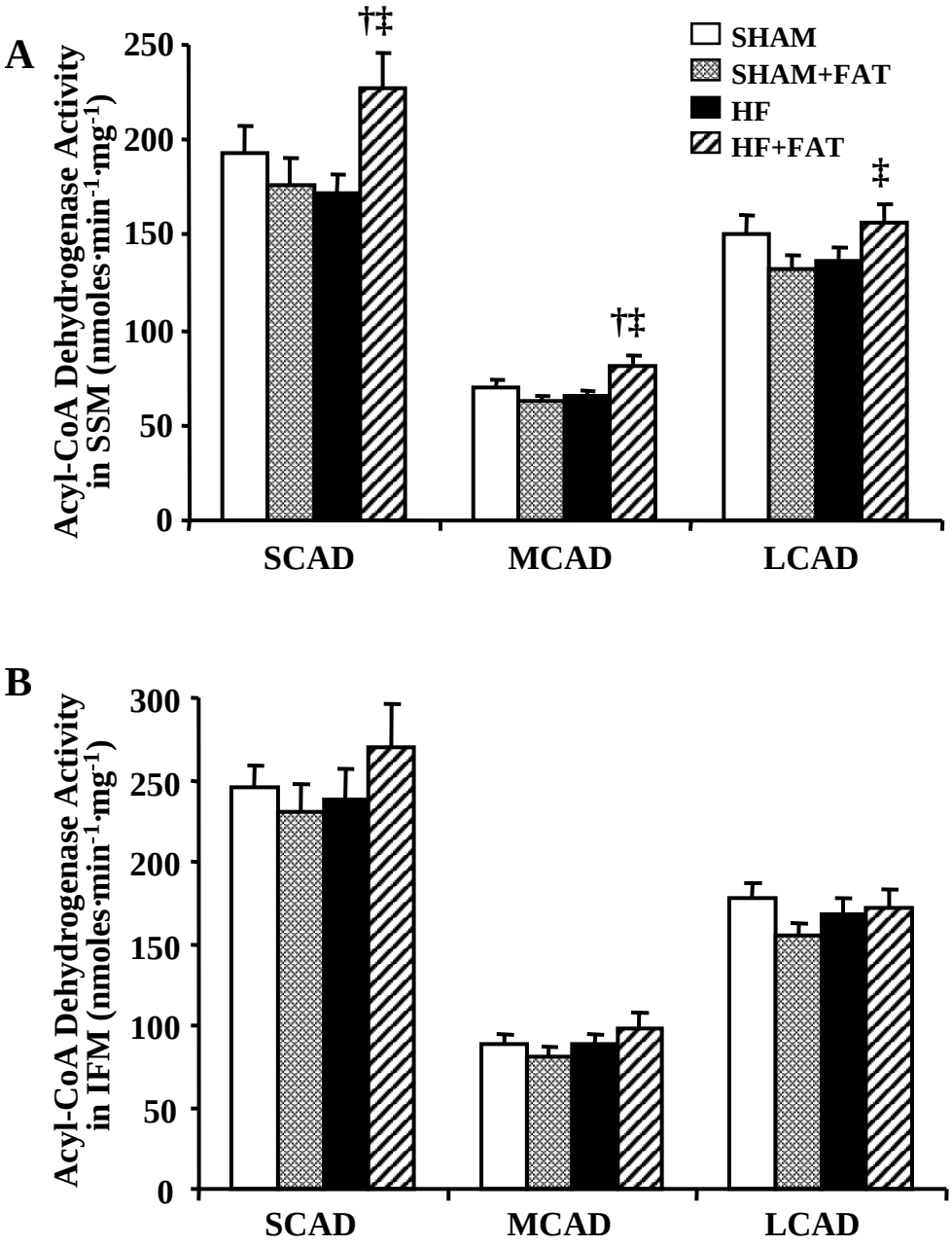

Figure 3-10. Activity of SCAD, MCAD, and LCAD in SSM (A) and IFM (B) of SHAM (n=10), SHAM+FAT (n=10), HF (n=9); and HF+FAT (n=10). Values are mean±SEM. *****P<0.05 compared to SHAM; †P<0.05 compared to SHAM+FAT; ‡P<0.05 compared to HF.

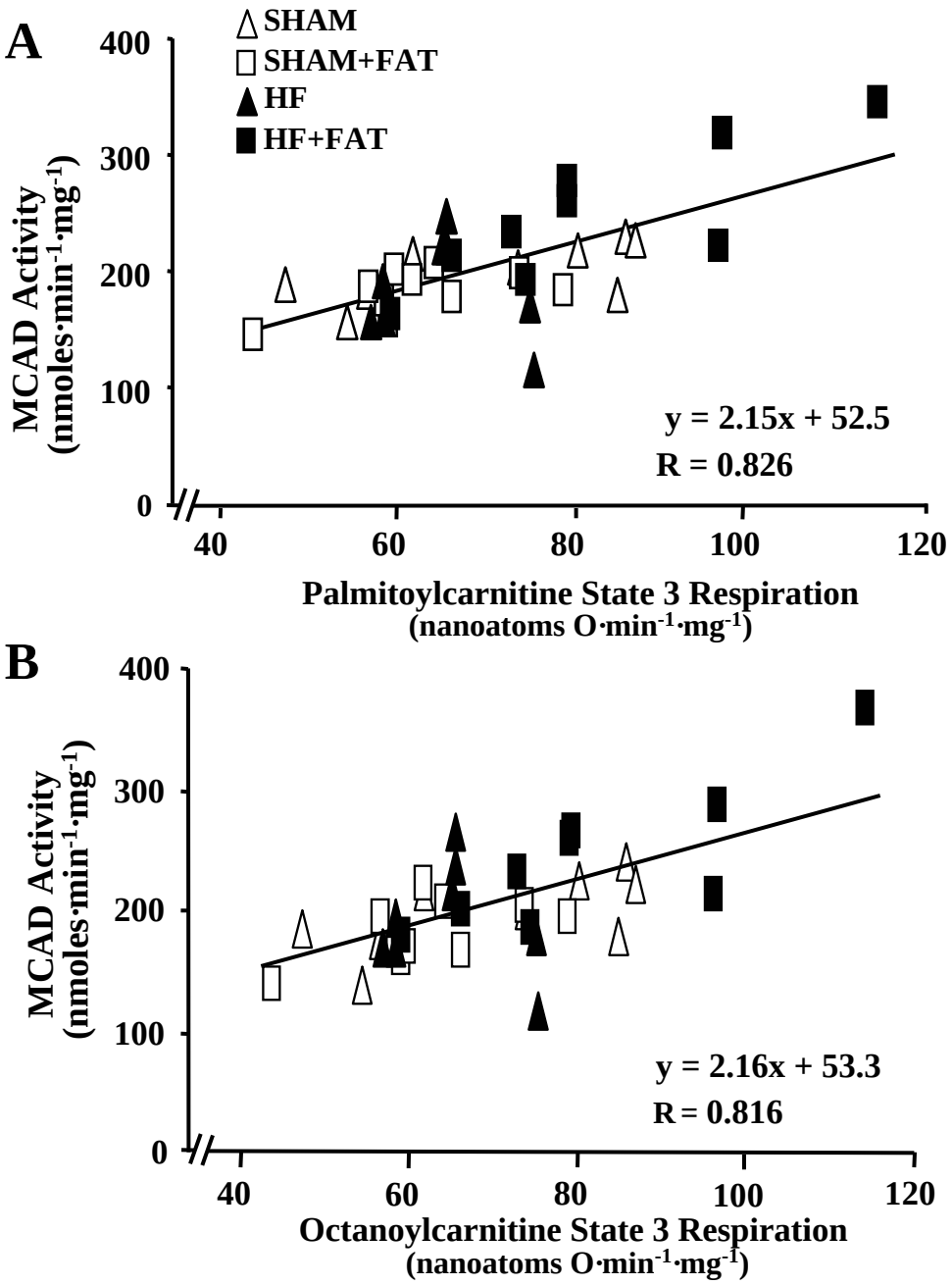

Figure 3-11. Activity of MCAD correlated to state 3 respiration in the SSM using (C) palmitoylcarnitine and (D) octanoylcarnitine.

CD36 and FATP-1 protein expression were not altered by heart failure or high fat diet (Figure 3-12), suggesting that the elevated state 3 respiration using lipid substrates and acyl-CoA dehydrogenase activity is not a result of changes in fatty acid uptake due to alterations in fatty acid transport protein content. However, because we measured protein expression of CD36 and FATP-1 in whole tissue, this assessment did not differentiate between CD36 and FATP-1 localized to the plasma membrane from that found in intracellular compartments.

3.3.9 Acylcarnitines

Total carnitine (carnitine+acylcarnitine) content in myocardial tissue was decreased in HF compared to SHAM (Figure 3-13A). High fat also decreased total carnitine in SHAM+FAT and HF+FAT compared to SHAM and HF, respectively. Because acylcarnitine content did not differ between groups, the decrease in total carnitine can be attributed to decreased carnitine. Additionally, the decreased carnitine content resulted in an increased acylcarnitine-to-carnitine ratio in both HF+FAT ($p<0.05$) and SHAM+FAT ($p<0.067$) (Figure 3-13A).

The content of individual acylcarnitines, palmitoylcarnitine, stearoylcarnitine, and oleoylcarnitine content were not altered in HF (Figure 3-13B). Only stearoylcarnitine was elevated in SHAM+FAT compared to SHAM. Palmitoylcarnitine, stearoylcarnitine, and oleoylcarnitine were elevated in HF+FAT compared to HF, but interestingly, stearoylcarnitine and oleoylcarnitine were elevated as well in HF+FAT compared to SHAM+FAT.

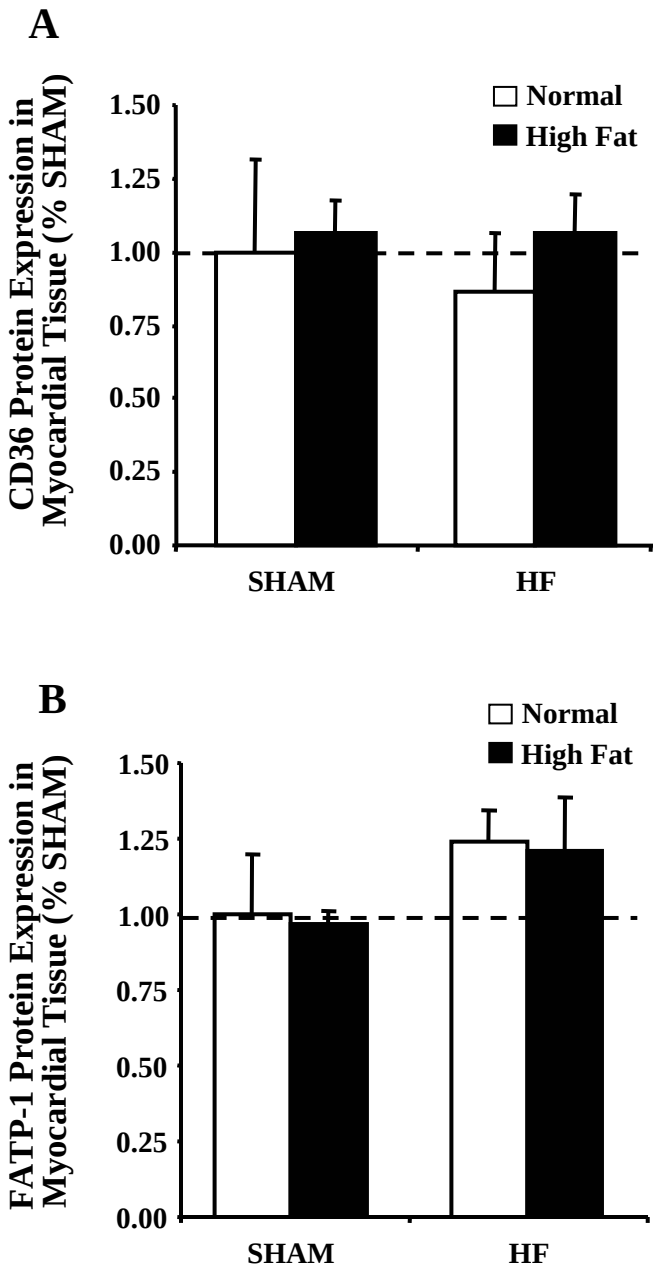

Figure 3-12. A) Densitometry of CD36 protein expression in myocardial tissue of SHAM (n=3), SHAM+FAT (n=9), HF (n=7), and HF+FAT (n=9). B) Densitometry of FATP-1 protein expression in myocardial tissue of SHAM (n=2), SHAM+FAT (n=4), HF (n=5), and HF+FAT (n=5). Each protein band was normalized to calsequestrin expression. Values are mean±SEM and expressed as a percentage of SHAM.

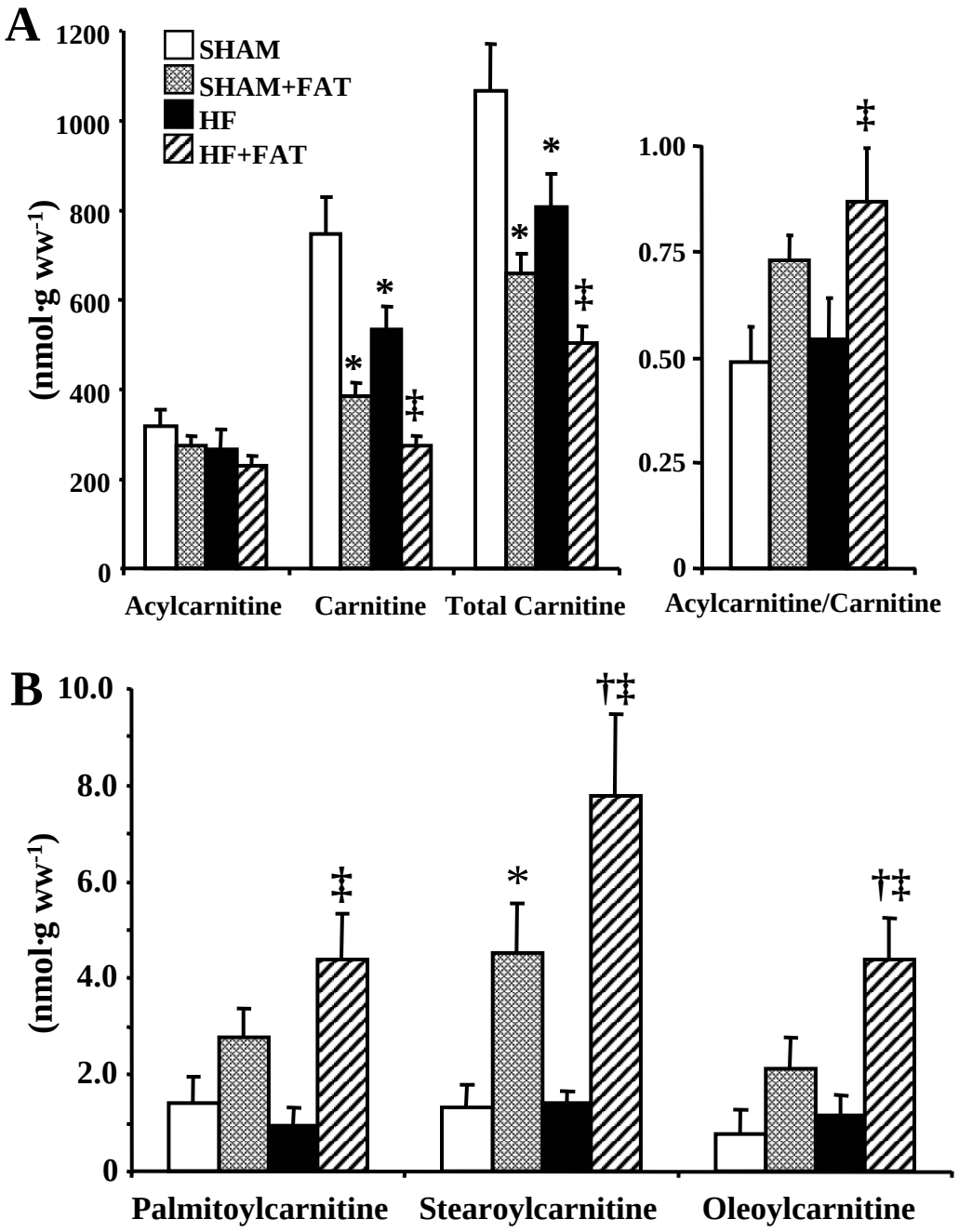

Figure 3-13. (A) Myocardial tissue carnitine, acylcarnitine, and total carnitine (carnitine+acylcarnitine) content, and acylcarnitine-to-carnitine ratio and (B) long-chain acylcarnitine content in SHAM (n=10), SHAM+FAT (n=10), HF (n=9); and HF+FAT (n=10). Values are mean±SEM. *****P<0.05 compared to SHAM; †P<0.05 compared to SHAM+FAT; ‡P<0.05 compared to HF.

3.4 Discussion

The present study shows that administration of a high fat diet in heart failure increased state 3 respiration and acyl-CoA dehydrogenase (SCAD, MCAD, and LCAD) activities, but did not affect the decreased mRNA expression of PPAR target genes associated with coronary artery ligation-induced heart failure. These findings are summarized in Table 3-6. The activity of acyl-CoA dehydrogenases showed a strong positive relationship with increased state 3 respiration when lipid respiratory substrates were utilized. These effects of high fat were not evident in normal animals, suggesting that the high fat effect on mitochondrial capacity is limited to heart failure. Additionally, eight weeks of high fat feeding in normal animals did not adversely affect mitochondrial respiration, the expression or activity of enzymes involved in β-oxidation, or LV contractile function.

We hypothesized that feeding rodents a high fat diet during heart failure would result in improved mitochondrial fatty acid oxidation and increased state 3 respiration by activating genes involved in fatty acid uptake and utilization. In the present study, mitochondrial respiration was assessed using the lipid substrates, octanoylcarnitine and palmitoylcarnitine. We observed increased state 3 respiration using both lipid substrates and an elevation in the activity of each chain-length specific acyl-CoA dehydrogenase. The first and rate-limiting step of β-oxidation, the α,β-dehydrogenation of fatty acyl-CoA is catalyzed by a family of flavoproteins known as the acyl-CoA dehydrogenases. This process shortens a fatty acid by two carbons resulting in acetyl-CoA units that enter the citric acid cycle and generate reducing equivalents that enter the ETC at complex I or complex II. A long-chain fatty acid would initially utilize LCAD, but as the fatty acid

Table 3-6. Summary of changes induced by high fat in heart failure.

	SSM	IFM	Myocardial Tissue
Protein Yield	↔	↓	n/a
Citrate Synthase	↑	↔	↔
mRNA and Protein Expression			
scad	n/a	n/a	↔
mcad	n/a	n/a	↔
lcad	n/a	n/a	↔
MCAD	n/a	n/a	↔
Acyl-CoA Dehydrogenase Activity			
SCAD	↑	↔	n/a
MCAD	↑	↔	n/a
LCAD	↑	↔	n/a
Mitochondrial State 3 Respiration			
Octanoylcarnitine	↑	↔	n/a
Palmitoylcarnitine	↑	↔	n/a
Glutamate	↑	↔	n/a

Depicted are changes in HF+FAT relative to HF only. ↑ increase, ↓ decrease, ↔ no change, n/a not applicable.

chain-length is repetitively shortened by two carbons, MCAD and SCAD would be utilized as well. Therefore, a diet high in long-chain fatty acids (like the one used in the present study) would provide substrate not just for LCAD, but for MCAD and SCAD as well. Both octanoylcarnitine and palmitoylcarnitine enter the mitochondria by the carnitine transport system; however, for the eight carbon octanoylcarnitine, the first step of β-oxidation is catalyzed by MCAD while the 16 carbon palmitoylcarnitine utilizes LCAD. We have shown an increase in state 3 respiration using both octanoylcarnitine and palmitoylcarnitine as respiratory substrates. Because both substrates enter the mitochondria by the same mechanism (the carnitine transport system), but utilize a different acyl-CoA dehydrogenase for the initial step of β-oxidation, this data indicates that the increase in state 3 respiration is not specific to the chain-length of a fatty acid.

In the current study, the activity of the acyl-CoA dehydrogenases was increased in the heart failure group fed high fat and showed a strong positive relationship with the increased state 3 respiration using lipid substrates. Previous studies using a direct PPARα agonist, clofibrate, also demonstrated good correlations between state 3 respiration using palmitoylcarnitine and acyl-CoA dehydrogenase activity in liver mitochondria (31; 139). We observed an elevation in the activity of each chain-length specific acyl-CoA dehydrogenase. One possible mechanism by which mitochondrial activity of these enzymes increases during high fat feeding may involve the absence of inhibitory effect of certain proteins on the activity of acyl-CoA dehydrogenases. Proteins that normally inhibit acyl-CoA dehydrogenase activity by targeting either the glutamate catalytic residue or the FAD cofactor (147) may themselves be altered so as to allow increased enzyme activity. It is also important to note that the activity of the fatty acid

oxidation enzymes SCAD, MCAD, and LCAD were increased in SSM despite no alterations in *scad, mcad*, *lcad*, or the protein expression of MCAD by high fat feeding in heart failure. These results suggest that the enhanced state 3 respiration observed in the present study was independent of transcriptional events, but might reflect post-transcriptional alterations of fatty acid oxidation enzymes. For example, Chu et al. (19) reported post-translational modifications of SCAD when fatty acid oxidation was up-regulated in an effort to meet the energetic demands of enhanced sarcoplasmic reticular calcium cycling and hyperdynamic function in phospholamban knockout hearts. These potential modifications affecting enzyme activity require further investigation to examine their potential role in the increased enzyme activity in heart failure following high fat feeding.

In general terms, the current transcriptional analysis is consistent with previous studies showing that genes promoting fatty acid oxidation are down-regulated in hypertrophy and failing hearts (34; 50; 71; 91; 108). As reported in this current investigation, however, alterations in mRNA expression are not always reflective of protein expression or enzyme activity. Morgan et al. (91) reported a repression of fatty acid oxidation genes in heart failure, but a 45% high fat diet initiated eight weeks following ligation surgery had no effect on mRNA, protein expression, or enzyme activity of MCAD. Interestingly, fenofibrate, a direct PPARα ligand, induced mRNA expression of PPARα regulated genes, as well as protein expression and activity of MCAD (91). In a study by Sack *et al.* (108), LV hypertrophy was associated with decreased mRNA expression of *mcad*, with no change in protein or enzyme activity. However, when LV hypertrophy progressed to heart failure, decreased *mcad* was

accompanied by decreased protein and enzyme activity. These data support the existence of a temporal pattern for changes in mRNA expression, protein expression, and enzyme activity that are contingent upon the stage or progression of contractile dysfunction/failure. In the present study, the level of LV dysfunction would be considered mild to moderate, having not progressed to more severe or decompensated heart failure; therefore, our findings may reflect an earlier stage in disease progression.

Conditions known to elevate fatty acid levels such as high fat feeding, obesity, and diabetes are associated with activation of PPARα and genes involved in fatty acid oxidation. We have shown that high fat feeding was associated with increased expression of *cte-1* and *pdk4,* but the expression of additional fatty acid-responsive genes (*pparα, pparδ, scad, mcad, lcad)* was not altered. Variations in the response of the PPARα regulated genes examined in this study might reflect differential effects of distinct fatty acid species (specifically in this study, palmitate, stearate, and oleate) on gene expression. For example, we have previously demonstrated that the fatty acid composition of high fat diets (specifically high saturated vs high unsaturated fat diets) differentially affected PPARα regulated gene expression (93). Furthermore, in isolated adult cardiomyocytes, long chain monounsaturated fatty acids such as oleate induced fatty acid responsive genes to a greater extent that long-chain saturated fatty acids such as palmitate (Young ME *et al.*, unpublished data). Future studies should examine the differential effects of distinct fatty acid species and also possible alternative pathways that could regulate the expression of genes involved in the transport and utilization of fatty acids.

It also was important to determine whether the effects of a high fat diet were independent of heart failure, so we assessed the effects of high saturated fat feeding on

mitochondrial and contractile function in normal rats. An interesting observation in the current study is that although high fat feeding in heart failure increased state 3 respiration and the activities of the acyl-CoA dehydrogenases, there was no effect on mitochondrial function or myocardial contractile dysfunction in normal rats. Additionally, expression of *anf*, a gene marker of LV hypertrophy, was not different in normal animals. These results indicate that the effects of high fat on cardiac mitochondrial function are exclusive to heart failure and that eight weeks of high fat feeding in normal animals does not adversely affect myocardial contractile or mitochondrial function. However, the effects of longer duration high fat feeding on mitochondrial and myocardial contractile function have not been assessed and should be a target of future investigations.

Carnitine facilitates the translocation of acyl-CoA across the mitochondrial membrane and buffers mitochondrial acetyl-CoA content (125). Decreased myocardial carnitine content is associated with hypertrophic cardiomyopathy (46; 112), whereas administration of propionyl L-carnitine prevents the decrease in cardiac work typically associated with hypertrophy (112). Consistent with these findings, free and total carnitine were decreased by heart failure (Figure 3-11). A high fat diet might be expected to induce a decrease in carnitine and a concomitant increase in acylcarnitine, but in our study high fat caused a further decrease in myocardial carnitine while acylcarnitine levels remained unchanged. The decreased carnitine content, though significant, is not severe enough to be associated with contractile dysfunction. However, the effect of the decreased carnitine content on the acylcarnitine-to-carnitine ratio is noteworthy. An increase in the acylcarnitine-to-carnitine ratio (which reflects the acyl-CoA-to-CoA ratio) indicates that more acyl-CoA is being synthesized than is being oxidized, and therefore serves as a

marker of metabolic distress. The increased acylcarnitine-to-carnitine ratio, evident in both SHAM+FAT and HF+FAT, may serve as an early indicator that mitochondrial dysfunction would be evident with a longer duration of high fat feeding.

In summary, our results clearly show that state 3 respiration and acyl-CoA dehydrogenase (SCAD, MCAD, and LCAD) activities are elevated in high fat fed heart failure animals. High fat attenuated a heart failure-induced repression of only a few of the PPAR target genes. Although high fat feeding did not influence expression of the acyl-CoA dehydrogenases investigated, activity of these enzymes are increased and show a strong positive relationship with state 3 respiration using lipid substrates. These effects of high fat on mitochondrial and contractile function are not evident in normal animals, indicating the high fat effect on mitochondrial capacity is specific to heart failure. The increased activity of the acyl-CoA dehydrogenases may be due to a decrease of inhibitory proteins or a post-translational modification of these enzymes, and requires further investigation to examine their potential role in the increased mitochondrial capacity associated with high fat fed heart failure animals.

Chapter 4

Summary and Future Directions

4.1 Primary Findings

The primary findings of this study are as follows:

1) Administration of a high saturated fat diet in a model of coronary artery ligation-induced heart failure did not adversely affect LV contractile function or the progression of LV remodeling. We originally hypothesized that high fat feeding would exacerbate the progression of LV dysfunction in heart failure, however given the findings that mitochondrial function was improved in this model, it was not suprising that myocardial contractile function was not decreased.
2) Administration of a high saturated fat diet in a model of coronary artery ligation-induced heart failure increased mitochondrial state 3 respiration using lipid substrates palmitoyl-CoA, palmitoylcarnitine, and octanoylcarnitine. These findings indicate that the increase in state 3 respiration is not due to alterations in the activity of CPT-I, nor is it specific to the chain-length fatty acid. Additionally, state 3 respiration was elevated using glutamate, but no

other complex specific substrates, indicating that the elevated state 3 respiration is due to a mitochondrial alteration upstream of the ETC.

3) Administration of a high saturated fat diet in heart failure increased acyl-CoA dehydrogenase (SCAD, MCAD, and LCAD) activities, but did not affect the decreased mRNA expression of PPAR target genes associated with heart failure. The activity of acyl-CoA dehydrogenases showed a strong positive relationship with increased state 3 respiration when lipid respiratory substrates were utilized. The acyl-CoA dehydrogenase family of proteins catalyze the first and rate-limiting step of β-oxidation, a step in the fatty acid utilization pathway that is located downstream of CPT-I and upstream of the ETC. These findings indicate that the elevated state 3 respiration is at least partially due to an increase in acyl-CoA dehydrogenase activity. This increased acyl-CoA dehydrogenase activity is not specific to a particular chain-length fatty acid and is not due to increased mRNA (SCAD, MCAD, or LCAD) or protein expression (MCAD).
4) Elevations in myocardial ceramide in an *in vivo* model of high fat feeding in heart failure were not accompanied by any evidence of a lipotoxic effect on either myocardial contractile or mitochondrial function.
5) Eight weeks of high fat feeding in normal animals did not adversely affect LV contractile function or remodeling, mitochondrial respiration, ETC complex activities, or the expression or activity of enzymes involved in β-oxidation, suggesting that the high fat effect on mitochondrial capacity is limited to heart failure.

6) Administration of high saturated fat diet for two weeks prior to coronary artery ligation increased surgical mortality rate in saturated fat fed compared to normal chow fed rats. These findings further support the concept that the beneficial effects of high saturated fat feeding on mitochondrial function is limited to an injury model.
7) Neither heart failure nor high fat feeding altered the morphology of isolated SSM and IFM. Mitochondrial shape, size, and density of both SSM and IFM within the myocardial tissue also were not altered by heart failure or high fat feeding. Given the improved mitochondrial function, we would expect no adverse alterations in mitochondrial morphology.

4.2 Future Directions

Given the provocative nature of our findings there are a number of questions that should be addressed in future projects.

4.2.1 Mechanism for Increased Acyl-CoA Dehydrogenase Activity

We observed an elevation in the activity of each chain-length specific acyl-CoA dehydrogenase only in heart failure animals fed a high fat diet. One possible mechanism by which mitochondrial activity of these enzymes increases during high fat feeding may involve the absence of inhibitory effect of certain proteins on the activity of acyl-CoA dehydrogenases. Proteins that normally inhibit acyl-CoA dehydrogenase activity by targeting either the glutamate catalytic residue or the FAD cofactor (147) may themselves be altered so as to allow increased enzyme activity. It is also important to note that the

activity of the fatty acid oxidation enzymes SCAD, MCAD, and LCAD were increased in SSM despite no alterations in *scad, mcad*, *lcad*, or the protein expression of MCAD. These results suggest that the enhanced state 3 respiration observed in the present study was independent of transcriptional events, but might reflect post-transcriptional alterations of fatty acid oxidation enzymes. Likely candidates for such post-transcriptional alterations are the glutamate catalytic residue and the FAD cofactor. However, as there are currently no studies that have reported post-transcriptional modifications that act to increase acyl-CoA dehydrogenase activity this is an important area for future investigation.

4.2.2 High Fat Diet and Substrate Utilization in Heart Failure

The current study examined the effects of high saturated fat feeding on isolated mitochondrial function using lipid and non-lipid respiratory substrates. Previous studies have shown that genes promoting fatty acid oxidation are down-regulated in hypertrophied and failing hearts (34; 50; 71; 91; 108). We have shown that heart failure animals fed a high fat diet have elevated mitochondrial state 3 respiration when supplied lipid substrates. Our data suggests that the mitochondria of high fat fed heart failure animals have an increased capacity for fatty acid utilization (increased state 3 respiration and acyl-CoA dehydrogenase activities). Additionally, we have shown that high fat feeding increased plasma free fatty acids, while plasma glucose concentrations were not altered. However, the current study did not assess whether high fat feeding alters the substrate preferences of the failing heart. Though the mitochondria have an increased capacity for fatty acid utilization, and the heart has an increased supply of fatty acids in

the plasma, it is unknown whether fatty acid oxidation is increased in the heart failure animals fed a high fat diet. This is an important area of future investigation.

4.2.3 The Role of High Fat Feeding in Increased Surgical Mortality

A novel finding in this study was that administration of high saturated fat diet for two weeks prior to coronary artery ligation resulted in an increased surgical mortality in saturated fat fed (30/45, 67%) compared to normal chow fed rats (9/24, 38%), however the mechanism for this effect was not investigated. A potential mechanism for the increased sudden death may be the accumulation of acylcarnitines. CPT-I converts fatty acyl-CoA to acylcarnitine thereby enabling transport of fatty acids across the inner mitochondrial membrane. Upon entering the mitochondria, the acylcarnitine is converted back to fatty acyl-CoA by CPT-II and enters β-oxidation. In conditions such as high fat feeding, if the increased availability of acylcarnitines is not matched by an increase in utilization through pathways such as β-oxidation, then acylcarnitines will accumulate. The excess fatty acids and acylcarnitines can alter the electrical activity of the heart (82; 95; 102) and the resulting arrhythmias could compound the effects of a myocardial infarction and increase the risk of sudden death. Future studies should examine the mechanism by which high fat feeding increases surgical mortality.

4.2.4 Specificity of Findings to Model Used

The protective effects of high fat on cardiac function has been shown in other animal models of LV dysfunction and heart failure (14; 93), however mitochondrial function was not assessed in these studies. Altered mitochondrial function has been

described in the rat model of coronary artery ligation-induced heart failure (56), the cardiomyopathic Syrian hamster model (46), the canine microembolization-induced model of heart failure (116), ischemia (8; 54; 75), and a pacing-induced canine model of heart failure (53; 85). It is important to note that defects in mitochondrial structure and function may be dependent upon the severity of LV dysfunction. The current study assessed mitochondrial function in hearts with what would be characterized as mild-to-moderate contractile dysfunction. However, it has been shown that myocardial substrate utilization favors glucose to a greater degree as myocardial dysfunction progresses (108). The impact of high fat feeding on myocardial contractile and mitochondrial function at a stage of heart failure where the heart prefers glucose as a fuel source was not assessed in the current study. Future studies should investigate the impact of a high fat diet on mitochondrial function in a model that represents a more decompensated stage of heart failure. Similarly, the current investigation assessed myocardial contractile function under conditions of rest. Future studies should evaluate *in vivo* cardiovascular responses to conditions of stress as would occur with exercise or alterations in preload.

4.2.5 Time Course for Alterations Induced by High Fat

We have shown that eight weeks of high fat feeding increased mitochondrial function in a ligation-induced model of heart failure. We did not determine whether this was an acute effect due to the presence of high fat during the recovery period immediately following the surgery or whether these effects were a result of prolonged high fat feeding. Additionally, the effects of high fat feeding for a duration longer than eight weeks on myocardial contractile and mitochondrial function have not been

examined. As noted in Chapter 3, an increase in the acylcarnitine-to-carnitine ratio serves as a marker of metabolic distress. The increased acylcarnitine-to-carnitine ratio, evident in both high fat fed groups, may serve as an early indicator that to this timepoint the mitochondria have adapted to handle the increased fat load, but that with a longer duration of high fat feeding mitochondrial dysfunction would be evident. Future studies should establish a time-course for the effects of high fat on myocardial contractile and mitochondrial function.

Our studies specifically assessed the impact of high fat feeding on the heart. While we have shown that high fat improved mitochondrial function and prevented the progression of LV dysfunction in heart failure, we did not assess the effects of high fat on other tissues. Obesity and elevated blood lipid levels are associated with other disease conditions that include hepatic steatosis, type 2 diabetes, and coronary artery disease (1; 6), all of which when left untreated are associated with increased rates of morbidity and mortality. Therefore, time-course studies should also assess the effects of long-term high fat feeding on extra-myocardial tissues.

4.2.6 Diet Composition- The Role of Carbohydrates

An inevitable result of producing a diet high in fat is that the carbohydrate content of the diet is decreased. Recent studies have shown a high fructose diet exacerbated LV dysfunction and increased mortality in a Dahl Salt-Sensitive rat model of hypertension (114) and a mouse model of transverse aortic constriction induced LV hypertrophy (13), suggesting that the protective effects of high fat may actually be a result of a low carbohydrate diet. In fact, the carbohydrate composition of the diet can play an essential

role. These effects of a high fructose diet were not evident with a diet that was composed of complex carbohydrates (13; 114). The effects of a high carbohydrate diet on mitochondrial oxidative phosphorylation and ETC activities have not been examined and should be the focus of future investigations.

4.3 Summary

These studies have shown that administration of a high saturated fat diet in a model of coronary artery ligation-induced heart failure did not adversely affect LV contractile function or the progression of LV remodeling. Elevations in myocardial ceramide were not accompanied by any evidence of a lipotoxic effect on either myocardial contractile or mitochondrial function. In fact, mitochondrial state 3 respiration using lipid substrates and acyl-CoA dehydrogenase (SCAD, MCAD, and LCAD) activities were elevated with high fat feeding in heart failure. Though the activity of acyl-CoA dehydrogenases showed a strong positive relationship with increased state 3 respiration, these alterations cannot be accounted for by increased mRNA (SCAD, MCAD, or LCAD) or protein expression (MCAD). Interestingly, these effects of high fat on mitochondrial function were not evident in normal animals fed a high fat diet suggesting that the high fat effect on mitochondrial capacity is limited to heart failure.

Reference List

1. American Heart Association. Heart Disease and Stroke Statistics - 2008 Update. 2008. Dallas, TX, American Heart Association.

2. **Argaud L, Prigent AF, Chalabreysse L, Loufouat J, Lagarde M and Ovize M**. Ceramide in the antiapoptotic effect of ischemic preconditioning. *Am J Physiol Heart Circ Physiol* 286: H246-H251, 2004.

3. **Atkinson LL, Fischer MA and Lopaschuk GD**. Leptin activates cardiac fatty acid oxidation independent of changes in the AMP-activated protein kinase-acetyl-CoA carboxylase-malonyl-CoA axis. *J Biol Chem* 277: 29424-29430, 2002.

4. **Baily RG, Lehman JC, Gubin SS and Musch TI**. Non-invasive assessment of ventricular damage in rats with myocardial infarction. *Cardiovasc Res* 27: 851-855, 1993.

5. **Barger PM and Kelly DP**. PPAR signaling in the control of cardiac energy metabolism. *Trends Cardiovasc Med* 10: 238-245, 2000.

6. **Begriche K, Igoudjil A, Pessayre D and Fromenty B**. Mitochondrial dysfunction in NASH: causes, consequences and possible means to prevent it. *Mitochondrion* 6: 1-28, 2006.

7. **Belke DD, Betuing S, Tuttle MJ, Graveleau C, Young ME, Pham M, Zhang D, Cooksey RC, McClain DA, Litwin SE, Taegtmeyer H, Severson D, Kahn CR and Abel ED**. Insulin signaling coordinately regulates cardiac size, metabolism, and contractile protein isoform expression. *J Clin Invest* 109: 629-639, 2002.

8. **Borutaite V, Budriunaite A, Morkuniene R and Brown GC**. Release of mitochondrial cytochrome c and activation of cytosolic caspases induced by myocardial ischaemia. *Biochim Biophys Acta* 1537: 101-109, 2001.

9. **Buchwald A, Till H, Unterberg C, Oberschmidt R, Figulla HR and Wiegand V**. Alterations of the mitochondrial respiratory chain in human dilated cardiomyopathy. *Eur Heart J* 11: 509-516, 1990.

10. **Bugger H and Abel ED**. Molecular mechanisms for myocardial mitochondrial dysfunction in the metabolic syndrome. *Clin Sci (Lond)* 114: 195-210, 2008.

11. **Chance B and Williams GR**. Respiratory enzymes in oxidative phosphorylation. I. Kinetics of oxygen utilization. *J Biol Chem* 217: 383-393, 1955.

12. **Chatelut M, Leruth M, Harzer K, Dagan A, Marchesini S, Gatt S, Salvayre R, Courtoy P and Levade T**. Natural ceramide is unable to escape the lysosome, in contrast to a fluorescent analogue. *FEBS Lett* 426: 102-106, 1998.

13. **Chess DJ, Lei B, Hoit BD, Azimzadeh AM and Stanley WC**. Deleterious effects of sugar and protective effects of starch on cardiac remodeling, contractile dysfunction, and mortality in response to pressure overload. *Am J Physiol Heart Circ Physiol* 293: H1853-H1860, 2007.

14. **Chess DJ, Lei B, Hoit BD, Azimzadeh AM and Stanley WC**. Effects of a high saturated fat diet on cardiac hypertrophy and dysfunction in response to pressure overload. *J Card Fail* 14: 82-88, 2008.

15. **Chiu HC, Kovacs A, Blanton RM, Han X, Courtois M, Weinheimer CJ, Yamada KA, Brunet S, Xu H, Nerbonne JM, Welch MJ, Fettig NM, Sharp TL, Sambandam N, Olson KM, Ory DS and Schaffer JE**. Transgenic expression of fatty acid transport protein 1 in the heart causes lipotoxic cardiomyopathy. *Circ Res* 96: 225-233, 2005.

16. **Chiu HC, Kovacs A, Ford DA, Hsu FF, Garcia R, Herrero P, Saffitz JE and Schaffer JE**. A novel mouse model of lipotoxic cardiomyopathy. *J Clin Invest* 107: 813-822, 2001.

17. **Chomczynski P and Sacchi N**. Single-step method of RNA isolation by acid guanidinium thiocyanate-phenol-chloroform extraction. *Anal Biochem* 162: 156-159, 1987.

18. **Christoffersen C, Bollano E, Lindegaard ML, Bartels ED, Goetze JP, Andersen CB and Nielsen LB**. Cardiac lipid accumulation associated with diastolic dysfunction in obese mice. *Endocrinology* 144: 3483-3490, 2003.

19. **Chu G, Kerr JP, Mitton B, Egnaczyk GF, Vazquez JA, Shen M, Kilby GW, Stevenson TI, Maggio JE, Vockley J, Rapundalo ST and Kranias EG**. Proteomic analysis of hyperdynamic mouse hearts with enhanced sarcoplasmic reticulum calcium cycling. *FASEB J* 18: 1725-1727, 2004.

20. **Cocco T, Di Paola M, Papa S and Lorusso M**. Arachidonic acid interaction with the mitochondrial electron transport chain promotes reactive oxygen species generation. *Free Radic Biol Med* 27: 51-59, 1999.

21. **Davos CH, Doehner W, Rauchhaus M, Cicoira M, Francis DP, Coats AJ, Clark AL and Anker SD**. Body mass and survival in patients with chronic heart failure without cachexia: the importance of obesity. *J Card Fail* 9: 29-35, 2003.

22. **Di Paola M, Cocco T and Lorusso M**. Ceramide interaction with the respiratory chain of heart mitochondria. *Biochemistry* 39: 6660-6668, 2000.

23. **Di Paola M, Zaccagnino P, Montedoro G, Cocco T and Lorusso M**. Ceramide induces release of pro-apoptotic proteins from mitochondria by either a Ca2+ -dependent or a Ca2+ -independent mechanism. *J Bioenerg Biomembr* 36: 165-170, 2004.

24. **Diniz YS, Cicogna AC, Padovani CR, Santana LS, Faine LA and Novelli EL**. Diets rich in saturated and polyunsaturated fatty acids: metabolic shifting and cardiac health. *Nutrition* 20: 230-234, 2004.

25. **Estabrook R**. Mitochondrial respiratory control and polarographic measurement of ADP/O ratios. In: Methods in Enzymology, 1967, p. 41-47.

26. **Finck BN**. The PPAR regulatory system in cardiac physiology and disease. *Cardiovasc Res* 73: 269-277, 2007.

27. **Finck BN, Han X, Courtois M, Aimond F, Nerbonne JM, Kovacs A, Gross RW and Kelly DP**. A critical role for PPARalpha-mediated lipotoxicity in the pathogenesis of diabetic cardiomyopathy: modulation by dietary fat content. *Proc Natl Acad Sci U S A* 100: 1226-1231, 2003.

28. **Finck BN, Lehman JJ, Leone TC, Welch MJ, Bennett MJ, Kovacs A, Han X, Gross RW, Kozak R, Lopaschuk GD and Kelly DP**. The cardiac phenotype induced by PPARalpha overexpression mimics that caused by diabetes mellitus. *J Clin Invest* 109: 121-130, 2002.

29. **Fonarow GC**. The relationship between body mass index and mortality in patients hospitalized with acute decompensated heart failure. *Am Heart J* 154: e21, 2007.

30. **Forman BM, Chen J and Evans RM**. Hypolipidemic drugs, polyunsaturated fatty acids, and eicosanoids are ligands for peroxisome proliferator-activated receptors alpha and delta. *Proc Natl Acad Sci U S A* 94: 4312-4317, 1997.

31. **Furuta S, Miyazawa S and Hashimoto T**. Induction of acyl-CoA dehydrogenases and electron transfer flavoprotein and their roles in fatty acid oxidation in rat liver mitochondria. *J Biochem (Tokyo)* 90: 1751-1756, 1981.

32. **Galante YM and Hatefi Y**. Resolution of complex I and isolation of NADH dehydrogenase and an iron--sulfur protein. *Methods Enzymol* 53: 15-21, 1978.

33. **Garcia-Ruiz C, Colell A, Mari M, Morales A and Fernandez-Checa JC**. Direct effect of ceramide on the mitochondrial electron transport chain leads to generation of reactive oxygen species. Role of mitochondrial glutathione. *J Biol Chem* 272: 11369-11377, 1997.

34. **Garnier A, Fortin D, Delomenie C, Momken I, Veksler V and Ventura-Clapier R**. Depressed mitochondrial transcription factors and oxidative capacity in rat failing cardiac and skeletal muscles. *J Physiol* 551: 491-501, 2003.

35. **Ghafourifar P, Klein SD, Schucht O, Schenk U, Pruschy M, Rocha S and Richter C**. Ceramide induces cytochrome c release from isolated mitochondria. Importance of mitochondrial redox state. *J Biol Chem* 274: 6080-6084, 1999.

36. **Ghisla S and Thorpe C**. Acyl-CoA dehydrogenases. A mechanistic overview. *Eur J Biochem* 271: 494-508, 2004.

37. **Gibson UE, Heid CA and Williams PM**. A novel method for real time quantitative RT-PCR. *Genome Res* 6: 995-1001, 1996.

38. **Gudz TI, Tserng KY and Hoppel CL**. Direct inhibition of mitochondrial respiratory chain complex III by cell-permeable ceramide. *J Biol Chem* 272: 24154-24158, 1997.

39. **Halvorsen B, Rustan AC, Madsen L, Reseland J, Berge RK, Sletnes P and Christiansen EN**. Effects of long-chain monounsaturated and n-3 fatty acids on fatty acid oxidation and lipid composition in rats. *Ann Nutr Metab* 45: 30-37, 2001.

40. **Han XX, Chabowski A, Tandon NN, Calles-Escandon J, Glatz JF, Luiken JJ and Bonen A**. Metabolic challenges reveal impaired fatty acid metabolism and translocation of FAT/CD36 but not FABPpm in obese Zucker rat muscle. *Am J Physiol Endocrinol Metab* 293: E566-E575, 2007.

41. **Hanaichi T, Sato T, Iwamoto T, Malavasi-Yamashiro J, Hoshino M and Mizuno N**. A stable lead by modification of Sato's method. *J Electron Microsc (Tokyo)* 35: 304-306, 1986.

42. **Hickson-Bick DL, Buja ML and McMillin JB**. Palmitate-mediated alterations in the fatty acid metabolism of rat neonatal cardiac myocytes. *J Mol Cell Cardiol* 32: 511-519, 2000.

43. **Higa M, Zhou YT, Ravazzola M, Baetens D, Orci L and Unger RH**. Troglitazone prevents mitochondrial alterations, beta cell destruction, and diabetes in obese prediabetic rats. *Proc Natl Acad Sci U S A* 96: 11513-11518, 1999.

44. **Hoppel C, DiMarco JP and Tandler B**. Riboflavin and rat hepatic cell structure and function. Mitochondrial oxidative metabolism in deficiency states. *J Biol Chem* 254: 4164-4170, 1979.

45. **Hoppel CL, Kerr DS, Dahms B and Roessmann U**. Deficiency of the reduced nicotinamide adenine dinucleotide dehydrogenase component of complex I of mitochondrial electron transport. Fatal infantile lactic acidosis and hypermetabolism with skeletal-cardiac myopathy and encephalopathy. *J Clin Invest* 80: 71-77, 1987.

46. **Hoppel CL, Tandler B, Parland W, Turkaly JS and Albers LD**. Hamster cardiomyopathy. A defect in oxidative phosphorylation in the cardiac interfibrillar mitochondria. *J Biol Chem* 257: 1540-1548, 1982.

47. **Horwich TB, Fonarow GC, Hamilton MA, MacLellan WR, Woo MA and Tillisch JH**. The relationship between obesity and mortality in patients with heart failure. *J Am Coll Cardiol* 38: 789-795, 2001.

48. **Howard BV, Van Horn L, Hsia J, Manson JE, Stefanick ML, Wassertheil-Smoller S, Kuller LH, LaCroix AZ, Langer RD, Lasser NL, Lewis CE, Limacher MC, Margolis KL, Mysiw WJ, Ockene JK, Parker LM, Perri MG, Phillips L, Prentice RL, Robbins J, Rossouw JE, Sarto GE, Schatz IJ, Snetselaar LG, Stevens VJ, Tinker LF, Trevisan M, Vitolins MZ, Anderson GL, Assaf AR, Bassford T, Beresford SA, Black HR, Brunner RL, Brzyski RG, Caan B, Chlebowski RT, Gass M, Granek I, Greenland P, Hays J, Heber D, Heiss G, Hendrix SL, Hubbell FA, Johnson KC and Kotchen JM**. Low-fat dietary pattern and risk of cardiovascular disease: the Women's Health Initiative Randomized Controlled Dietary Modification Trial. *JAMA* 295: 655-666, 2006.

49. **Hunt SA, Baker DW, Chin MH, Cinquegrani MP, Feldman AM, Francis GS, Ganiats TG, Goldstein S, Gregoratos G, Jessup ML, Noble RJ, Packer M, Silver MA, Stevenson LW, Gibbons RJ, Antman EM, Alpert JS, Faxon DP, Fuster V, Gregoratos G, Jacobs AK, Hiratzka LF, Russell RO and Smith SC**. ACC/AHA guidelines for the evaluation and management of chronic heart failure in the adult: executive summary. *J Heart Lung Transplant* 21: 189-203, 2002.

50. **Huss JM and Kelly DP**. Nuclear receptor signaling and cardiac energetics. *Circ Res* 95: 568-578, 2004.

51. **Huss JM and Kelly DP**. Mitochondrial energy metabolism in heart failure: a question of balance. *J Clin Invest* 115: 547-555, 2005.

52. **Ide T, Tsutsui H, Hayashidani S, Kang D, Suematsu N, Nakamura K, Utsumi H, Hamasaki N and Takeshita A**. Mitochondrial DNA damage and dysfunction associated with oxidative stress in failing hearts after myocardial infarction. *Circ Res* 88: 529-535, 2001.

53. **Ide T, Tsutsui H, Kinugawa S, Utsumi H, Kang D, Hattori N, Uchida K, Arimura K, Egashira K and Takeshita A**. Mitochondrial electron transport complex I is a potential source of oxygen free radicals in the failing myocardium. *Circ Res* 85: 357-363, 1999.

54. **Iwai T, Tanonaka K, Inoue R, Kasahara S, Kamo N and Takeo S**. Mitochondrial damage during ischemia determines post-ischemic contractile dysfunction in perfused rat heart. *J Mol Cell Cardiol* 34: 725-738, 2002.

55. **Jarreta D, Orus J, Barrientos A, Miro O, Roig E, Heras M, Moraes CT, Cardellach F and Casademont J**. Mitochondrial function in heart muscle from patients with idiopathic dilated cardiomyopathy. *Cardiovasc Res* 45: 860-865, 2000.

56. **Javadov S, Huang C, Kirshenbaum L and Karmazyn M**. NHE-1 inhibition improves impaired mitochondrial permeability transition and respiratory function during postinfarction remodelling in the rat. *J Mol Cell Cardiol* 38: 135-143, 2005.

57. **Kantor P**. Myocardial Energy Metabolism. In: Heart Physiology and Pathophysiology, edited by Opie L. Orlando, FL: Academic, 2004, p. 543-569.

58. **Karbowska J and Kochan Z**. Role of adiponectin in the regulation of carbohydrate and lipid metabolism. *J Physiol Pharmacol* 57 Suppl 6: 103-113, 2006.

59. **Kenchaiah S, Narula J and Vasan RS**. Risk factors for heart failure. *Med Clin North Am* 88: 1145-1172, 2004.

60. **Kenchaiah S, Pocock SJ, Wang D, Finn PV, Zornoff LA, Skali H, Pfeffer MA, Yusuf S, Swedberg K, Michelson EL, Granger CB, McMurray JJ and Solomon SD**. Body mass index and prognosis in patients with chronic heart failure: insights from the Candesartan in Heart failure: Assessment of Reduction in Mortality and morbidity (CHARM) program. *Circulation* 116: 627-636, 2007.

61. **Kerner J and Hoppel C**. Fatty acid import into mitochondria. *Biochim Biophys Acta* 1486: 1-17, 2000.

62. **Kerner J, Turkaly PJ, Minkler PE and Hoppel CL**. Aging skeletal muscle mitochondria in the rat: decreased uncoupling protein-3 content. *Am J Physiol Endocrinol Metab* 281: E1054-E1062, 2001.

63. **Kong JY and Rabkin SW**. Palmitate-induced cardiac apoptosis is mediated through CPT-1 but not influenced by glucose and insulin. *Am J Physiol Heart Circ Physiol* 282: H717-H725, 2002.

64. **Kong JY and Rabkin SW**. Reduction of palmitate-induced cardiac apoptosis by fenofibrate. *Mol Cell Biochem* 258: 1-13, 2004.

65. **Koonen DP, Glatz JF, Bonen A and Luiken JJ**. Long-chain fatty acid uptake and FAT/CD36 translocation in heart and skeletal muscle. *Biochim Biophys Acta* 1736: 163-180, 2005.

66. **Krahenbuhl S, Chang M, Brass EP and Hoppel CL**. Decreased activities of ubiquinol:ferricytochrome c oxidoreductase (complex III) and ferrocytochrome c:oxygen oxidoreductase (complex IV) in liver mitochondria from rats with hydroxycobalamin[c-lactam]-induced methylmalonic aciduria. *J Biol Chem* 266: 20998-21003, 1991.

67. **Krahenbuhl S, Talos C, Wiesmann U and Hoppel CL**. Development and evaluation of a spectrophotometric assay for complex III in isolated mitochondria, tissues and fibroblasts from rats and humans. *Clin Chim Acta* 230: 177-187, 1994.

68. **Lavie CJ, Osman AF, Milani RV and Mehra MR**. Body composition and prognosis in chronic systolic heart failure: the obesity paradox. *Am J Cardiol* 91: 891-894, 2003.

69. **Lee Y, Naseem RH, Duplomb L, Park BH, Garry DJ, Richardson JA, Schaffer JE and Unger RH**. Hyperleptinemia prevents lipotoxic cardiomyopathy in acyl CoA synthase transgenic mice. *Proc Natl Acad Sci U S A* 101: 13624-13629, 2004.

70. **Lee Y, Wang MY, Kakuma T, Wang ZW, Babcock E, McCorkle K, Higa M, Zhou YT and Unger RH**. Liporegulation in diet-induced obesity. The antisteatotic role of hyperleptinemia. *J Biol Chem* 276: 5629-5635, 2001.

71. **Lehman JJ, Barger PM, Kovacs A, Saffitz JE, Medeiros DM and Kelly DP**. Peroxisome proliferator-activated receptor gamma coactivator-1 promotes cardiac mitochondrial biogenesis. *J Clin Invest* 106: 847-856, 2000.

72. **Lesnefsky EJ, Chen Q, Slabe TJ, Stoll MS, Minkler PE, Hassan MO, Tandler B and Hoppel CL**. Ischemia, rather than reperfusion, inhibits respiration through cytochrome oxidase in the isolated, perfused rabbit heart: role of cardiolipin. *Am J Physiol Heart Circ Physiol* 287: H258-H267, 2004.

73. **Lesnefsky EJ and Hoppel CL**. Ischemia-reperfusion injury in the aged heart: role of mitochondria. *Arch Biochem Biophys* 420: 287-297, 2003.

74. **Lesnefsky EJ, Moghaddas S, Tandler B, Kerner J and Hoppel CL**. Mitochondrial dysfunction in cardiac disease: ischemia--reperfusion, aging, and heart failure. *J Mol Cell Cardiol* 33: 1065-1089, 2001.

75. **Lesnefsky EJ, Tandler B, Ye J, Slabe TJ, Turkaly J and Hoppel CL**. Myocardial ischemia decreases oxidative phosphorylation through cytochrome oxidase in subsarcolemmal mitochondria. *Am J Physiol* 273: H1544-H1554, 1997.

76. **Leverve XM**. Mitochondrial function and substrate availability. *Crit Care Med* 35: S454-S460, 2007.

77. **Li YY, Chen D, Watkins SC and Feldman AM**. Mitochondrial abnormalities in tumor necrosis factor-alpha-induced heart failure are associated with impaired DNA repair activity. *Circulation* 104: 2492-2497, 2001.

78. **Liao Y, Takashima S, Maeda N, Ouchi N, Komamura K, Shimomura I, Hori M, Matsuzawa Y, Funahashi T and Kitakaze M**. Exacerbation of heart failure in adiponectin-deficient mice due to impaired regulation of AMPK and glucose metabolism. *Cardiovasc Res* 67: 705-713, 2005.

79. **Lichtenstein AH, Appel LJ, Brands M, Carnethon M, Daniels S, Franch HA, Franklin B, Kris-Etherton P, Harris WS, Howard B, Karanja N, Lefevre M, Rudel L, Sacks F, Van Horn L, Winston M and Wylie-Rosett J**. Summary of

American Heart Association Diet and Lifestyle Recommendations revision 2006. *Arterioscler Thromb Vasc Biol* 26: 2186-2191, 2006.

80. **Listenberger LL, Han X, Lewis SE, Cases S, Farese RV, Jr., Ory DS and Schaffer JE**. Triglyceride accumulation protects against fatty acid-induced lipotoxicity. *Proc Natl Acad Sci U S A* 100: 3077-3082, 2003.

81. **Listenberger LL, Ory DS and Schaffer JE**. Palmitate-induced apoptosis can occur through a ceramide-independent pathway. *J Biol Chem* 276: 14890-14895, 2001.

82. **Longo N, Amat di San FC and Pasquali M**. Disorders of carnitine transport and the carnitine cycle. *Am J Med Genet C Semin Med Genet* 142: 77-85, 2006.

83. **Lopaschuk GD, Folmes CD and Stanley WC**. Cardiac energy metabolism in obesity. *Circ Res* 101: 335-347, 2007.

84. **Mann DL and Bristow MR**. Mechanisms and models in heart failure: the biomechanical model and beyond. *Circulation* 111: 2837-2849, 2005.

85. **Marin-Garcia J, Goldenthal MJ and Moe GW**. Abnormal cardiac and skeletal muscle mitochondrial function in pacing-induced cardiac failure. *Cardiovasc Res* 52: 103-110, 2001.

86. **McMurray JJ and Pfeffer MA**. Heart failure. *Lancet* 365: 1877-1889, 2005.

87. **Minkler PE, Ingalls ST and Hoppel CL**. Strategy for the isolation, derivatization, chromatographic separation, and detection of carnitine and acylcarnitines. *Anal Chem* 77: 1448-1457, 2005.

88. **Moghaddas S, Hoppel CL and Lesnefsky EJ**. Aging defect at the QO site of complex III augments oxyradical production in rat heart interfibrillar mitochondria. *Arch Biochem Biophys* 414: 59-66, 2003.

89. **Moghaddas S, Stoll MS, Minkler PE, Salomon RG, Hoppel CL and Lesnefsky EJ**. Preservation of cardiolipin content during aging in rat heart interfibrillar mitochondria. *J Gerontol A Biol Sci Med Sci* 57: B22-B28, 2002.

90. **Morgan EE, Faulx MD, McElfresh TA, Kung TA, Zawaneh MS, Stanley WC, Chandler MP and Hoit BD**. Validation of echocardiographic methods for assessing left ventricular dysfunction in rats with myocardial infarction. *Am J Physiol Heart Circ Physiol* 287: H2049-H2053, 2004.

91. **Morgan EE, Rennison JH, Young ME, McElfresh TA, Kung TA, Tserng KY, Hoit BD, Stanley WC and Chandler MP**. Effects of chronic activation of peroxisome proliferator-activated receptor-alpha or high-fat feeding in a rat infarct model of heart failure. *Am J Physiol Heart Circ Physiol* 290: H1899-H1904, 2006.

92. **Okere IC, Chandler MP, McElfresh TA, Rennison JH, Kung TA, Hoit BD, Ernsberger P, Young ME and Stanley WC**. Carnitine palmitoyl transferase-I inhibition is not associated with cardiac hypertrophy in rats fed a high-fat diet. *Clin Exp Pharmacol Physiol* 34: 113-119, 2007.

93. **Okere IC, Chandler MP, McElfresh TA, Rennison JH, Sharov V, Sabbah HN, Tserng KY, Hoit BD, Ernsberger P, Young ME and Stanley WC**. Differential effects of saturated and unsaturated fatty acid diets on cardiomyocyte apoptosis, adipose distribution, and serum leptin. *Am J Physiol Heart Circ Physiol* 291: H38-H44, 2006.

94. **Okere IC, Chess DJ, McElfresh TA, Johnson J, Rennison J, Ernsberger P, Hoit BD, Chandler MP and Stanley WC**. High-fat diet prevents cardiac hypertrophy and improves contractile function in the hypertensive dahl salt-sensitive rat. *Clin Exp Pharmacol Physiol* 32: 825-831, 2005.

95. **Oliver MF**. Metabolic causes and prevention of ventricular fibrillation during acute coronary syndromes. *Am J Med* 112: 305-311, 2002.

96. **Ouchi N, Shibata R and Walsh K**. Cardioprotection by adiponectin. *Trends Cardiovasc Med* 16: 141-146, 2006.

97. **Ouwens DM, Boer C, Fodor M, de Galan P, Heine RJ, Maassen JA and Diamant M**. Cardiac dysfunction induced by high-fat diet is associated with altered myocardial insulin signalling in rats. *Diabetologia* 48: 1229-1237, 2005.

98. **Ouwens DM, Diamant M, Fodor M, Habets DD, Pelsers MM, El Hasnaoui M, Dang ZC, van den Brom CE, Vlasblom R, Rietdijk A, Boer C, Coort SL, Glatz JF and Luiken JJ**. Cardiac contractile dysfunction in insulin-resistant rats fed a high-fat diet is associated with elevated CD36-mediated fatty acid uptake and esterification. *Diabetologia* 50: 1938-1948, 2007.

99. **Palmer JW, Tandler B and Hoppel CL**. Biochemical properties of subsarcolemmal and interfibrillar mitochondria isolated from rat cardiac muscle. *J Biol Chem* 252: 8731-8739, 1977.

100. **Panchal AR, Stanley WC, Kerner J and Sabbah HN**. Beta-receptor blockade decreases carnitine palmitoyl transferase I activity in dogs with heart failure. *J Card Fail* 4: 121-126, 1998.

101. **Paumen MB, Ishida Y, Muramatsu M, Yamamoto M and Honjo T**. Inhibition of carnitine palmitoyltransferase I augments sphingolipid synthesis and palmitate-induced apoptosis. *J Biol Chem* 272: 3324-3329, 1997.

102. **Pepe S and McLennan PL**. (n-3) Long chain PUFA dose-dependently increase oxygen utilization efficiency and inhibit arrhythmias after saturated fat feeding in rats. *J Nutr* 137: 2377-2383, 2007.

103. **Quillet-Mary A, Jaffrezou JP, Mansat V, Bordier C, Naval J and Laurent G**. Implication of mitochondrial hydrogen peroxide generation in ceramide-induced apoptosis. *J Biol Chem* 272: 21388-21395, 1997.

104. **Relling DP, Hintz KK and Ren J**. Acute exposure of ceramide enhances cardiac contractile function in isolated ventricular myocytes. *Br J Pharmacol* 140: 1163-1168, 2003.

105. **Rennison JH, McElfresh TA, Okere IC, Vazquez EJ, Patel HV, Foster AB, Patel KK, Chen Q, Hoit BD, Tserng KY, Hassan MO, Hoppel CL and Chandler MP**. High-fat diet postinfarction enhances mitochondrial function and does not exacerbate left ventricular dysfunction. *Am J Physiol Heart Circ Physiol* 292: H1498-H1506, 2007.

106. **Rosamond W, Flegal K, Friday G, Furie K, Go A, Greenlund K, Haase N, Ho M, Howard V, Kissela B, Kittner S, Lloyd-Jones D, McDermott M, Meigs J, Moy C, Nichol G, O'Donnell CJ, Roger V, Rumsfeld J, Sorlie P, Steinberger J, Thom T, Wasserthiel-Smoller S and Hong Y**. Heart disease and stroke statistics--2007 update: a report from the American Heart Association Statistics Committee and Stroke Statistics Subcommittee. *Circulation* 115: e69-171, 2007.

107. **Sabbah HN, Sharov V, Riddle JM, Kono T, Lesch M and Goldstein S**. Mitochondrial abnormalities in myocardium of dogs with chronic heart failure. *J Mol Cell Cardiol* 24: 1333-1347, 1992.

108. **Sack MN, Rader TA, Park S, Bastin J, McCune SA and Kelly DP**. Fatty acid oxidation enzyme gene expression is downregulated in the failing heart. *Circulation* 94: 2837-2842, 1996.

109. **Sanbe A, Tanonaka K, Hanaoka Y, Katoh T and Takeo S**. Regional energy metabolism of failing hearts following myocardial infarction. *J Mol Cell Cardiol* 25: 995-1013, 1993.

110. **Saraste M**. Oxidative phosphorylation at the fin de siecle. *Science* 283: 1488-1493, 1999.

111. **Schaffer JE**. Lipotoxicity: when tissues overeat. *Curr Opin Lipidol* 14: 281-287, 2003.

112. **Schonekess BO, Allard MF and Lopaschuk GD**. Propionyl L-carnitine improvement of hypertrophied rat heart function is associated with an increase in cardiac efficiency. *Eur J Pharmacol* 286: 155-166, 1995.

113. **Sharma N, Okere IC, Duda MK, Chess DJ, O'Shea KM and Stanley WC**. Potential impact of carbohydrate and fat intake on pathological left ventricular hypertrophy. *Cardiovasc Res* 73: 257-268, 2007.

114. **Sharma N, Okere IC, Duda MK, Johnson J, Yuan CL, Chandler MP, Ernsberger P, Hoit BD and Stanley WC**. High fructose diet increases mortality in hypertensive rats compared to a complex carbohydrate or high fat diet. *Am J Hypertens* 20: 403-409, 2007.

115. **Sharma S, Adrogue JV, Golfman L, Uray I, Lemm J, Youker K, Noon GP, Frazier OH and Taegtmeyer H**. Intramyocardial lipid accumulation in the failing human heart resembles the lipotoxic rat heart. *FASEB J* 18: 1692-1700, 2004.

116. **Sharov VG, Goussev A, Lesch M, Goldstein S and Sabbah HN**. Abnormal mitochondrial function in myocardium of dogs with chronic heart failure. *J Mol Cell Cardiol* 30: 1757-1762, 1998.

117. **Sharov VG, Todor AV, Silverman N, Goldstein S and Sabbah HN**. Abnormal mitochondrial respiration in failed human myocardium. *J Mol Cell Cardiol* 32: 2361-2367, 2000.

118. **Sordahl LA, McCollum WB, Wood WG and Schwartz A**. Mitochondria and sarcoplasmic reticulum function in cardiac hypertrophy and failure. *Am J Physiol* 224: 497-502, 1973.

119. **Sparagna GC, Chicco AJ, Murphy RC, Bristow MR, Johnson CA, Rees ML, Maxey ML, McCune SA and Moore RL**. Loss of cardiac tetralinoleoyl cardiolipin in human and experimental heart failure. *J Lipid Res* 48: 1559-1570, 2007.

120. **Sparagna GC, Hickson-Bick DL, Buja LM and McMillin JB**. A metabolic role for mitochondria in palmitate-induced cardiac myocyte apoptosis. *Am J Physiol Heart Circ Physiol* 279: H2124-H2132, 2000.

121. **Srere PA**. Citrate Synthase. *Methods Enzymol* 13: 3-5, 1969.

122. **Stanley WC and Chandler MP**. Energy metabolism in the normal and failing heart: potential for therapeutic interventions. *Heart Fail Rev* 7: 115-130, 2002.

123. **Stanley WC, Recchia FA and Lopaschuk GD**. Myocardial substrate metabolism in the normal and failing heart. *Physiol Rev* 85: 1093-1129, 2005.

124. **Stavinoha MA, RaySpellicy JW, Essop MF, Graveleau C, Abel ED, Hart-Sailors ML, Mersmann HJ, Bray MS and Young ME**. Evidence for mitochondrial thioesterase 1 as a peroxisome proliferator-activated receptor-

alpha-regulated gene in cardiac and skeletal muscle. *Am J Physiol Endocrinol Metab* 287: E888-E895, 2004.

125. **Steiber A, Kerner J and Hoppel CL**. Carnitine: a nutritional, biosynthetic, and functional perspective. *Mol Aspects Med* 25: 455-473, 2004.

126. **Stryer L**. *Biochemistry*. New York: W.H. Freeman and Company, 1995.

127. **Swedberg K, Cleland J, Dargie H, Drexler H, Follath F, Komajda M, Tavazzi L, Smiseth OA, Gavazzi A, Haverich A, Hoes A, Jaarsma T, Korewicki J, Levy S, Linde C, Lopez-Sendon JL, Nieminen MS, Pierard L and Remme WJ**. Guidelines for the diagnosis and treatment of chronic heart failure: executive summary (update 2005): The Task Force for the Diagnosis and Treatment of Chronic Heart Failure of the European Society of Cardiology. *Eur Heart J* 26: 1115-1140, 2005.

128. **Taegtmeyer H, King LM and Jones BE**. Energy substrate metabolism, myocardial ischemia, and targets for pharmacotherapy. *Am J Cardiol* 82: 54K-60K, 1998.

129. **Taha M and Lopaschuk GD**. Alterations in energy metabolism in cardiomyopathies. *Ann Med* 39: 594-607, 2007.

130. **Tomassini B and Testi R**. Mitochondria as sensors of sphingolipids. *Biochimie* 84: 123-129, 2002.

131. **Tomec RJ and Hoppel CL**. Carnitine palmitoyltransferase in bovine fetal heart mitochondria. *Arch Biochem Biophys* 170: 716-723, 1975.

132. **Tserng KY and Griffin R**. Quantitation and molecular species determination of diacylglycerols, phosphatidylcholines, ceramides, and sphingomyelins with gas chromatography. *Anal Biochem* 323: 84-93, 2003.

133. **Ueta H, Ogura R, Sugiyama M, Kagiyama A and Shin G**. O2-. spin trapping on cardiac submitochondrial particles isolated from ischemic and non-ischemic myocardium. *J Mol Cell Cardiol* 22: 893-899, 1990.

134. **Unger RH**. Hyperleptinemia: protecting the heart from lipid overload. *Hypertension* 45: 1031-1034, 2005.

135. **Unger RH**. Longevity, lipotoxicity and leptin: the adipocyte defense against feasting and famine. *Biochimie* 87: 57-64, 2005.

136. **Unger RH and Orci L**. Diseases of liporegulation: new perspective on obesity and related disorders. *FASEB J* 15: 312-321, 2001.

137. **Van Blitterswijk WJ, Van Der Luit AH, Veldman RJ, Verheij M and Borst J**. Ceramide: second messenger or modulator of membrane structure and dynamics? *Biochem J* 369: 199-211, 2003.

138. **Van der Vusse GJ, van Bilsen M and Glatz JF**. Cardiac fatty acid uptake and transport in health and disease. *Cardiovasc Res* 45: 279-293, 2000.

139. **Veitch K, Draye JP, Van Hoof F and Sherratt HS**. Effects of riboflavin deficiency and clofibrate treatment on the five acyl-CoA dehydrogenases in rat liver mitochondria. *Biochem J* 254: 477-481, 1988.

140. **Venkataraman K and Futerman AH**. Ceramide as a second messenger: sticky solutions to sticky problems. *Trends Cell Biol* 10: 408-412, 2000.

141. **Weiss B and Stoffel W**. Human and murine serine-palmitoyl-CoA transferase--cloning, expression and characterization of the key enzyme in sphingolipid synthesis. *Eur J Biochem* 249: 239-247, 1997.

142. **Weiss R**. Fat distribution and storage: how much, where, and how? *Eur J Endocrinol* 157 Suppl 1: S39-S45, 2007.

143. **Wharton DC and Tzagoloff A**. Cytochrome Oxidase. *Methods Enzymol* 10: 245-250, 1967.

144. **Young ME, Guthrie PH, Razeghi P, Leighton B, Abbasi S, Patil S, Youker KA and Taegtmeyer H**. Impaired long-chain fatty acid oxidation and contractile dysfunction in the obese Zucker rat heart. *Diabetes* 51: 2587-2595, 2002.

145. **Young ME, Laws FA, Goodwin GW and Taegtmeyer H**. Reactivation of peroxisome proliferator-activated receptor alpha is associated with contractile dysfunction in hypertrophied rat heart. *J Biol Chem* 276: 44390-44395, 2001.

146. **Young ME, Patil S, Ying J, Depre C, Ahuja HS, Shipley GL, Stepkowski SM, Davies PJ and Taegtmeyer H**. Uncoupling protein 3 transcription is regulated by peroxisome proliferator-activated receptor (alpha) in the adult rodent heart. *FASEB J* 15: 833-845, 2001.

147. **Zeng J, Deng G, Yu W and Li D**. Inactivation of medium-chain acyl-CoA dehydrogenase by oct-4-en-2-ynoyl-CoA. *Bioorg Med Chem Lett* 16: 1445-1448, 2006.

148. **Zhou YT, Grayburn P, Karim A, Shimabukuro M, Higa M, Baetens D, Orci L and Unger RH**. Lipotoxic heart disease in obese rats: implications for human obesity. *Proc Natl Acad Sci U S A* 97: 1784-1789, 2000.